



National Library
of Canada

Acquisitions and
Bibliographic Services Branch

395 Wellington Street
Ottawa, Ontario
K1A 0N4

Bibliothèque nationale
du Canada

Direction des acquisitions et
des services bibliographiques

395, rue Wellington
Ottawa (Ontario)
K1A 0N4

Your file - Votre référence

Our file - Notre référence

NOTICE

The quality of this microform is heavily dependent upon the quality of the original thesis submitted for microfilming. Every effort has been made to ensure the highest quality of reproduction possible.

If pages are missing, contact the university which granted the degree.

Some pages may have indistinct print especially if the original pages were typed with a poor typewriter ribbon or if the university sent us an inferior photocopy.

Reproduction in full or in part of this microform is governed by the Canadian Copyright Act, R.S.C. 1970, c. C-30, and subsequent amendments.

AVIS

La qualité de cette microforme dépend grandement de la qualité de la thèse soumise au microfilmage. Nous avons tout fait pour assurer une qualité supérieure de reproduction.

S'il manque des pages, veuillez communiquer avec l'université qui a conféré le grade.

La qualité d'impression de certaines pages peut laisser à désirer, surtout si les pages originales ont été dactylographiées à l'aide d'un ruban usé ou si l'université nous a fait parvenir une photocopie de qualité inférieure.

La reproduction, même partielle, de cette microforme est soumise à la Loi canadienne sur le droit d'auteur, SRC 1970, c. C-30, et ses amendements subséquents.

Canada

UNIVERSITY OF ALBERTA

THE EFFECT OF FLOW RATE AND CORE LENGTH ON THE
LONGITUDINAL DISPERSION COEFFICIENT

by

TUYET HUYNH LE



A thesis submitted to the Faculty of Graduate Studies and Research in partial fulfilment
of the requirements for the degree of MASTER OF SCIENCE

in

PETROLEUM ENGINEERING

DEPARTMENT OF MINING, METALLURGICAL and PETROLEUM
ENGINEERING

EDMONTON, ALBERTA

SPRING 1995



National Library
of Canada

Acquisitions and
Bibliographic Services Branch

395 Wellington Street
Ottawa, Ontario
K1A 0N4

Bibliothèque nationale
du Canada

Direction des acquisitions et
des services bibliographiques

395, rue Wellington
Ottawa (Ontario)
K1A 0N4

Your file *Votre référence*

Our file *Notre référence*

THE AUTHOR HAS GRANTED AN IRREVOCABLE NON-EXCLUSIVE LICENCE ALLOWING THE NATIONAL LIBRARY OF CANADA TO REPRODUCE, LOAN, DISTRIBUTE OR SELL COPIES OF HIS/HER THESIS BY ANY MEANS AND IN ANY FORM OR FORMAT, MAKING THIS THESIS AVAILABLE TO INTERESTED PERSONS.

L'AUTEUR A ACCORDE UNE LICENCE IRREVOCABLE ET NON EXCLUSIVE PERMETTANT A LA BIBLIOTHEQUE NATIONALE DU CANADA DE REPRODUIRE, PRETER, DISTRIBUER OU VENDRE DES COPIES DE SA THESE DE QUELQUE MANIERE ET SOUS QUELQUE FORME QUE CE SOIT POUR METTRE DES EXEMPLAIRES DE CETTE THESE A LA DISPOSITION DES PERSONNE INTERESSEES.

THE AUTHOR RETAINS OWNERSHIP OF THE COPYRIGHT IN HIS/HER THESIS. NEITHER THE THESIS NOR SUBSTANTIAL EXTRACTS FROM IT MAY BE PRINTED OR OTHERWISE REPRODUCED WITHOUT HIS/HER PERMISSION.

L'AUTEUR CONSERVE LA PROPRIETE DU DROIT D'AUTEUR QUI PROTEGE SA THESE. NI LA THESE NI DES EXTRAITS SUBSTANTIELS DE CELLE-CI NE DOIVENT ETRE IMPRIMES OU AUTREMENT REPRODUITS SANS SON AUTORISATION.

ISBN 0-612-01621-8

UNIVERSITY OF ALBERTA

RELEASE FORM

NAME OF AUTHOR : TUYET HUYNH LE

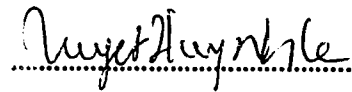
TITLE OF THESIS : *The Effect of Flow Rate and Core Length on the
Longitudinal Dispersion Coefficient.*

DEGREE FOR WHICH THESIS WAS PRESENTED : MASTER OF SCIENCE

YEAR THIS DEGREE WAS GRANTED : 1995

Permission is hereby granted to the University of Alberta Library to reproduce single copies of this thesis and to lend or sell such copies for private, scholarly or scientific research purposes only.

The author reserves all other publication and other rights in association with the copyright in the thesis, and except as hereinbefore provided, neither the thesis nor any substantial portion thereof may be printed or otherwise reproduced in any material form whatever without the author's prior written permission.




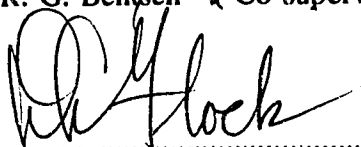
219 Osland Close
Edmonton, Alberta
Canada

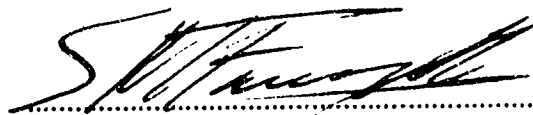
DATE : Jan 30 / 95

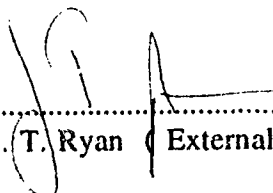
UNIVERSITY OF ALBERTA
FACULTY OF GRADUATE STUDIES AND RESEARCH

The undersigned certify that they have read, and recommend to the Faculty of Graduate Studies and Research, for acceptance, a thesis entitled " *The Effect of Flow Rate and Core Length on the Longitudinal Dispersion Coefficient* " submitted by *Tuyet Huynh Le* in partial fulfilment of the requirements for the degree of *Master of Science in Petroleum Engineering*.


.....
Dr. R. G. Bentsen (Co-supervisor)


.....
Dr. D. L. Flock (Co-supervisor)


.....
Dr. S. M. Farouq Ali (Chairman, Examiner)


.....
Dr. J. T. Ryan (External Examiner)

DATED : *January 23, 1995*

This work is dedicated to my parents and my family for their support and encouragement.

ABSTRACT

Laboratory experiments conducted to study diffusion and dispersion in a miscible displacement in a Berea sandstone cores are presented in this thesis. The work involved several miscible displacement tests conducted with n-hexane as the resident oil and cyclohexane as the solvent. The tests were performed in three core lengths at six flow rates. A longitudinal dispersion coefficient, which was based on Fickian dispersion theory, was calculated for each case to study the effect of core length and flow rate on the miscible displacement process. The experimental results were compared with theoretical results which were calculated based on Brigham's model³, an analytical solution based on Fick's first law of diffusion.

It was found that the dispersion coefficient depends on both core length and flow rate. The dispersion coefficient increases with increasing flow rate. The effect was minor in the short core, but becomes more significant in the longer cores. The dispersion coefficient increases with increasing core length and becomes independent of core length at high flow rates. Laboratory dispersion in Berea sandstone is not Fickian as the predicted concentration profile and the experimental concentration profile do not match in every test. There was always a deviation between the experimental and the predicted concentration profile. It is believed that Brigham's model failed to match the predicted and experimental results in this case because the model did not take into account the heterogeneity of the consolidated core. Similar work done by Walsh and Withjack¹⁶ recently has produced evidence of non-Fickian dispersion phenomena in Berea sandstone.

ACKNOWLEDGEMENT

The author is grateful to Dr. D. L. Flock and Dr. R. G. Bentsen for their encouragement and support in the completion of this study. Special thanks should be made to Dr. R. G. Bentsen for reviewing the manuscript and giving valuable advice.

Appreciation is extended to Dr. S. M. Farouq Ali for permission to use some equipment for the experiments. Appreciation is also extended to Mr. Bob Smith for his assistance in setting up the equipment.

The author would like to acknowledge the financial support provided by the Alberta Oil Sands Technology and Research Authority , Texaco Canada Incorporated and the Department of Mining, Metallurgical and Petroleum Engineering, University of Alberta.

TABLE OF CONTENTS

1.	INTRODUCTION	1
2.	LITERATURE REVIEW	3
	2.1 Diffusion of miscible fluids	3
	2.2 Dispersion in porous media	7
	2.3 The dispersion coefficients	8
	2.3.1 The Brigham model	12
	2.3.2 The Coats and Smith model	15
	2.3.3 Other related work	18
	2.4 Factors affecting the dispersion coefficient	19
3.	STATEMENT OF THE PROBLEM	22
4.	EXPERIMENTAL	24
	4.1 Experimental apparatus	24
	4.2 Displacement test procedure	26
	4.2.1 Preparation of the core	27
	4.2.2 Packing the core	27
	4.2.3 Saturating the core	28
	4.2.4 Permeability test	29
	4.2.5 The displacement test	29
	4.3 Calculation of the results	30

5.	RESULTS AND DISCUSSION	34
5.1	The effect of solvent injection rate	35
5.2	The effect of core length	45
5.3	Miscible displacement in unfavourable mobility case	58
5.4	Comparison of theoretical and experimental concentration profiles	60
6.	CONCLUSIONS AND RECOMMENDATIONS	69
7.	REFERENCES	71
8.	APPENDIX A	74
9.	APPENDIX B	77
10.	APPENDIX C	84

LIST OF TABLES

1.	Properties of the miscible components	26
2.	Displacement test results for 122 cm core	40
3.	Displacement test results for 183 cm length	41
4.	Displacement test results for 242 cm length	41
B1.	Experimental effluent concentration for the favourable mobility case 122 cm core length	78
B2.	Experimental effluent concentration for the favourable mobility case 183 cm core length	79
B3.	Experimental effluent concentration for the favourable mobility case 242 cm core length	80
B4.	Experimental effluent concentration for the unfavourable mobility case 122 cm core length	81
B5.	Experimental effluent concentration for the unfavourable mobility case 183 cm core length	82
B6.	Experimental effluent concentration for the unfavourable mobility case 242 cm core length	83

LIST OF FIGURES

2.1.1	Concentration profile on arithmetic probability paper to be used for the calculation of D_0 from Equation (2.1.3)	5
2.3.1	Longitudinal dispersion coefficient	9
2.3.2	Transverse dispersion coefficient	11
4.1	Schematic diagram of the miscible flood apparatus	25
5.1.1	A typical concentration profile	36
5.1.2	Effluent concentration plotted on arithmetic probability paper for core length of 122 cm	36
5.1.3	Concentration profile for core length of 122 cm	38
5.1.4	Concentration profile for core length of 183 cm	38
5.1.5	Concentration profile for core length of 242 cm	39
5.1.6	The effect of fluid velocity on the dispersion coefficient	43
5.2.1	Concentration profile at low flow rate ($0.0732 \text{ cm}^3/\text{s}$)	47
5.2.2	Concentration profile at high flow rate ($0.1146 \text{ cm}^3/\text{s}$)	47
5.2.3	The effect of core length on the dispersion coefficient	48
5.2.4a	The effect of fluid velocity on the dispersion coefficient	49

5.2.4b	The effect of core length on the dispersion coefficient	50
5.2.5	The effect of velocity and core length on the dispersion coefficient	52
5.2.6	The effect of core length on the recovery factor at a solvent injection rate of 0.0732 cm ³ /s	53
5.2.7	The effect of core length on the recovery factor at a solvent injection rate of 0.1446 cm ³ /s	54
5.2.8	The effect of core length on the recovery factor at a solvent injection rate of 0.1896 cm ³ /s	55
5.2.9	The effect of flow rate on the recovery factor at 1 pore volume of production	56
5.2.10	The effect of velocity and core length on the recovery factor at 1 PV	57
5.3.1	The effect of mobility ratio on the concentration profile Core length = 122 cm - Fluid velocity = 0.0118 cm/s	59
5.3.2	The effect of flow rate on the concentration profile for an unfavorable mobility case	59
5.4.1	Concentration profile - experimental versus predicted Core length = 122 cm - fluid velocity = 0.0118 cm/s	63

5.4.2	Concentration plotted on arithmetic probability paper	
	Core length = 122 cm - fluid velocity = 0.0118 cm/s	63
5.4.3	Concentration profile - experimental versus predicted	
	Core length = 183 cm - fluid velocity = 0.0146 cm/s	64
5.4.4	Concentration profile - experimental versus predicted	
	Core length = 242 cm - fluid velocity = 0.0115 cm/s	64
5.4.5	Concentration profile - experimental versus predicted	
	Core length = 122 cm - fluid velocity = 0.0483 cm/s	65
5.4.6	Concentration profile - experimental versus predicted	
	Core length = 183 cm - fluid velocity = 0.0391 cm/s	65
5.4.7	Concentration profile - experimental versus predicted	
	Core length = 242 cm - fluid velocity = 0.0461 cm/s	66
B1	Standard concentration curve	
	Refractive index versus % cyclohexane	77
C1	Concentration profile - experimental versus predicted	
	Core length = 122cm - fluid velocity = 0.0187 cm/s	93
C2	Concentration profile - experimental versus predicted	
	Core length = 122cm - fluid velocity = 0.0241 cm/s	93

C3	Concentration profile - experimental versus predicted	
	Core length = 183cm - fluid velocity = 0.0166 cm/s	94
C4	Concentration profile - experimental versus predicted	
	Core length = 183cm - fluid velocity = 0.0195 cm/s	94
C5	Concentration profile - experimental versus predicted	
	Core length = 183cm - fluid velocity = 0.0293 cm/s	95
C6	Concentration profile - experimental versus predicted	
	Core length = 242cm - fluid velocity = 0.0178 cm/s	95
C7	Concentration profile - experimental versus predicted	
	Core length = 242cm - fluid velocity = 0.0192 cm/s	96
C8	Concentration profile - experimental versus predicted	
	Core length = 242cm - fluid velocity = 0.0221 cm/s	96
C9	Concentration profile - experimental versus predicted	
	Core length = 242cm - fluid velocity = 0.0338 cm/s	97

NOMENCLATURE

A	Cross-sectional area, (cm^2)
a	Rate group, dimensionless
	Mixing coefficient, dimensionless
C	In-situ solvent concentration, dimensionless
C*	Solvent concentration in the stagnant fluid, dimensionless
C _o	Feed concentration, dimensionless
C'	Effluent concentration, dimensionless
D	Apparent diffusion coefficient, (cm^2/s)
D _o	Molecular diffusion coefficient, (cm^2/s)
d _p	Average particle diameter, (cm)
E	Longitudinal dispersion coefficient, (cm^2/s)
F	Formation electrical resistivity factor, dimensionless
f	Fraction of pore space occupied by mobile fluid, dimensionless
G	Quantity of material diffusing across a plane, (cm^3)
\dot{G}	Fluid volume flow rate, (cm^3/s)
I	Pore volumes injected, dimensionless
K _e	Effective dispersion coefficient, (cm^2/s)
K _l	Longitudinal dispersion coefficient, (cm^2/s)
K _t	Transverse dispersion coefficient, (cm^2/s)
L	Length of the porous medium, (cm)
P _e	Peclet number
r	Average diameter of glass bead, (cm)
t	Time, (s)
V _i	Injected volume, (cm^3)
V _p	Pore volume, (cm^3)
x	Distance, (cm)

- x_{10} Distance from the initial interface where the composition is 10% of the fluid under consideration, (cm)
- x_{90} Distance from the initial interface where the composition is 90% of the fluid under consideration, (cm)
- y Distance, (cm)
-
- α Mixing coefficient, dimensionless
- γ Dimensionless dispersion
- λ Volume function
- v Pore velocity, (cm/s)
Interstitial velocity, (cm/s)
- Φ Fractional porosity
- σ Inhomogeneity factor

1. INTRODUCTION

An oil reservoir which undergoes primary and then secondary recovery still leaves behind from 40 to 60 percent residual oil. In order to recover the rest of the oil, several enhanced oil recovery methods have been studied in the laboratory and then field tested. Amongst these miscible-flooding has become a major tertiary recovery method where a solvent is injected into the reservoir to reduce the interfacial tension and the capillary forces. In this case, the solvent (displacing fluid) is mixed with the oil (displaced fluid) on first contact to form a mixing zone where the interfacial tension is eliminated. The oil recovery by this method leaves behind minimal residual oil saturation.

There are two kinds of miscible displacement:

- " first-contact miscible " where the displacing fluid mixes directly with the displaced fluid on first contact,
- " multiple contact " where miscibility between the two fluids is obtained by repeated contact and mixing.

The mixing process is governed by three main mechanisms:

- molecular diffusion where the two fluids are immobile and diffuse into each other as a result of the thermal motion of molecules.
- microscopic convective dispersion where mixing is due to the movement of the fluid in the pores without channelling,
- macroscopic convective dispersion where mixing is due to the channelling of the displacing fluid through the porous medium.

Miscible displacement is normally described by a dispersion coefficient. Mixing which occurs in the fluid flow direction is represented by the longitudinal dispersion coefficient and that in the direction perpendicular to flow is described by the transverse dispersion coefficient. Both dispersion coefficients can be evaluated by laboratory models as well as mathematically. Laboratory experiments on miscible displacement have shown that the dispersion coefficient magnitude is affected by:

1. the fluid flow velocity,
2. the geometry of the model: dimension, shape,
3. mobility ratio,
4. density ratio,
5. porous medium type,

Most of the research papers found in this field deal with the effect of the above-mentioned factors on the transverse dispersion coefficient and very few data are available for the longitudinal dispersion coefficient.

The purpose of this research was to study the effect of solvent injection rate and core length on the longitudinal dispersion coefficient. The experiments are conducted in a consolidated medium and with a favourable mobility ratio where mixing due to adverse mobility is negligible. The study involves a series of miscible flood experiments using hexane as the resident oil and cyclohexane as the solvent. The displacement tests are performed for three different core lengths and six different flow rates. In addition, during the process of bringing the cores back to their original nature, a reflush test is performed where cyclohexane becomes the resident oil to be displaced by hexane. The reflush experiments will serve as a study of miscible displacement where mixing is due to diffusion and channelling as a result of adverse mobility.

2. LITERATURE REVIEW

Miscible displacement has become an important method for enhanced oil recovery. In this process, a solvent is injected into the reservoir to form a less viscous mixture of oil-solvent to increase the oil recovery. The mixing may be by diffusion or by dispersion.

2.1 Diffusion of miscible fluids

When two miscible fluids are in contact with each other under a no flow condition, one fluid diffuses into the other as a result of the thermal motion of the molecules. This phenomenon is known as molecular diffusion. A sharp interface initially separates the two fluids. This interface then grows with time to form a single-phase mixed zone grading from one pure fluid to the other. If the volume of the two fluids is conserved during the diffusion process, then the net material transported across any arbitrary plane can be determined by Fick's diffusion equation¹³, which may be stated as follows:

$$\frac{\partial G}{\partial t} = -D_0 A' \frac{\partial C}{\partial x} \quad (2.1.1)$$

where

G = the quantity of material diffusing across a plane (cm^3)

t = time (s)

D_0 = molecular diffusion coefficient (cm^2/s)

A' = cross sectional area for diffusion (cm^2)

C = concentration, volume fraction

and

x = distance (cm)

In the above equation, the diffusion coefficient may be a function of concentration. To solve Equation (2.1.1) mathematically with a variable diffusion coefficient is fairly complicated. To simplify the problem, Perkins and Johnston¹³ introduced an "effective average diffusion coefficient", which is constant and independent of concentration. As D_0 is now a constant, Equation (2.1.1) can be integrated to give the fluid concentration as a function of time and distance for a system of miscible fluids mixing by diffusion :

$$C = \frac{1}{2} \left[1 \pm \operatorname{erf} \left(\frac{x}{2\sqrt{D_0 t}} \right) \right] \quad (2.1.2)$$

where

C = the concentration of fluid under consideration
(volume fraction)

x = the distance measured from the original position of the
interface (cm)

and

erf = error function.

The minus or plus sign of equation depends on the boundary conditions:

If at $t = 0$, $C = 1$ for $x < 0$ and $C = 0$ for $x > 0$ then use a minus sign.

If at $t = 0$, $C = 0$ for $x < 0$ and $C = 1$ for $x > 0$ then use a plus sign.

A plot of Equation (2.1.2) on probability co-ordinate paper gives a straight line as shown in Figure 2.1.1. The diffusion coefficient can be calculated as:

$$D_o = \left[\frac{1}{t} \right] \left[\frac{x_{90} - x_{10}}{3.625} \right]^2 \quad (2.1.3)$$

where

x_{90} = the distance from the initial interface where the composition is 90 percent of the fluid under consideration

and

x_{10} = the distance from the initial interface where the composition is 10 percent of the fluid under consideration.

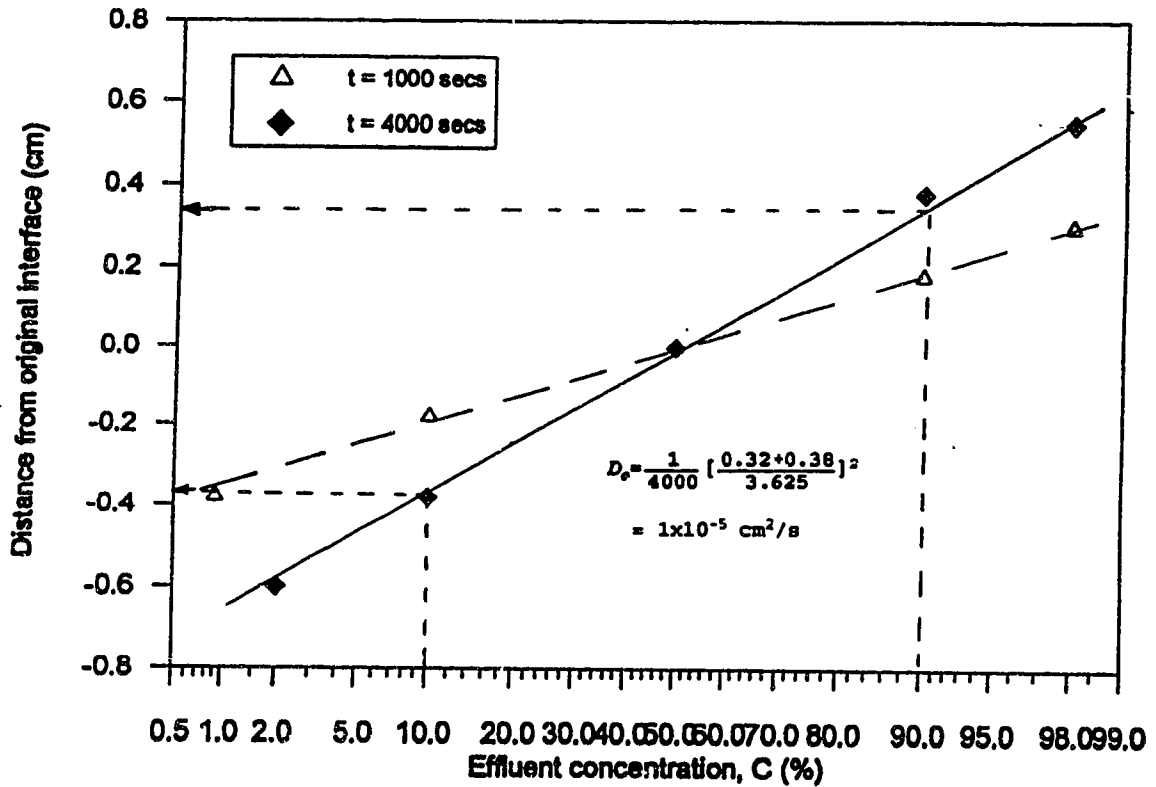


Figure 2.1.1 : Plot of concentration profile on arithmetic probability paper to be used for the calculation of D_o from Equation (2.1.3)

In a porous medium, an apparent diffusion coefficient, D , is normally based on the average cross sectional area open for diffusion and the overall length of the medium. For steady state diffusion in a porous medium, Equation (2.1.1) can be written as:

$$\dot{G} = -DA \frac{\Delta C}{L} \quad (2.1.4)$$

where

A is the area open for diffusion.

Carman⁵ has shown that, in a porous medium, fluids usually travel in a direction 45° to the net direction of flow. Therefore, the actual distance of travel in Equation (2.1.4) is $L\sqrt{2}$ and the diffusion model applied for porous rock is:

$$\frac{D}{D_o} = 0.707 \quad (2.1.5)$$

Brigham et al.⁴ took a more complicated approach to the solution of Equation (2.1.1) and, along with Crane and Gardner⁸ and Van der Poel¹⁶, found that there is an analogy between diffusion and electrical conductivity in porous media. They introduced another model for the evaluation of the diffusion coefficient in porous medium as:

$$\frac{D}{D_o} = \frac{1}{F\Phi} \quad (2.1.6)$$

where

F = the formation electrical resistivity factor,

and

Φ = fractional porosity.

Verification of both of these models has been reported by several investigators^{1,2,4,10,13}.

2.2. Dispersion in porous media

When fluid is flowing through porous media, fluid movement creates mixing in addition to that due to diffusion. The increased mixing due to diffusion and fluid flow is called dispersion.

When miscible displacement occurs in a homogenous medium with a mobility ratio less than 1, the mixing is defined as microscopic convective dispersion. Mixing of fluid can also be caused by the permeability heterogeneity of the reservoir. If the degree of heterogeneity is large, the mixing front is unstable and channelling may occur. The dispersion in this case is defined as macroscopic dispersion which normally occurs in the case of miscible displacement in a porous medium with a mobility ratio greater than 1.

There are two types of microscopic convective dispersion:

- longitudinal dispersion where mixing occurs in the flow direction due to diffusion and gross fluid movement,
- transverse dispersion where mixing occurs in the direction transverse to fluid flow due mainly to the permeability heterogeneity of the porous medium.

These two types of dispersion are not the same.

2.3 The dispersion coefficients

The mixing of fluids due to microscopic convective dispersion is normally described by a combination of the longitudinal dispersion coefficient and the transverse dispersion coefficient.

For fluid flow at a constant velocity in the x direction, the overall transport and mixing of fluids can be described by the following diffusion-convection equation:

$$K_1 \frac{\partial^2 C}{\partial x^2} + K_t \frac{\partial^2 C}{\partial y^2} + K_t \frac{\partial^2 C}{\partial z^2} - v \frac{\partial C}{\partial x} = \frac{\partial C}{\partial t} \quad (2.3.1)$$

where

$K_1 = D+E$, the total coefficient of longitudinal dispersion

and

$K_t =$ the total coefficient of transverse dispersion.

The first term in Equation (2.3.1) takes care of the longitudinal dispersion in the x direction and the second and third terms account for the transverse dispersion in the y and z directions.

For mixing of fluids of equal density and viscosity, Raimondi and Gardener as referred to in Perkins and Johnson¹³ proposed the equation for longitudinal dispersion coefficient as:

$$\frac{K_1}{D_o} = \frac{1}{Pe} + 0.5 \left(\frac{v \sigma d_p}{D_o} \right) \quad \text{for } Pe < 50 \quad (2.3.2)$$

where

v = the interstitial velocity, cm/s,

K_1 = the longitudinal dispersion coefficient, cm²/s,

σ = the inhomogeneity factor,

and

d_p = the average particle diameter, cm.

Figure 2.3.1 is a graphical interpretation of Equation (2.3.2) where the dimensionless term (K_1/D_0) is plotted as a function of the Peclet number (P_e).

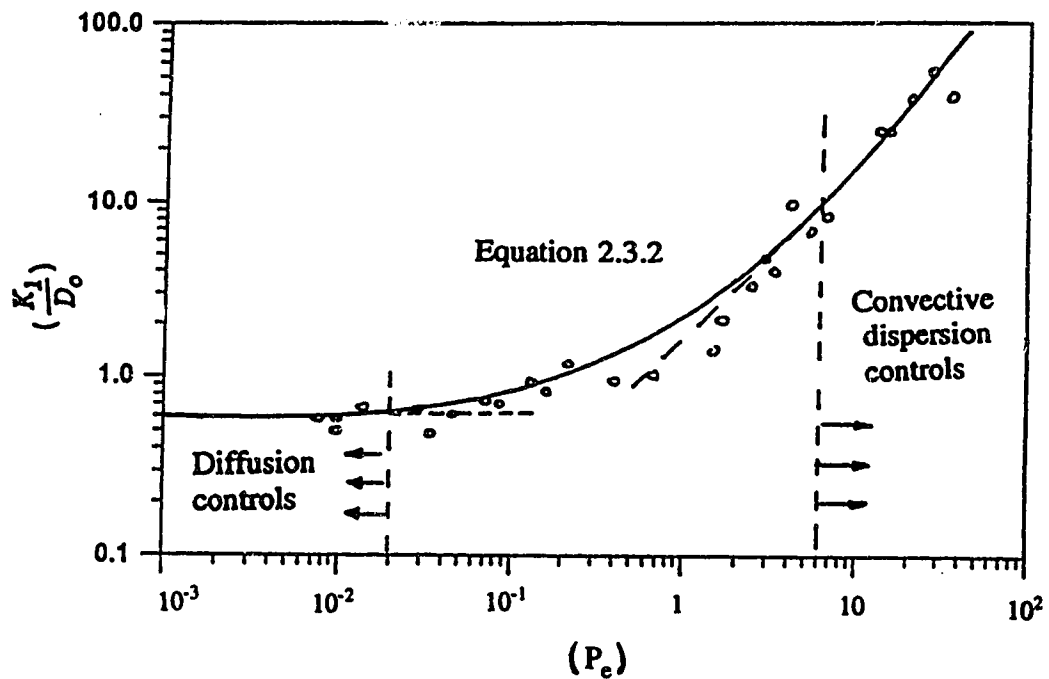


Figure 2.3.1 : Longitudinal dispersion coefficient

The figure shows three regions of mixing dependence ¹³:

- for $P_e < 0.1$, low flow rate, molecular diffusion dominates the longitudinal mixing,
- for $0.1 < P_e < 4$, moderate flow rate, both molecular and convection dispersion play an important role in longitudinal mixing,
- for $4 < P_e < 50$, high flow rate, convective dispersion dominates the longitudinal mixing and the dispersion coefficient is proportional to the flow rate,
- for $P_e > 50$, the dispersion is greater than that predicted by mixing cell theory and most data available show that (K_l/D_o) is proportional to $(P_e)^{1.2}$.

In the case of the transverse dispersion coefficient, Perkins and Johnston¹³ proposed the following equation for the calculation of the transverse dispersion coefficient for fluids of equal density and viscosity:

$$\frac{K_t}{D_o} = \frac{1}{Fr\Phi} + 0.0157 \left(\frac{v\sigma D_p}{D_o} \right) \quad \text{for } P_e < 10^4 \quad (2.3.3)$$

Again, Figure 2.3.2 shows the relationship between (K_l/D_o) and Peclet number according to Equation (2.3.3). For $P_e < 50$ molecular diffusion controls the transverse mixing and for $P_e > 300$, convective dispersion dominates.

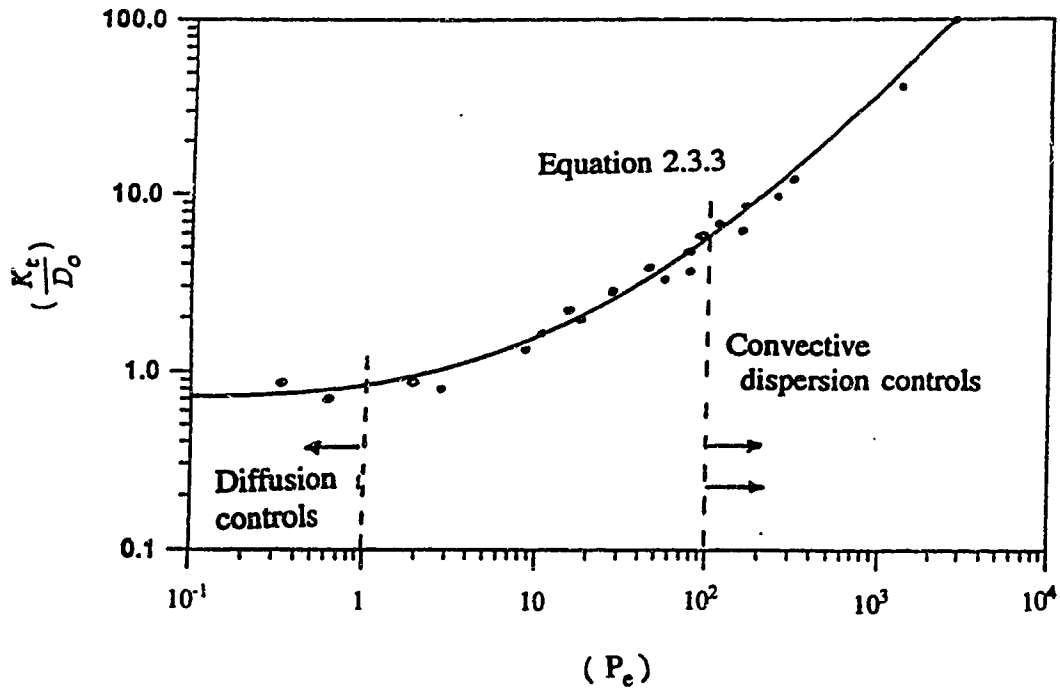


Figure 2.3.2 : Transverse dispersion coefficient

Longitudinal and transverse dispersion coefficients are normally determined by laboratory miscible displacement experiments. Several authors^{3,4,5,7,11,12} have recommended different methods for the determination of dispersion coefficients. Most of these methods are trying to fit the solvent concentration profile from the displacement test to various solutions of the diffusion-convection equation. The dispersion coefficient is determined from the best fit solution where the experimental concentration profile is closest to the calculated concentration profile.

2.3.1 The Brigham model

Brigham³ used the solution to the convective dispersion equation to match an effluent concentration profile obtained from a miscible displacement experiment.

Assume that the miscible displacement involves:

- one dimensional flow of incompressible fluid and dispersion occurs only in the direction of flow,
- first contact miscibility and
- a favourable mobility ratio.

Then the displacement can be described by the following diffusion equation :

$$K_1 \frac{\partial^2 C}{\partial x^2} - v \frac{\partial C}{\partial x} = \frac{\partial C}{\partial t} \quad (2.3.1.1)$$

where

- K_1 = the longitudinal dispersion coefficient,
- x = the distance from the inlet end of the core,
- v = the pore velocity,

and

- C = the in-situ solvent concentration

To solve the above equation, the boundary conditions must be defined since each set of boundary conditions yields a different solution. For a miscible displacement where the mixing zone is large compared to the porous medium, the boundary affects the

solution significantly. However, if the mixing zone is short compared to the length of the medium, the solutions to the diffusion equation are almost the same for any boundary condition chosen.

Consider the infinite medium case where the boundary conditions are chosen as:

$$\text{as } x \rightarrow +\infty \quad C(x,t) \rightarrow 0$$

and

$$\text{at } x = vt \quad C(x,t) = 1/2$$

Then the solution to the equation is:

$$C = \frac{1}{2} \operatorname{erfc}\left(\frac{x-vt}{2\sqrt{Kt}}\right) \quad (2.3.1.2)$$

In a laboratory experiment, one measures the effluent concentration at the outlet end of the core. This concentration is called the flowing concentration, C' , and is defined as :

$$C' = \frac{q}{vA\Phi} = C - \frac{K}{v} \left(\frac{\partial C}{\partial x}\right) \quad (2.3.1.3)$$

If one takes the derivative of Equation (2.3.1.2) and substitutes the result into Equation (2.3.1.3), the flowing concentration becomes:

$$C' = \frac{1}{2} \operatorname{erfc}\left(\frac{x-vt}{2\sqrt{Kt}}\right) + \left(\frac{K}{v}\right) \frac{1}{2\sqrt{Kt\pi}} e^{-\left(\frac{x-vt}{2\sqrt{Kt}}\right)^2} \quad (2.3.1.4)$$

Then by setting $x = L$, core length, and by introducing the dimensionless dispersion⁷, $\gamma = vL/K$, Equation (2.3.1.4) becomes:

$$C' = \frac{1}{2} \operatorname{erfc}\left(\frac{1-I}{2\sqrt{I/\gamma}}\right) + \frac{1}{2\sqrt{\pi\gamma I}} e^{-\left(\frac{1-I}{2\sqrt{I/\gamma}}\right)^2} \quad (2.3.1.5)$$

where

$$I = \text{pore volumes injected, } V_i/V_p \text{ or } vt/L$$

Equation (2.3.1.5) is often used to predict the effluent concentration profile of a miscible displacement test.

Brigham^{3,4} also introduced a simple method to determine the effective dispersion coefficient, K_e , using the experimental effluent concentration of the displacing fluid via a volume modifying function, λ , which is defined as :

$$\lambda = \frac{(V_i/V_p)}{\sqrt{V_i/V_p}} = \frac{I-1}{\sqrt{I}} \quad (2.3.1.6)$$

A plot of the volume modifying function versus effluent concentration on probability paper should yield a straight line, if the model is applicable. The value of γ in Equation (2.3.1.5) can be calculated as:

$$\gamma = \left(\frac{3.625}{\lambda_{90} - \lambda_{10}}\right)^2 \quad (2.3.1.7)$$

where

$$\lambda_{90} \text{ and } \lambda_{10} = \text{values of modified volume function at effluent concentrations of 90\% \& 10\%, respectively.}$$

The effective dispersion coefficient is then calculated as :

$$K_e = \frac{vL}{\gamma} = vL \left(\frac{\lambda_{90} - \lambda_{10}}{3.625} \right)^2 \quad (2.3.1.8)$$

where

K_e = effective dispersion coefficient (cm²/s)

v = pore velocity (cm/s)

and

L = core length (cm)

2.3.2 Coats and Smith model

Coats and Smith⁶ introduced a model for matching the effluent concentration profile of a miscible displacement test to compensate for the residual oil trapped in the dead end pores. This was a modified capacitance model which took into account the additional effect the diffusion of residual oil trapped in the dead-end pore space had on the overall dispersion coefficient.

In this model, the oil trapped in the occluded pore space was believed to have access to the flowing solvent at a single point with mass transfer between the two fluids by diffusion only. By defining (1-f) as the fraction of the total volume that was stagnant and C^* as the average concentration in these pores, the displacement can be represented by the following equation :

$$K \frac{\partial^2 C}{\partial x^2} - v \frac{\partial C}{\partial x} = f \left(\frac{\partial C}{\partial t} \right) + (1-f) \frac{\partial C^*}{\partial t} \quad (2.3.2.1)$$

and

$$(1-f) \frac{\partial C^*}{\partial t} = K'(C-C^*) \quad (2.3.2.2)$$

or in dimensionless terms as :

$$\frac{1}{\gamma} \frac{\partial^2 C}{\partial y^2} - \frac{\partial C}{\partial y} = f \frac{\partial C}{\partial I} + (1-f) \frac{\partial C^*}{\partial I} \quad (2.3.2.3)$$

and

$$(1-f) \frac{\partial C^*}{\partial I} = a(C-C^*) \quad (2.3.2.4)$$

where

$\gamma = vL/K$, dimensionless dispersion

$y =$ dimensionless distance, x/L

$C =$ concentration of injected fluid

$f =$ fraction of pore space occupied by mobile fluid

$I =$ pore volumes injected, vt/L

$C^* =$ concentration in stagnant fluid

and

$a =$ rate group , KL/v .

At low flow rates, where the fluid moves with sufficiently small velocity, the rate group, KL/v , is large so the mass transfer between the flowing fluid and the fluid trapped in the stagnant space is almost instantaneous. The model reduces to the simple diffusion model proposed by Brigham³. In this case, the solution to Equation (2.3.2.3) is as follows :

$$\frac{C}{C_0} = \frac{1}{2} \operatorname{erfc}\left(\frac{\sqrt{Y}}{2} \cdot \frac{y-I}{\sqrt{I}}\right) - \frac{\sqrt{I}}{\sqrt{\pi Y}(y+I)} e^{-Y(y-I)^2/4I} \left(1 - \frac{2I}{1+I}\right) \quad (2.3.2.5)$$

where

C_0 is the feed concentration

At high flow rates, the rate group becomes very small and can be neglected. Again the model degenerates to the diffusion model. However, in this case, the solution to Equation (2.3.2.3) is in the same form as Equation (2.3.2.5) with the I replaced by $J = (l/f)$.

The dispersion coefficient is normally determined from the results of miscible displacement tests conducted in a laboratory. In such cases, the fluid velocity, v , is always larger and the core length is smaller than the actual field conditions. Therefore, the rate group, KL/v , may be sufficiently small so the mixing-by-capacitance effect is almost negligible. In the field, where L is many times greater and v is much smaller, the rate group becomes important and significantly affects the mixing process. Hence, to apply the laboratory miscible displacement test results to field-case mixing requires the inclusion of both the convective dispersion mechanism and the capacitance mechanism.

The Coats and Smith⁶ model is a more accurate model to use in cases where the existence of a stagnant volume is important because it takes into account the mass transfer from the dead-end pore space by the diffusion mechanism. Giesbrecht⁹ found that the Coats and Smith model worked very well in the case of miscible displacement tests conducted with a Golden Spike limestone core.

2.3.3 Other related work

Recently, Giesbrecht⁹ and Zhang¹⁸ have done miscible displacement tests in the laboratory with long and short cores to determine the dispersion coefficient.

Giesbrecht studied the relationship between several heterogeneity indicators and the mixing behaviour of a first-contact miscible process. In his work, where n-hexane and cyclohexane were used as the displacing and displaced fluids, respectively, he found, for various rock types, that :

- The recovery efficiency was inversely proportional to the flood velocity and that it showed an inverse logarithmic correlation with the convective dispersion coefficient for the Berea sandstone case.
- Displacement tests done with carbonate rocks yielded higher dispersion coefficients than those obtained with sandstone rock.
- The more homogeneous the rock type, the greater the effect of convective dispersion on the recovery factor.
- There was no good correlation between permeability, porosity or mean pore throat size and the dispersion coefficient. However, it was suspected that there may be a correlation between core length and the convective dispersion coefficient.

Zhang¹⁸ in her study of the effect of the core length on miscible displacement has found that the length of the porous medium played an important role in the mixing process of miscible fluids. The longer the system, the earlier the break through occurred. The displacement was stable in a short bead-packed core but not in a long one. Both the longitudinal dispersion coefficient and the stable mixing zone length are dependent on core length. The dependence of the dispersion coefficient on core length was more pronounced as the fluid velocity became larger. The study also led

to a conclusion that the theoretical error function curve in the Brigham³ model may still be valid in the unstable displacement case provided that a properly defined longitudinal dispersion coefficient was used.

Another recent work on the determination of the dispersion coefficient from a laboratory miscible displacement test was conducted by Walsh and Withjack¹⁷. The investigation involved re-examining the applicability of Fickian dispersion theory to consolidated porous media. The results obtained from miscible displacement tests conducted in uni-directional, equal viscosity, equal density fluids in Berea sandstone revealed that :

- Fickian dispersion theory accurately modelled the effluent history in a Berea sandstone sample but failed to model the mixing-zone growth.
- Dispersion in Berea sandstone is Fickian-dominated in short cores and non-Fickian-dominated in long cores .
- In systems where permeability variation and length were small, the dispersion was likely Fickian-dominated.

The authors have found a new method which can predict mixing zone growth as well as elution history performance in Berea sandstone cores more accurately than the Fickian model.

2.4 Factors affecting the dispersion coefficient

In miscible displacement processes, the mixing rate is normally quantified as a dispersion coefficient . There are several factors affecting the dispersion coefficient which are determined by a laboratory miscible displacement test.

Brigham et al⁴, in a study of mixing during miscible displacement in porous media,

found that the dispersion coefficient was affected by :

- the length of travel
- viscosity ratio
- pack diameter
- flow velocity
- porous medium type

The investigation revealed that, for a stable displacement, the amount of mixing was proportional to the square root of the distance travelled and the dispersion coefficient seemed to be proportional to the viscosity ratio. When the viscosity ratio increased to greater than one, the displacement became unstable and evidence of viscous fingering was very obvious. The pack diameter also played an important role in the mixing process and greater mixing was found in a small-diameter pack.

There was no doubt that fluid flow velocity was one of the most important factors influencing the mixing process of a miscible displacement. At very low flow rates, the dispersion coefficient was directly proportional to the Fick diffusion coefficient:

$$\frac{K}{D} = \frac{1}{F\Phi}$$

where

K = dispersion coefficient (cm²/s)

D = Fick diffusion coefficient (cm²/s)

F = formation resistivity factor

and

Φ = fractional porosity

At high fluid flow rates, the dispersion coefficient and Fick diffusion coefficient were

correlated as follows :

$$\frac{K}{D} = \alpha \frac{rv^{1.2}}{D}$$

where

α = mixing coefficient which is a function of the viscosity ratio of the flowing fluids and the homogeneity of the porous medium

v = average pore velocity (cm/s)

and

r = average diameter of glass beads or sand grains (cm)

The fluid velocity also affected the length of the mixing zone. The zone length was found to increase at very low flow rates, as well as very high flow rates, and there was a velocity at which the zone length was a minimum.

It was also found that, at reservoir flow rates, the dispersion coefficient in sandstone was proportional to $(v)^{1.2}$ and the dispersion rate in this type of medium was higher than that in the glass bead packs.

3. STATEMENT OF THE PROBLEM

As natural resources become depleted due to high energy demand, the oil industry has sought more effective methods to recover oil from the ground. One of the most effective ways to enhance oil recovery is miscible flooding where a solvent is injected into the reservoir to drive the oil out by a first-contact mixing process. There are several factors affecting the mixing of fluids at the flood front such as the viscosity ratio, the difference in fluid density, the solvent injection rate and the heterogeneity and geometry of the porous medium. The literature review has showed that the miscible displacement of oil in porous media is governed mainly by diffusion and dispersion phenomena^{2,3,5,6,7,18,24}. Several laboratory experiments have been conducted to investigate microscopic dispersion phenomena in porous media using bead-packs and consolidated cores. Most of the studies concentrated on the effect of injection rate or type of medium on the dispersion coefficient which serves as a basic factor for the application of the laboratory results to solve field problems. There has been very little work done on the effect of core length on the dispersion coefficient, especially the longitudinal dispersion coefficient. Blackwell² has done a few miscible displacement tests in two different core lengths but the tests were conducted in unconsolidated cores and the investigation concentrated on the transverse dispersion coefficient. Since the core length and flood rate are the most important scaling factors for the application of laboratory experimental results to field cases, experiments should be done to carefully investigate these factors.

The purpose of this research is to investigate the effect of core length and injection rate on the longitudinal dispersion coefficient. The cores used are consolidated Berea sandstone cores with lengths from 122 cm to 242 cm. The miscible displacement tests are designed to be performed in such a way that a first-contact miscible flood is guaranteed in the flow rate range from 0.0469 cm³/s to 0.1866 cm³/s. Calculation of the longitudinal dispersion coefficient follows the Brigham⁵ model which is a

convective dispersion model based on the Fick diffusion equation.

It was expected that the experimental results would lead to a correlation between the dispersion coefficient and the core length as well as the solvent injection rate and that scaling of the results can be applied to field cases.

4. EXPERIMENTAL

The purpose of this research was to study the effect of solvent injection rate and core length on the dispersion coefficient. The study involved a series of miscible flood experiments using n-hexane as the resident oil and cyclohexane as the solvent. The displacement tests were conducted using three different core lengths and up to six different flow rates. In addition, a reflush test, where cyclohexane became the resident oil to be displaced by n-hexane, was performed immediately after the original displacement test.

4.1 Experimental apparatus

Figure 4.1 is a schematic diagram of the core-flooding apparatus which consists of the following :

- a double cylinder Ruska pump
- a set of stainless steel cylinders
- a core holder rotating unit
- pressure gauges at the upstream and the downstream end of the core
- a back pressure regulator
- a sample collection unit
- a refractometer.

A Ruska positive displacement pump was used to inject solvent into a consolidated core which acted as a porous medium. The pump had two 1000 cm³ capacity cylinders and could be operated to a maximum pressure of 6.90 MPa. Each cylinder had a discharge rate from 10 to 330 cm³/hr. The injection rate could be varied by changing the gear of the pump transmission system. The pump was connected to cylinders containing n-hexane and cyclohexane, respectively. By using a four-way valve, a specific solvent was selected for injection into the core.

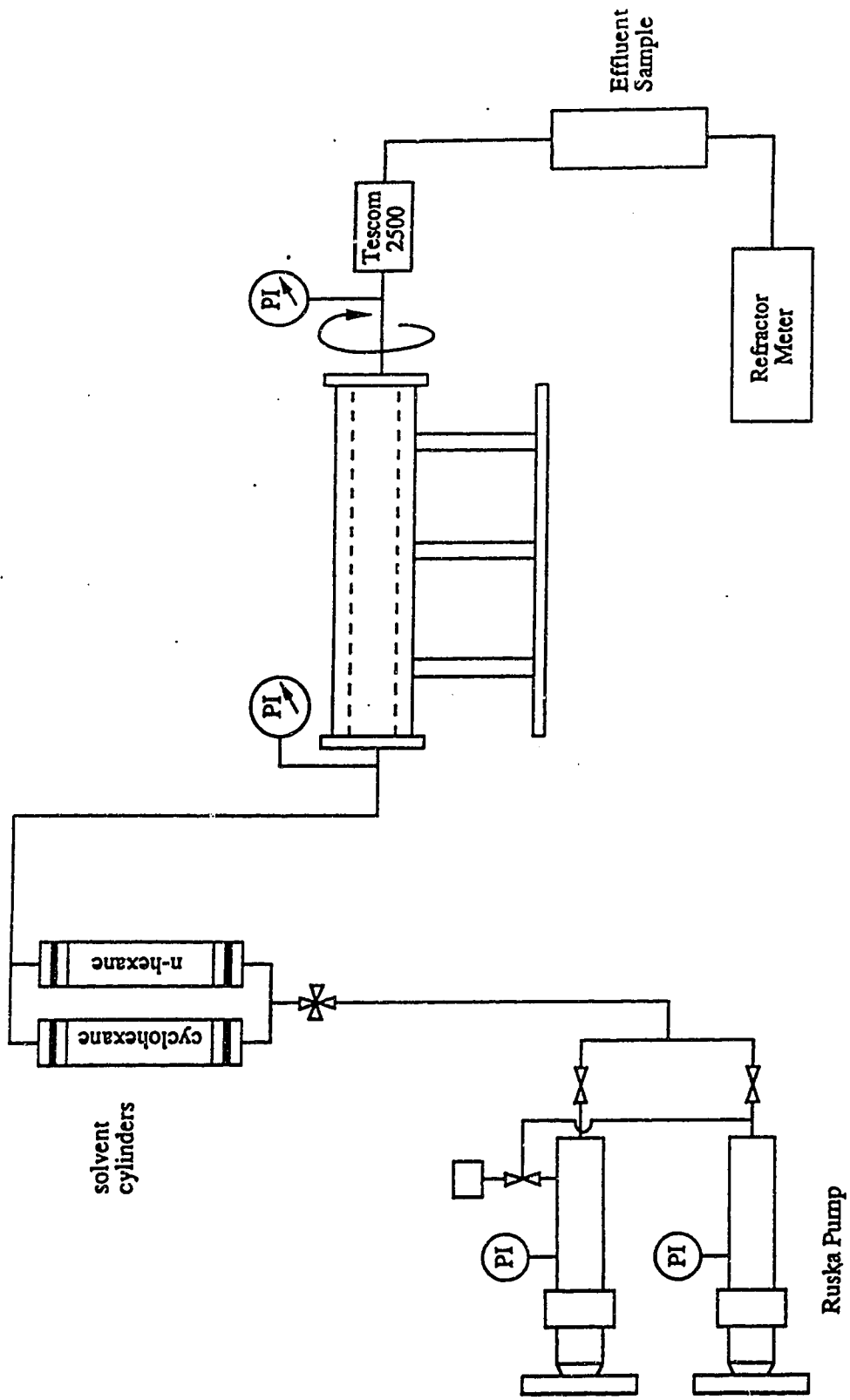


Figure 4.1 : Schematic diagram of the miscible flood apparatus

The coreholders were made of stainless steel with an internal diameter of 6.35 cm and lengths varying from 61 cm to 122 cm. The core holder was rotated at a rate of four revolution per hour to minimize the effect of gravity⁹. The pressure gauge at the upstream end of the core measured pressure from 0 MPa to 13.80 MPa \pm 0.01 MPa; the one at the downstream end measured up to 6.89 MPa \pm 0.01 MPa.

A Tescom 2500 back pressure regulator was used to maintain the downstream pressure at 2.07 MPa with an accuracy of \pm 0.35 MPa. Therefore, while the pressure gauge at downstream end of the core read 2.07 MPa, the actual downstream pressure may have been between 1.72 MPa and 2.42 MPa.

The refractometer used was an ABBE model A303 refractometer. The refractive index of distilled water ranged from 1.3310 to 1.3315, depending on room temperature.

4.2 Displacement test procedure

The displacement tests were conducted with n-hexane as the residual oil (displaced fluid) and cyclohexane as the solvent (displacing fluid) in a favourable mobility case. The properties of the fluids are listed in Table 1.

Table 1. Properties on the miscible component.

Component	Density (g/cm ³)	Refractive index	Viscosity at 25°C (cp)
n-hexane (C ₆ H ₁₄)	0.6627	1.3770	0.30
Cyclohexane (C ₆ H ₁₂)	0.7820	1.4235	0.88

A favourable mobility case is defined as the case in which the mobility ratio is less than one. The mobility ratio in this case is simply the ratio of the two fluids' viscosities since the relative permeability of the displaced fluid (n-hexane) and the displacing fluid (cyclohexane) are the same.

Each test was performed as follows :

- preparation of the consolidated core
- packing the core
- conducting permeability test
- core flood test.

4.2.1 Preparation of the core

Consolidated Berea sandstone cores having diameters of 4.45 cm to 5.10 cm and lengths of 61 cm and 122 cm were purchased from Cleveland Quarries. Each core was painted with two coats of phenolic material to prevent resident oil/solvent from leaking outwards and to prevent any absorption of molten metal into the pore space during packing.

4.2.2 Packing the core

The painted core was placed at the centre of the coreholder using a three-pin end cap which sealed one end of the coreholder. Melted Cerrobend alloy was poured into the annular space between the core and the inside wall of the coreholder¹⁰. The system was cooled over night. Cerrobend is an alloy made of tin, cadmium, bismuth and lead. Cerrobend was chosen as the packing material because it had a low melting point, 70 °C, and expanded slightly upon cooling to provide a tight seal around the core.

After the core had cooled, the two ends were machined so as to be flush with the coreholder and flanges. Two endcaps with o-ring type seals were then bolted to each end of the coreholder. The endcaps were designed in such a way that they would allow the core to rotate without twisting the inlet and outlet line. The ready packed core was then located on a rotating rack and the displacement test was conducted with the core rotating at four revolutions per hour. By rotating the core during the displacement of n-hexane by cyclohexane, the effect of gravity was almost eliminated⁹.

Since the available coreholders were of fixed length, 61 cm and 122 cm, respectively, the coreholders were connected together to provide the core length required for the experiment. In this case, a few layers of filter paper were placed between the connecting core faces to ensure capillary contact. The fluid was expected to flow continuously from one core to the other. Again, the ends of the two coreholders were equipped with o-ring seals to provide a gap-free connection and a completely sealed system.

4.2.3 Saturating the core

The core was saturated with n-hexane after a vacuum had been drawn to remove the residual water and air from the pore space. The drawing of a vacuum was conducted by connecting the core to a vacuum pump for at least 24 hours with the core in a horizontal position. The core was connected to the vacuum pump at one end and to a vacuum gauge at the other end. This allowed the quality of the vacuum to be monitored during the time the vacuum was being drawn.

Once the vacuum had been drawn, the coreholder was connected to a pressurized n-hexane-filled bomb and the n-hexane was allowed to flow into the core to fill up the pore space until the vacuum gauge read zero. The vacuum gauge was then removed

and the outlet line was connected. The inlet end of the core was removed from the bomb and connected to the Ruska pump. N-hexane was injected continuously into the core until the back pressure gauge read 2.07 MPa. This additional injection was done to compensate for the extra fluid that would enter the core if it were positioned vertically. At this point the core was completely saturated with n-hexane at 2.07 MPa. The amount of n-hexane injected was used to determine the porosity of the core using the bulk volume calculated from the core dimensions.

4.2.4 Permeability test

Once the pore volume was determined at 2.07 MPa back pressure, a required condition for all displacement tests, the back pressure was reduced to zero MPa to let the effluent discharge at atmospheric pressure. Fluid was injected into the core at various flow rates and the pressure difference between the inlet and outlet end of the core was recorded. The results were used to determine the permeability of the system. The back pressure was then reset at 2.07 MPa before starting the displacement test.

4.2.5 The displacement test

Once the core was ready for a test, the Ruska pump was set to inject cyclohexane into the core at a certain flow rate while the core was rotating at a rate of 4 revolutions per hour. The effluent was collected in a series of cylinders at the down-stream end of the core. Each sample contained approximately 0.05 PV. The refractive index of each sample was then measured and the process continued until 2 PV of cyclohexane was injected into the core. A computer program was used to interpret the results based on the refractive indexes.

At the completion of each displacement test, a reflush test was conducted. The test now had cyclohexane as the displaced fluid and n-hexane as the displacing fluid. It

should be noticed that the reflush test always started with a small amount of residual oil (n-hexane). This gave rise to an additional observation on the effect of unfavourable mobility on miscible displacement. The main purpose of the investigation was to determine the effect of injection rate and core length on miscible displacement for a favourable mobility system.

It was found that an amount of at least 4 PV of n-hexane had to be injected into the system to completely remove the cyclohexane and to make sure that the core was again saturated 100% with n-hexane.

The three core lengths used were 122 cm, 183 cm and 242 cm.

At each core length, six nominal injection rates were used :

- 169 cm³/hr (0.0469 cm³/s)
- 258 cm³/hr (0.0717 cm³/s)
- 288 cm³/hr (0.0800 cm³/s)
- 333 cm³/hr (0.0925 cm³/s)
- 505 cm³/hr (0.1403 cm³/s)
- 672 cm³/hr (0.1866 cm³/s)

These are set flow rates defined by the selection of an appropriate transmission gear on the Ruska pump. During the actual displacement test the flow rate values obtained by cumulative effluent volumes divided by the test durations yielded flow rates within $\pm 2\%$ of the set rates.

4.3 Calculation of the results

The purpose of this study is to investigate the effect of core length and injection rate on miscible displacement by establishing a correlation between the dispersion coefficient and core length / flow rate.

Appendix A contains the computer program EFFPLOT⁹ which was used to analyze the raw data of the displacement test as well as the reflush test results. The program has been modified slightly to work with the set of data obtained in this study.

The computer program utilized calibration data which were the refractive indexes of a series of mixtures of n-hexane and cyclohexane ranging from 100% n-hexane (0% cyclohexane) to 0% n-hexane (100% cyclohexane) by volume. The composition of these mixtures was varied at increments of 10%. The computer data file consisted of the refractive index values of effluent samples ranging from zero cumulative injection to 2 PV cumulative injection with an increment of 0.05 PV. The program EFFPLOT used a linear interpolation method to convert the refractive index to the concentration of cyclohexane and used the pore volume to calculate the modified volume used in the Brigham³ method :

$$\lambda = \frac{(V_i/V_p) - 1}{\sqrt{(V_i/V_p)}} \quad (4.3.1)$$

where

V_i is the cumulative volume injected (cm^3)

and

V_p is the total pore volume (cm^3)

This equation assumes that there was a conservation of volume throughout the test where the injected volume was exactly equal to the produced volume.

The computer program output consisted of pore volume, cyclohexane concentration and the lambda value for each sample data input (Appendix B).

The effective dispersion coefficient was calculated as:

$$K_e = vL \left(\frac{\lambda_{90} - \lambda_{10}}{3.625} \right)^2 \quad (4.3.2)$$

where

K_e = effective dispersion coefficient, (cm²/s)

v = pore velocity, (cm/s)

L = core length, (cm)

λ_{10} = lambda value at 10% cyclohexane

and

λ_{90} = lambda value at 90% cyclohexane

and calculated as follows:

$$\lambda_{10} = \frac{(V_{10}/V_p) - 1}{\sqrt{V_{10}/V_p}}$$

and

$$\lambda_{90} = \frac{(V_{90}/V_p) - 1}{\sqrt{V_{90}/V_p}}$$

The pore velocity, v , was defined as :

$$v = \frac{q}{\Phi A} \quad (4.3.3)$$

where

q = injection rate, (cm³/s)

Φ = core porosity

and

$$A = \text{core cross-sectional area (cm}^2 \text{)}$$

The last step of the EFFPLOT program calculated the area underneath the curve of cyclohexane versus cumulative pore volumes injected and output the recovery factor of the displacement test.

The recovery factor for n-hexane was calculated from:

$$R.F_n = 100 - \int_0^n C_s dC_s \quad (4.3.4)$$

where

$$n = 1, 1.5, 2 \text{ PV}$$

and

$$C_s = \text{concentration of solvent, (\% cyclohexane)}$$

The integral in Equation (2.3.4) was evaluated numerically using Simpson's 1/3 rule. The computer program output the recovery factor at 1 PV, 1.5 PV and 2 PV, respectively.

The resulting effective dispersion coefficients were plotted against core length and injection rate to establish a correlation between dispersion coefficient and core length and injection rate for the Berea sandstone core.

5. RESULTS AND DISCUSSION

The results of a laboratory investigation of the process of miscible displacement where the resident oil was displaced from a porous medium by a solvent which was miscible with the oil on first contact are presented in this thesis. The mixing process was mainly a microscopic one which resulted from velocity variation within the pore space of the medium, convective dispersion, and from molecular diffusion. Several research papers have pointed out that flood rate and core length affect the dispersion coefficient significantly. However, very little work has been done to investigate this matter. Blackwell¹ studied microscopic dispersion in unconsolidated cores and found that there were similar correlations between flow rate and the transverse dispersion coefficient as well as the longitudinal dispersion coefficient. Stalkup¹⁶ found that the following factors affected the dispersion coefficient:

- particle size distribution of the porous medium
- fluid saturation
- mobility ratio
- density ratio
- ratio of particle diameter to column diameter in the laboratory core
- particle shape.

The main purpose of this study is to quantify the effect of injection rate and core length on the effective dispersion coefficient. The investigation used n-hexane and cyclohexane to create a two component first contact miscible system. The choice of the two solvents satisfied the following requirements for a first-contact miscible flood:

- first-contact miscibility at standard conditions of temperature and pressure
- small difference in density
- a large difference in refractive index.

All tests were conducted with consolidated Berea sandstone cores to eliminate the effect of pore structure as a variable on miscible displacement. During the displacement process, the core was constantly rotated at a rate of 4 revolutions per hour to eliminate the effect of gravity segregation⁹. In this case the transverse dispersion was almost eliminated and the effective dispersion coefficient involved was mainly the longitudinal one. The use of n-hexane as the resident oil and cyclohexane as the solvent resulted in a mobility ratio of 0.34 assuming that the permeability of n-hexane and cyclohexane are of the same magnitude. This led to a favourable mobility condition where the effect of viscous fingering can be considered as negligible.

The reflush tests were done with cyclohexane as the resident oil and n-hexane as the displacing fluid. This provides a set of data for the unfavourable mobility case, where the mobility ratio equals 2.94.

The displacement of n-hexane by cyclohexane was conducted at six different injection rates and three different core lengths.

5.1 The effect of solvent injection rate

Figure 5.1.1 and Figure 5.1.2 present, respectively, typical concentration profile and lambda-function plots on probability paper for the favourable mobility case.

Figure 5.1.1 shows the length of the mixing zone is very short, as compared to the porous medium, and that the concentration curve has the typical "S" shape of the error function integral. A straight line, in Figure 5.1.2, between concentrations of 10% and 90% cyclohexane confirms that the application of Brigham's model to this case is valid.

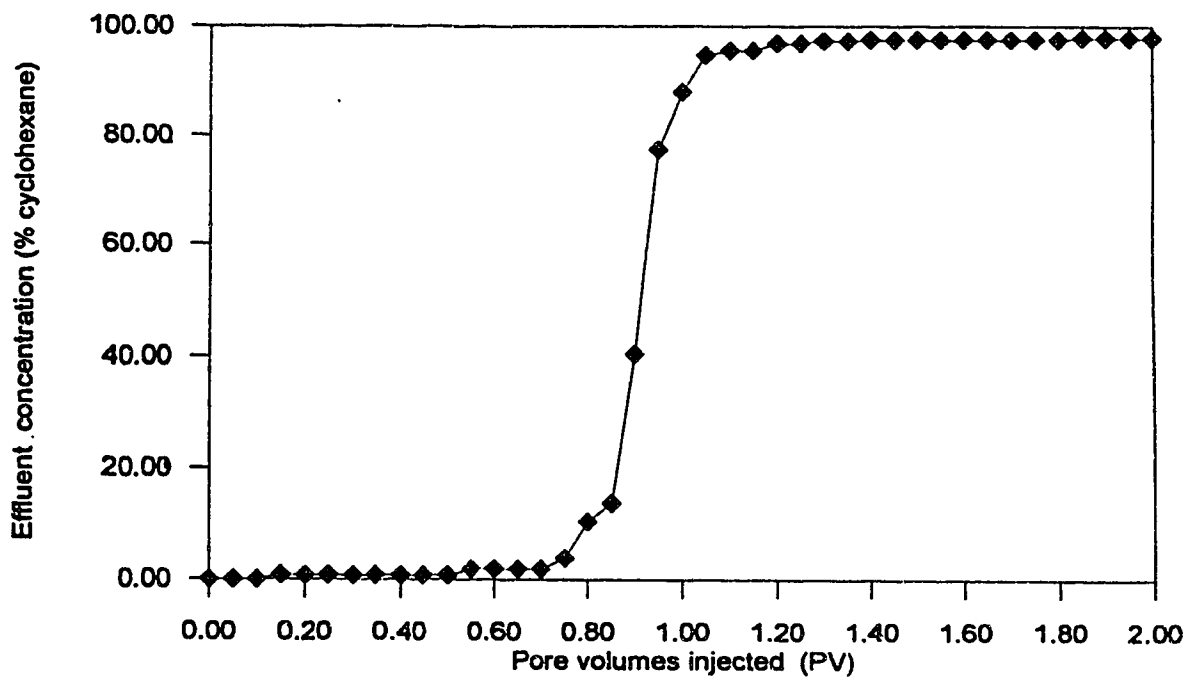


Figure 5.1.1 : A typical concentration profile

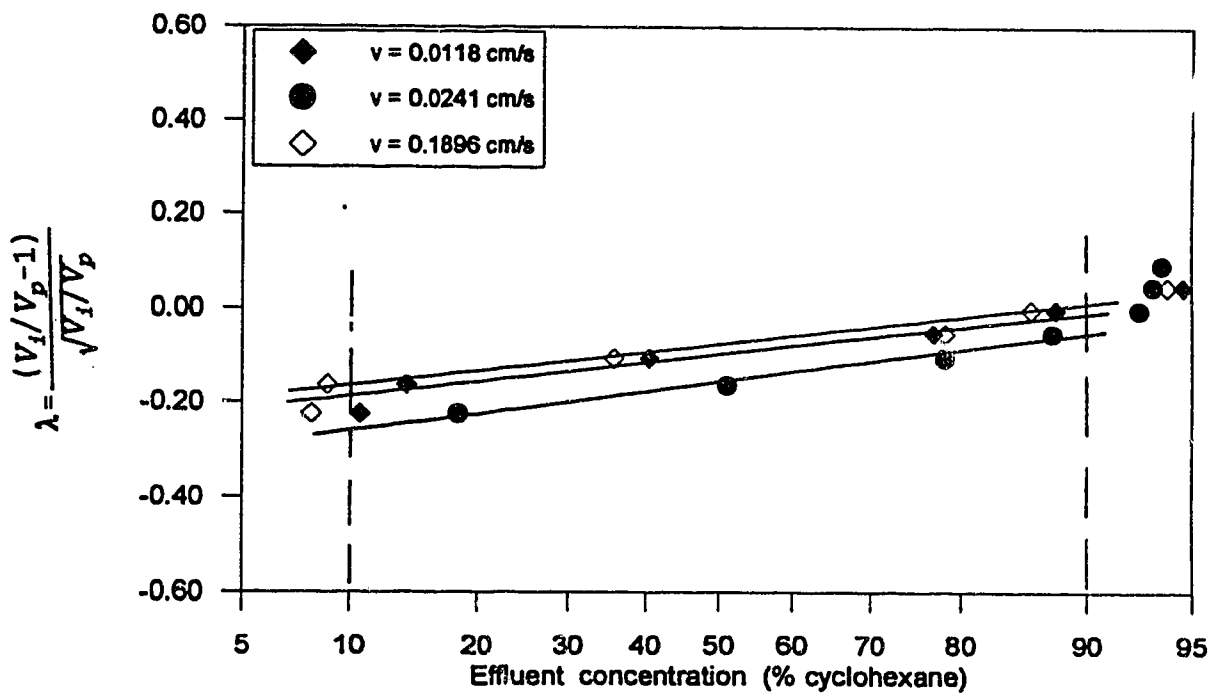


Figure 5.1.2 : Effluent concentration plotted on arithmetic probability paper for core length of 122 cm

The effective dispersion coefficient can be calculated from the formula:

$$K_e = vL \left(\frac{\lambda_{90} - \lambda_{10}}{3.625} \right)^2 \quad (2.3.1.8)$$

where

K_e = effective dispersion coefficient (cm^2/s)

v = pore velocity (cm/s)

L = core length (cm)

λ_{90} = Lambda function value at 90% cyclohexane

and

λ_{10} = Lambda function value at 10% cyclohexane

For a constant core length, the concentration profile is shifted to the right as the fluid velocity increases. This effect is very pronounced in the case of the 122 cm core (Figure 5.1.3) and somewhat less pronounced in the case of the 183 cm core (Figure 5.1.4). When the core length increases to 242 cm, the effect becomes reversed; that is, the concentration profile seems to shift to the left slightly (Figure 5.1.5). This may be explained by the effect of velocity on diffusion and dispersion in first-contact mixing. Normally, as the fluid velocity increases the mixing in the large pores becomes less complete. As a consequence, less soluble material is transported through them which delays breakthrough of the solvent. This results in a shift of the " S " curve to the right (see Figure 5.1.3). As the core increases in length, more time is available for mixing which results in more complete mixing. This results in earlier breakthrough of the solvent, which results in a shift of the " S " curve for the higher velocity to the left (see Figure 5.1.4). In the longest core (see Figure 5.1.5), the second effect is larger than the first. This results in the higher velocity curve falling to the left of the lower velocity curve, contrary to what was observed in the two shorter cores (see Figures 5.1.3 and 5.1.4).

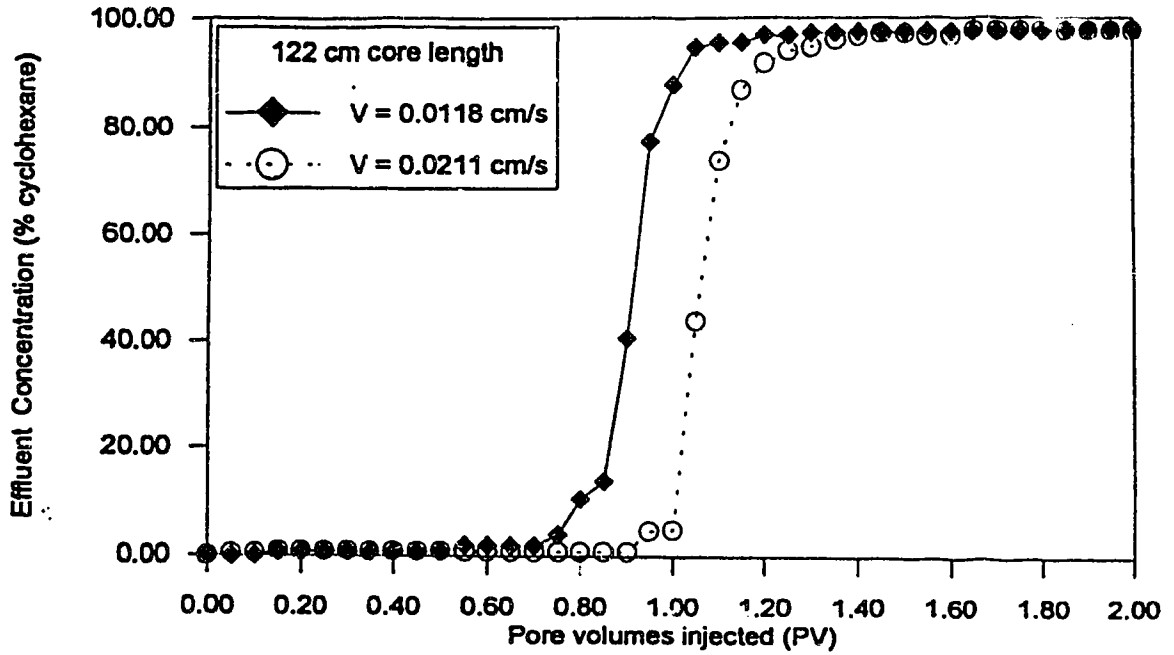


Figure 5.1.3 : Concentration profile for core length of 122 cm.

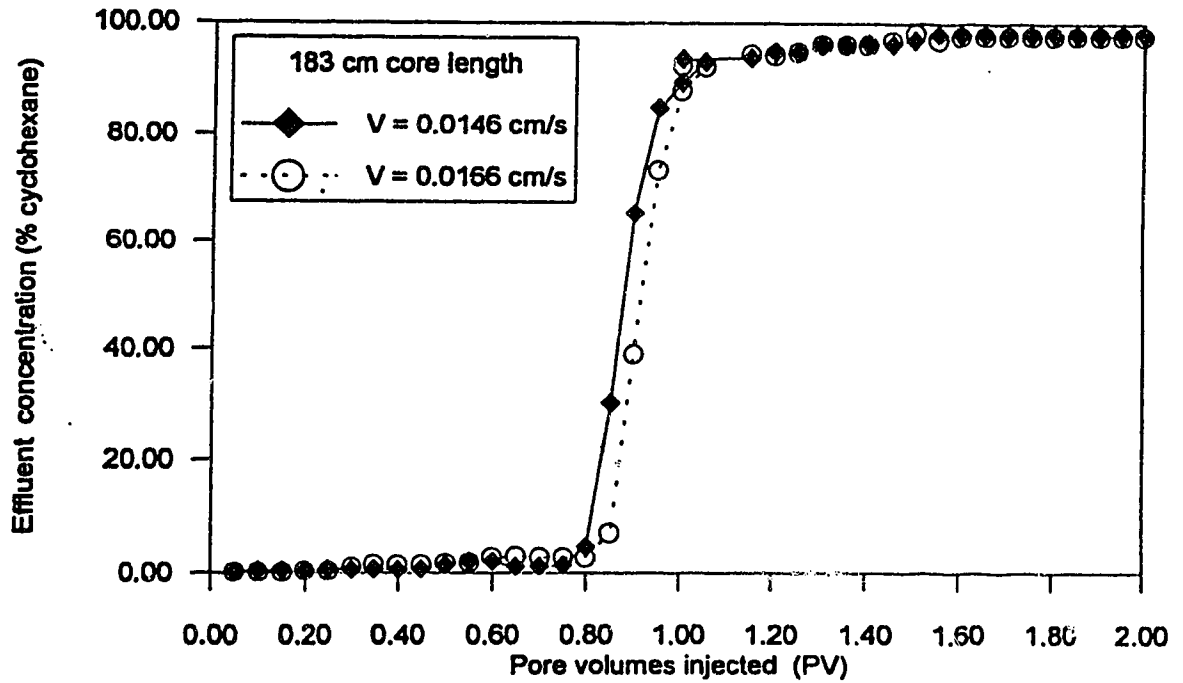


Figure 5.1.4 : Concentration profile for core length of 183 cm

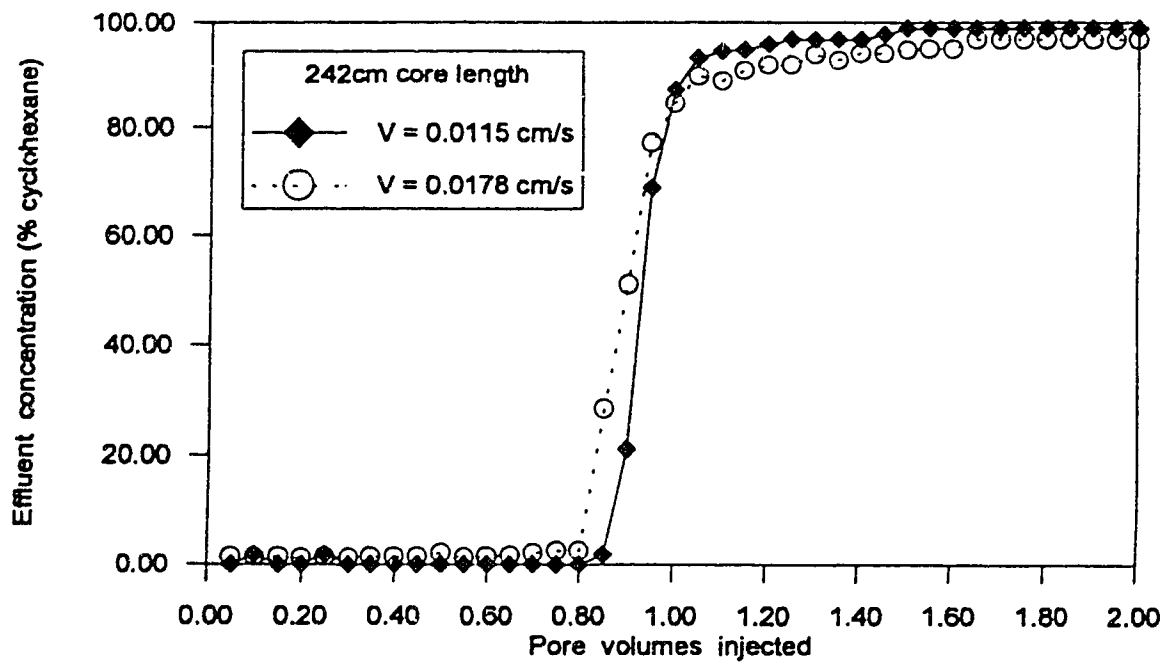


Figure 5.1.5 : Concentration profile for core length of 242 cm

The concentration profile provides data for the calculation of the dispersion coefficient which is the factor of most interest in this study. The effective dispersion coefficients are tabulated in Tables 2, 3 and 4 for core lengths of 122 cm, 183 cm and 242 cm, respectively.

Table.2 : Displacement test results for 122 cm core length

q (cm ³ /s)	v (cm/s)	K _d (cm ² /s)	R.F (%)		
			@ 1PV	@ 1.5PV	@ 2PV
0.0462	0.0118	0.00655	88.85	90.71	91.86
0.0732	0.0187	0.00917	88.30	91.26	92.00
0.0827	0.0211	0.00584	96.13	100	100
0.0944	0.0241	0.01266	83.54	85.29	85.38
0.1446	0.0368	0.00805	94.58	99.26	100
0.1896	0.0483	0.01513	87.58	89.10	90.07

Table.3 : Displacement test results for 183 cm core length

q (cm ³ /s)	v (cm/s)	K _e (cm ² /s)	R.F (%)		
			@ 1PV	@ 1.5PV	@ 2PV
0.0685	0.0146	0.00951	87.77	90.33	91.36
0.0781	0.0166	0.00838	86.03	88.29	89.43
0.0916	0.0195	0.01068	84.31	86.09	86.60
0.1377	0.0293	0.02765	86.31	89.53	91.09
0.1843	0.0391	0.04770	84.50	86.31	87.02

Table.4 : Displacement test results for 242 cm core length

q (cm ³ /s)	v (cm/s)	K _e (cm ² /s)	R.F (%)		
			@ 1PV	@1.5PV	@ 2PV
0.0472	0.0115	0.00553	92.93	95.08	95.62
0.0732	0.0178	0.00917	88.55	92.62	94.37
0.0791	0.0192	0.00993	86.23	88.80	91.26
0.0909	0.0221	0.01254	87.05	89.96	92.43
0.1390	0.0338	0.04610	87.01	92.28	93.24
0.1896	0.0461	0.08226	84.41	87.61	88.71

The resulting dispersion coefficients are plotted in Figure 5.1.6 as a function of flow velocity (pore velocity). It is observed that the dispersion coefficient increases with increasing velocity. The effect is minor in the short core (122 cm core length) and becomes more and more significant as the core length increases to 183 cm then to 242 cm. The three curves converge at a flow velocity of 0.018 cm/s and a dispersion coefficient of approximately 0.008 cm²/s. The dispersion coefficient seems to stay almost constant at flow velocities of 0.018 cm/s or lower. This characteristic is expected because at low flow rates the molecular diffusion dominates longitudinal mixing and the dispersion coefficient is independent of flow rate. Both Brigham et al.⁴ and Blackwell et al.² found similar relationships for the dispersion coefficient at low flow rates when they did their work with glass bead packs. They proposed an equation for the dispersion coefficient for the low flow rate case as :

$$\frac{K}{D} = \frac{1}{F\Phi} \quad (5.1.1)$$

where

K = dispersion coefficient (cm²/s)

D = Fick diffusion coefficient (cm²/s)

F = formation resistivity factor

and

Φ = fractional porosity

The term 1/FΦ is normally varied between 0.2 to 0.7 depending on the lithology of the porous medium. However, in this study FΦ and D are constant, indicating that K should be constant which is consistent with the results in this study.

At high flow rates, convective dispersion dominates longitudinal mixing and the dispersion coefficient becomes dependent on flow rate. Again Brigham et al.⁴

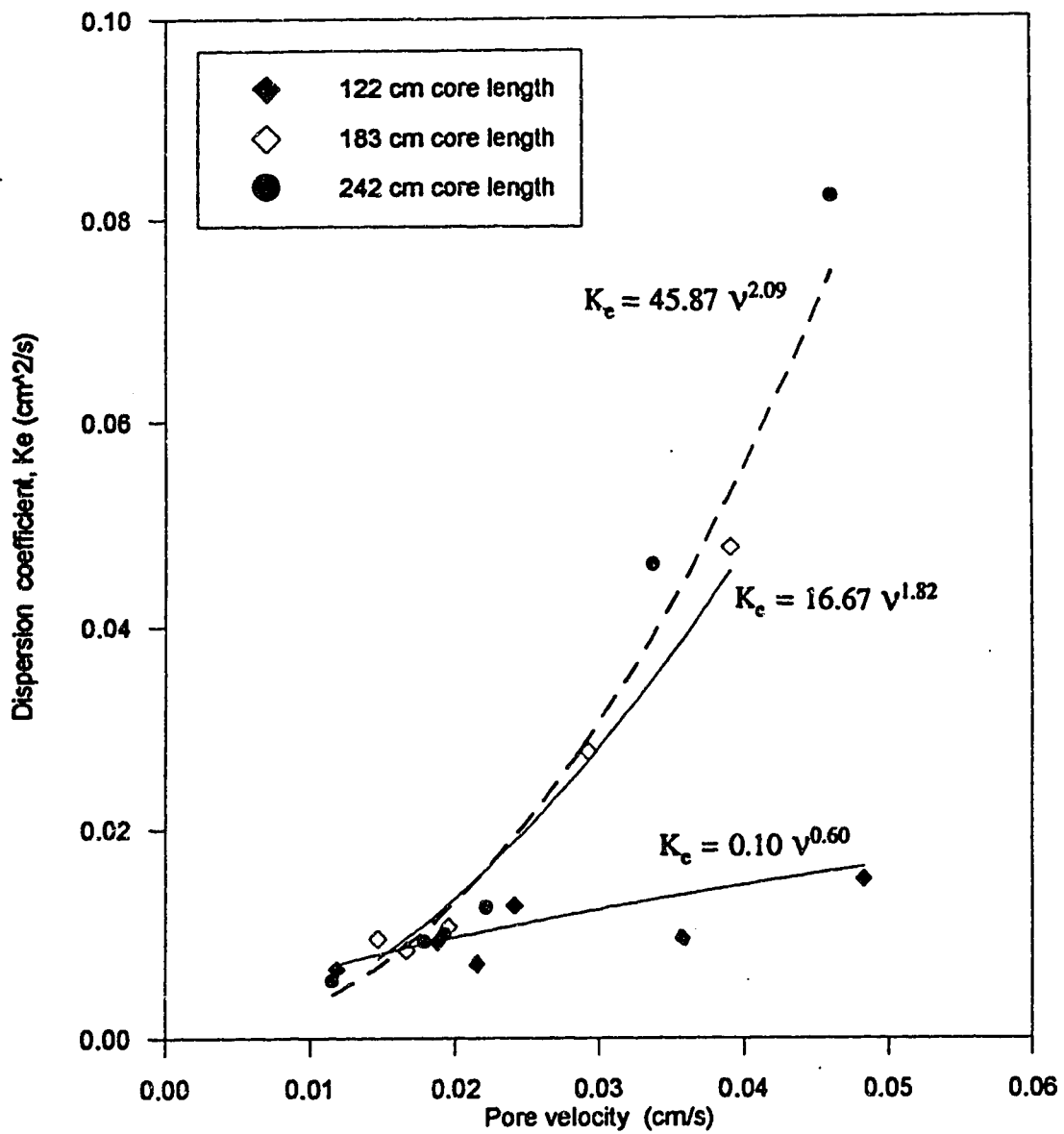


Figure 5.1.6 : The effect of fluid velocity on the dispersion coefficient

suggested the following relationship:

$$\frac{K}{D} = \alpha \left(\frac{rv}{D} \right)^{1.2} \quad (5.1.2)$$

where

K and D are defined as above

α = mixing coefficient

r = average radius of glass beads or sand grains (cm)

and

v = average pore velocity (cm/s)

The exponent value was experimentally determined to be 1.19 for Berea sandstone⁴. Blackwell et al.² found this value to be 1.17 while conducting experiments with sandstone cores.

Since this thesis is concerned with the effect of flow rate on the dispersion coefficient, one type of core is used (Berea sandstone) for all experiments. Hence, the Brigham equation applied to this case can be rewritten as:

$$K = B^m \quad (5.1.3)$$

where

B = a constant accounting for D, α and r

v = pore velocity (cm/s)

and

m = value of the exponent for this case.

Also from Figure 5.1.6, a plot of dispersion coefficient versus pore velocity for three

different cores, it is observed that, for velocities less than 0.02 cm/s, the dispersion coefficient seems to be independent of core length. As the velocity increases the dispersion coefficient becomes dependent on core length as well as velocity. For the core having a length of 122 cm, there appears to be a minimum in the dispersion coefficient versus pore velocity plot at 0.0211 cm/s and then again at 0.0368 cm/s. Replicate experiments performed at two flow rates, 0.0211 cm/s and 0.0368 cm/s, yielded no change in the magnitude of the dispersion coefficient. Consequently, it is thought that the minimum in the curve is not due to experimental error. Rather, it is thought to be due to interaction between length and velocity effects on the dispersion coefficient.

Curve fitting the data in Figure 5.1.6 yields values of m in Equation (5.1.3) of 1.82 and 2.09 for core lengths of 183 cm and 242 cm, respectively. For the 122 cm core the value of the exponent, m , is 0.47 if curve fitting is done with all data points and m is equal to 0.60 if the two minimum points are excluded from the curve fitting .

For cores having lengths of 183 cm and 242 cm, the dispersion coefficient is a relatively strong function of velocity , v , while for the core having a length of 122 cm, it is a relatively weak function of v .

5.2 The effect of core length

Laboratory miscible displacement studies normally take the core length as one of the most important factors to decide on what model should be used for interpreting effluent concentrations. Normally the diffusion equation is used to describe the displacement :

$$K_L \left(\frac{\partial^2 C}{\partial x^2} \right) - v \left(\frac{\partial C}{\partial x} \right) = \left(\frac{\partial C}{\partial t} \right) \quad (2.3.1.1)$$

The solution to this equation varies in form depending on the boundary conditions. In miscible displacements in short cores, where the mixed-zone length is almost equal to the length of the porous medium, the effect of the boundary condition is noticeable. The solution to Equation (2.3.1.1) has to be carefully chosen. Coats and Smith⁶ introduced the dimensionless dispersion term $\gamma = vL/K$, which served as a basis for choosing a solution to Equation (2.3.1.1). The smaller γ is, the greater the dispersion and the greater the boundary effect. The value of γ in this work is between 150 and 675, so the boundary condition doesn't affect which solution is chosen for Equation (2.3.1.1). When the value of γ is about 14 or less the boundary condition effects become very important³.

Figure 5.2.1 and Figure 5.2.2 display the concentration profiles for a low flow rate (0.0732 cm³/s) and a higher flow rate (0.1446 cm³/s) case, respectively. The correlation between the effective dispersion coefficient and the core length is presented in Figure 5.2.3. It is observed that, at the low flow rate, 0.0732 cm³/s, K_e is independent of core length. As the flow rate increases to higher values, 0.1446 cm³/s and 0.1896 cm³/s, the effective dispersion coefficient becomes dependent on core length.

Figure 5.2.4a is a plot of the dispersion coefficient versus pore velocity on a log-log scale. It is observed that the dispersion coefficient can be considered as independent of core length except for the case of the short core, the 122 cm core. A curve fit through the scattered data points for the 183 cm and 242 cm cores yields a curve with data points located within 10% of the average curve, which is reasonable, given the magnitude of the experimental error. This result agrees well with Blackwell's¹ results. In his study of microscopic dispersion phenomena done with

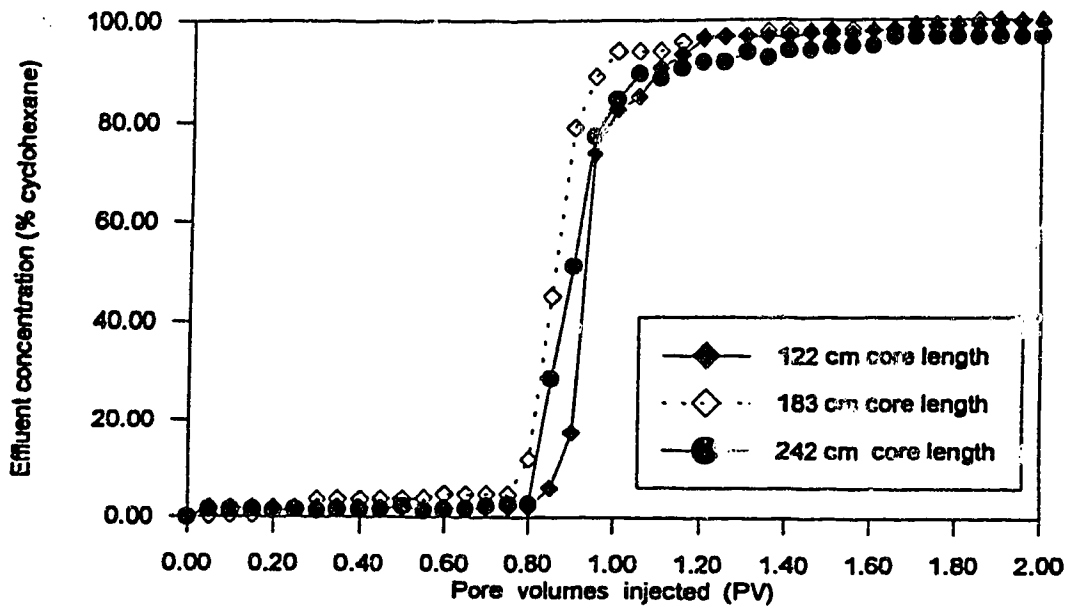


Figure 5.2.1 : Concentration profile at low flow rate (0.0732 cm³/s)

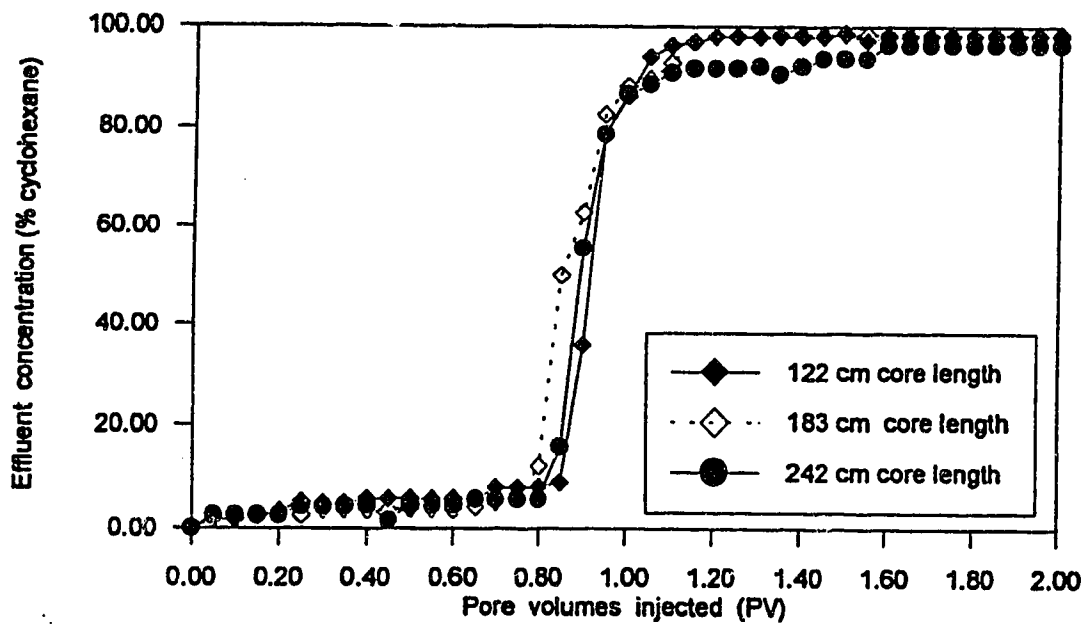


Figure 5.2.2 : Concentration profile at high flow rate (0.1146 cm³/s)

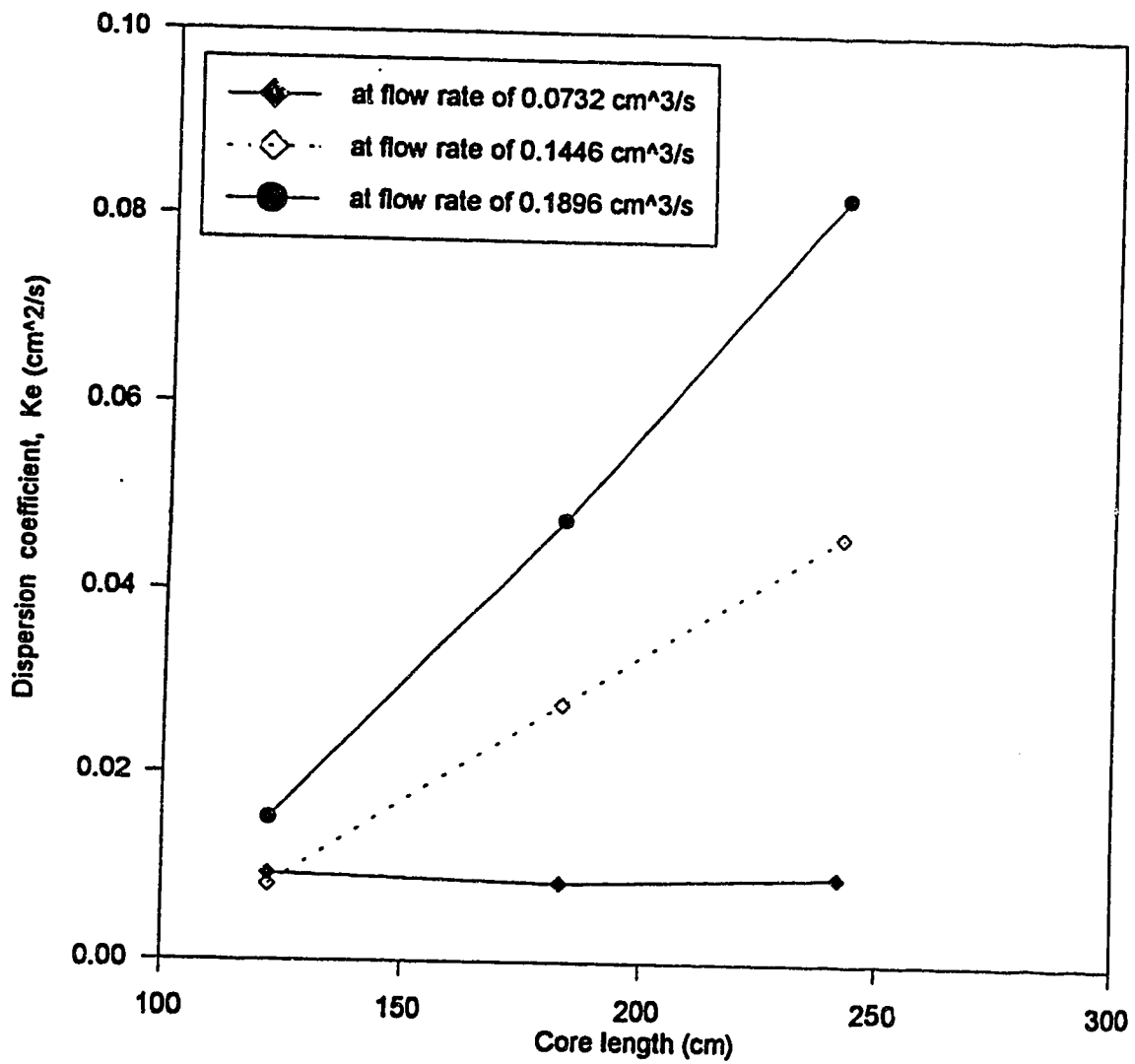


Figure 5.2.3: The effect of core length on the dispersion coefficient

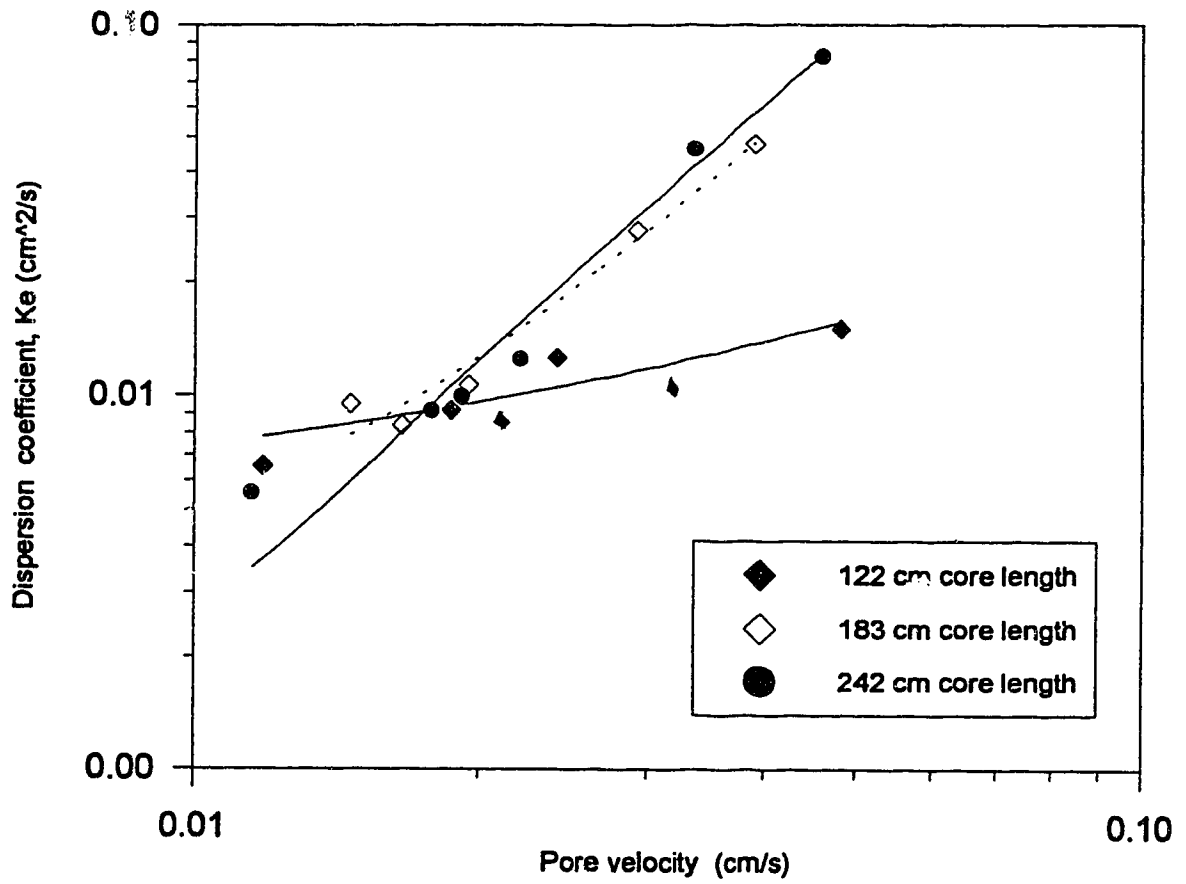


Figure 5.2.4a : The effect of fluid velocity on the dispersion coefficient

unconsolidated cores having lengths varying from 30.5 to 129.5 cm and volumetric flow rates from 0.0125 to 0.2500 cm^3/s , Blackwell found that the dispersion coefficients, transverse and longitudinal, are independent of core length. However, both this work and Blackwell's determined the dispersion coefficient using Fickian dispersion theory and this traditional method of analyzing laboratory dispersive flows may not accurately represent laboratory mixing phenomena. Walsh and Withjack¹⁷ have found that dispersion in Berea sandstone is not Fickian in some cases and that the dispersion mechanism is controlled by core length.

In order to determine whether the core length really affects the dispersion coefficient, the values of the exponent, m , from Equation (5.1.3) are plotted as a function of core length in Figure 5.2.4b. It is observed that the effect of core length on the dispersion coefficient is less pronounced as core length increases.

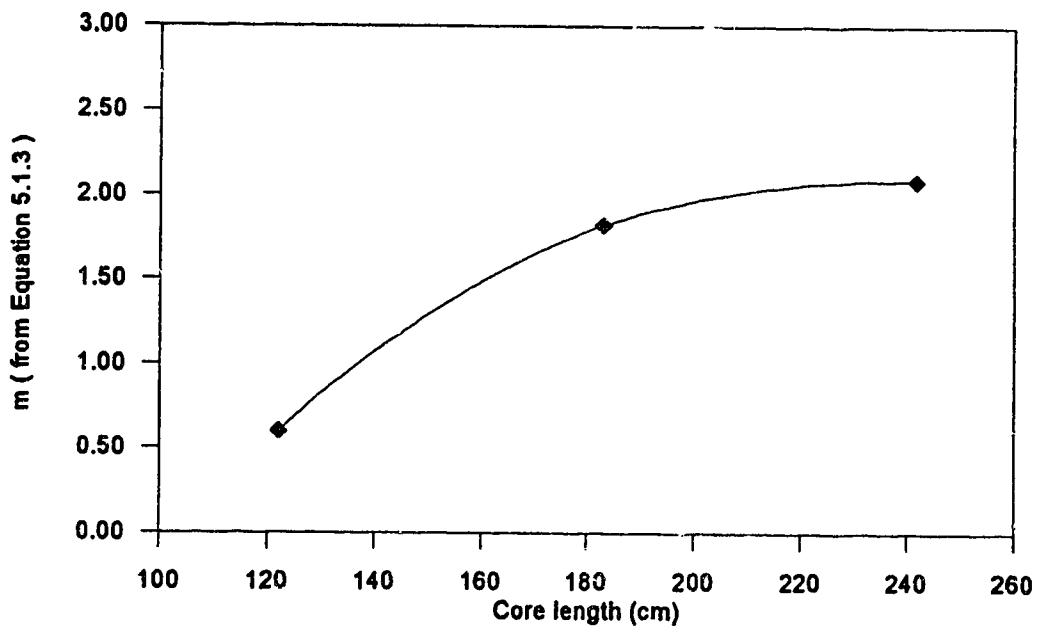


Figure 5.2.4b : The effect of core length on the dispersion coefficient

Since the dispersion coefficient is a function of flow rate and core length, it is difficult to depict the relationship between the dispersion coefficient and flow rate and core length at the same time. Figure 5.2.5 is a three-dimensional graph created to display the relationship between dispersion coefficient and flow rate and core length. The plot shows that both core length and velocity affect the dispersion coefficient and the effect is more pronounced as the core gets longer. The perturbations on the surface are thought to be due to experimental error.

Since the core length definitely affects the dispersion coefficient, it is important to study how much the core length affects the recovery factor which in turn determines the success of a displacement process. Figures 5.2.6, 5.2.7 and 5.2.8 show the recovery factor at 1 PV, 1.5 PV and 2 PV obtained at flow rates of $0.0732 \text{ cm}^3/\text{s}$, $0.1446 \text{ cm}^3/\text{s}$ and $0.1896 \text{ cm}^3/\text{s}$, respectively, for three core lengths. These figures show that the correlation between the recovery factor and core length is not simple. At constant flow rate, the recovery factor displays a minimum value at the intermediate core length of 183 cm .

Figure 5.2.9 shows the recovery factor obtained at 1 pore volume of production versus core length at three different flow rates. It is observed that the recovery factor increases as the flow rate decreases for core lengths of 183 cm and 242 cm. This is expected because, in a stable displacement, the effect of convective dispersion is proportional to the flow rate¹⁴. However, for the case of the 122 cm core, the recovery factor does not follow the same trend. In this case, the recovery factor at the intermediate flow rate is the highest one. This may be either an experimental error or a random combination of core length and flow rate at which the solvent works best to provide the maximum recovery.

Figure 5.2.10 is a three-dimensional plot of recovery factor versus core length and velocity at one pore volume of production. It is observed that the recovery factor

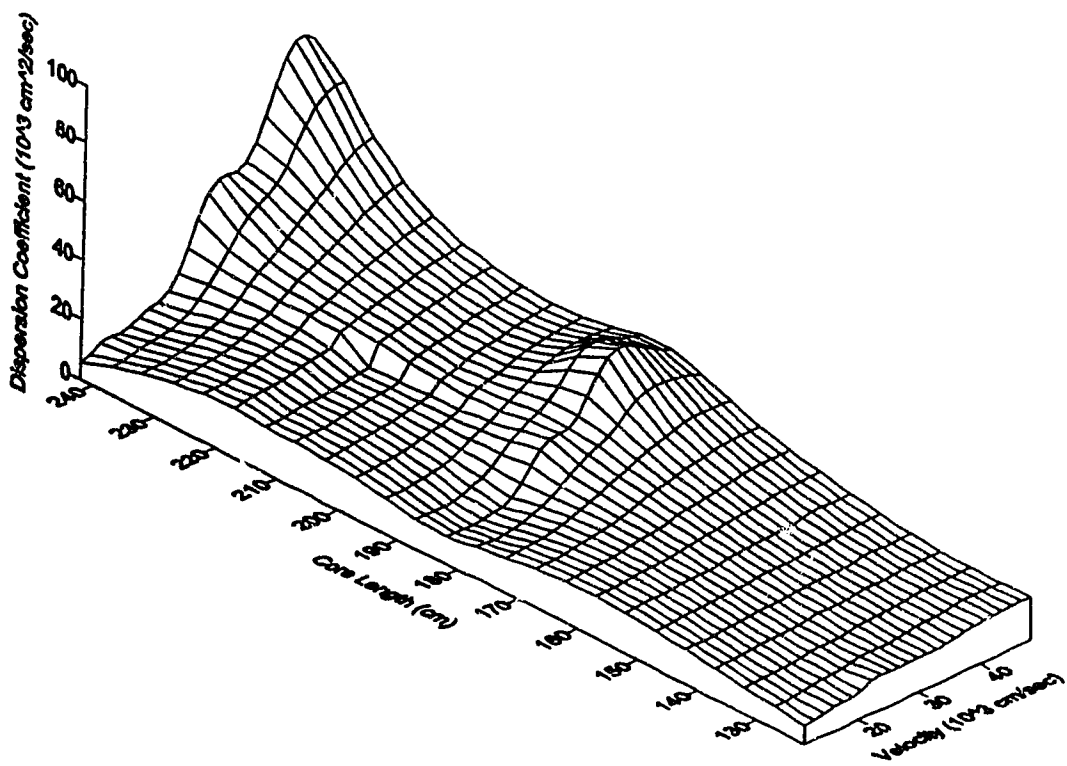


Figure 5.2.5 : The effect of velocity and core length on the dispersion coefficient

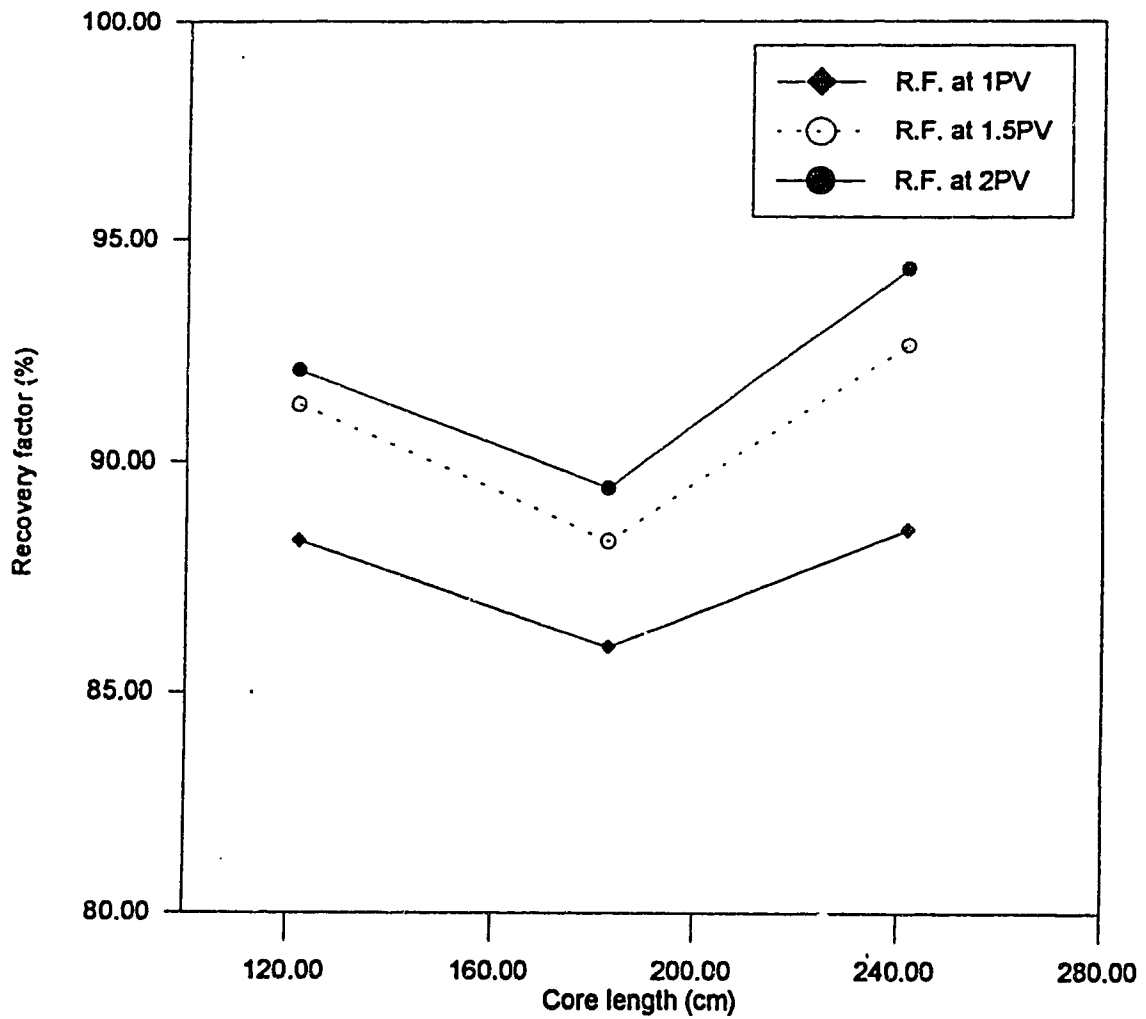


Figure 5.2.6 : The effect of core length on the recovery factor at a solvent injection rate of $0.0732 \text{ cm}^3/\text{s}$

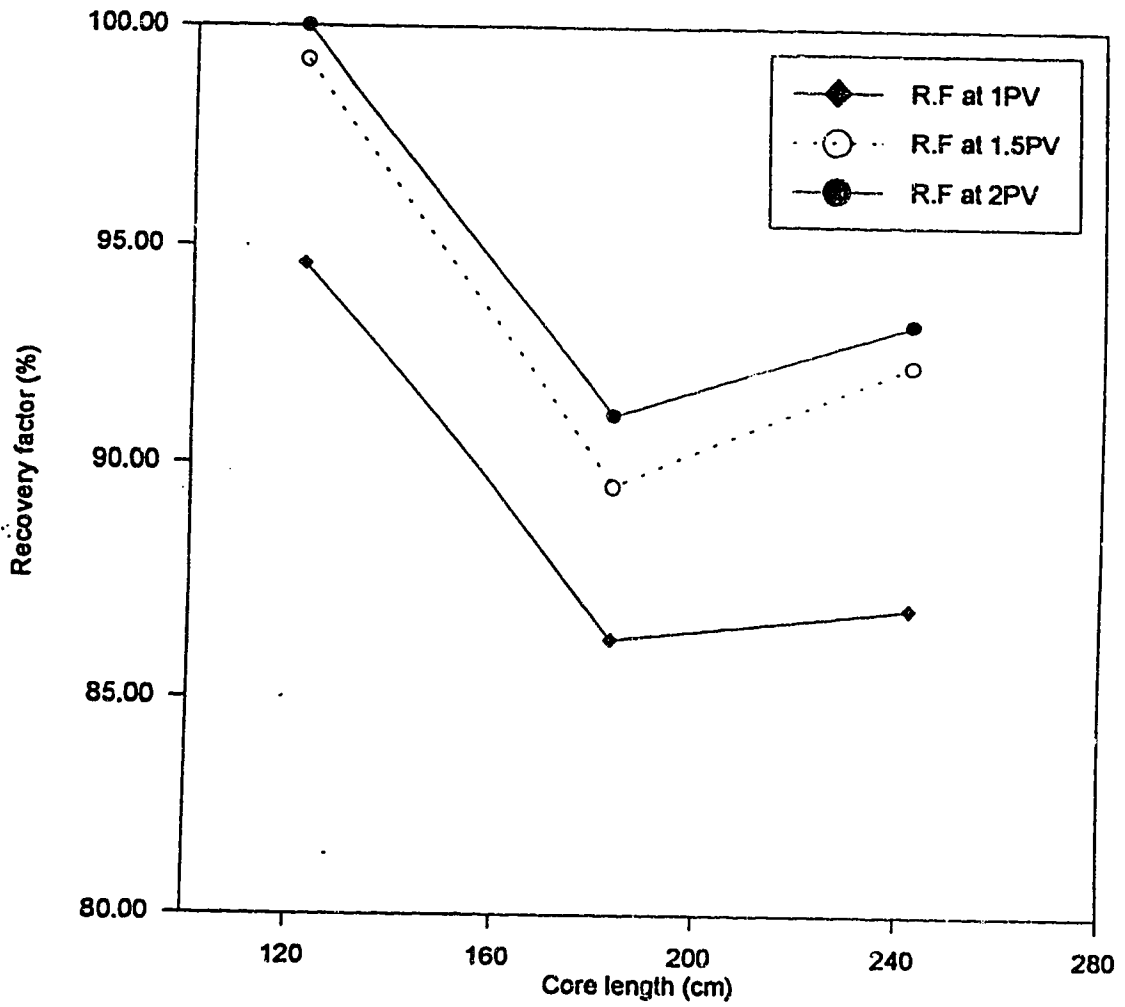


Figure 5.2.7 : The effect of core length on the recovery factor at a solvent injection rate of 0.1446 cm³/s

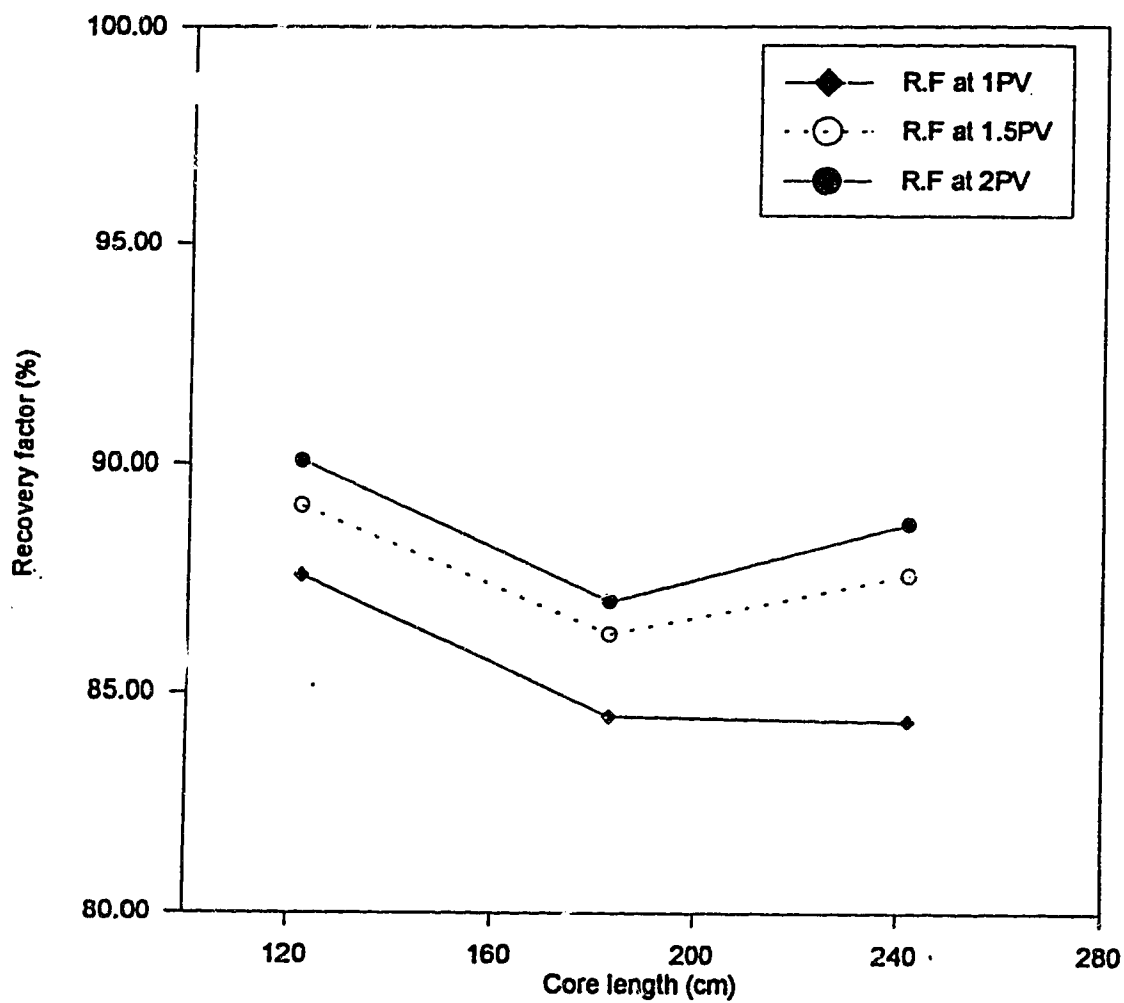


Figure 5.2.8 : The effect of core length on the recovery factor at a solvent injection rate of $0.1896 \text{ cm}^3/\text{s}$

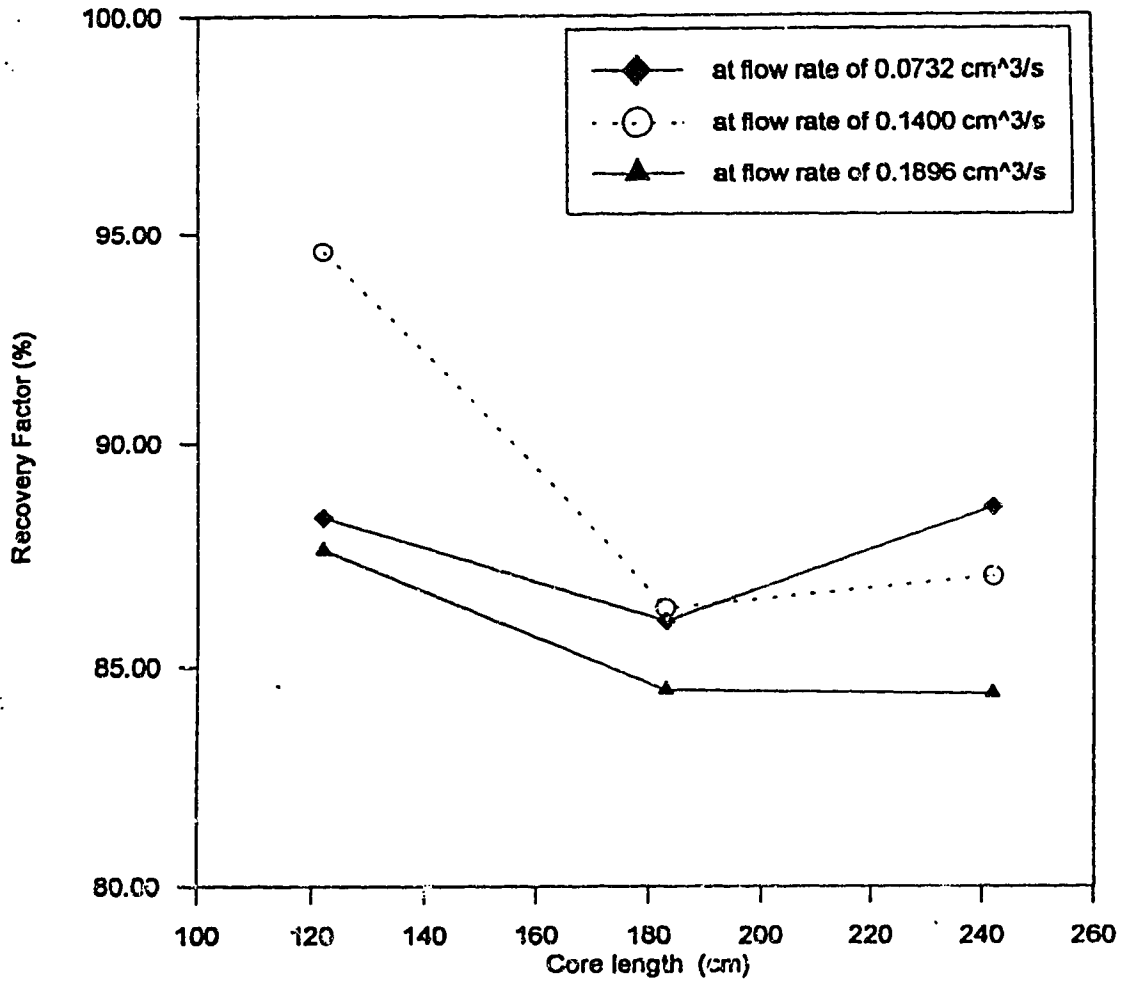


Figure 5.2.9 : The effect of flow rate on the recovery factor at 1 pore volume of production.

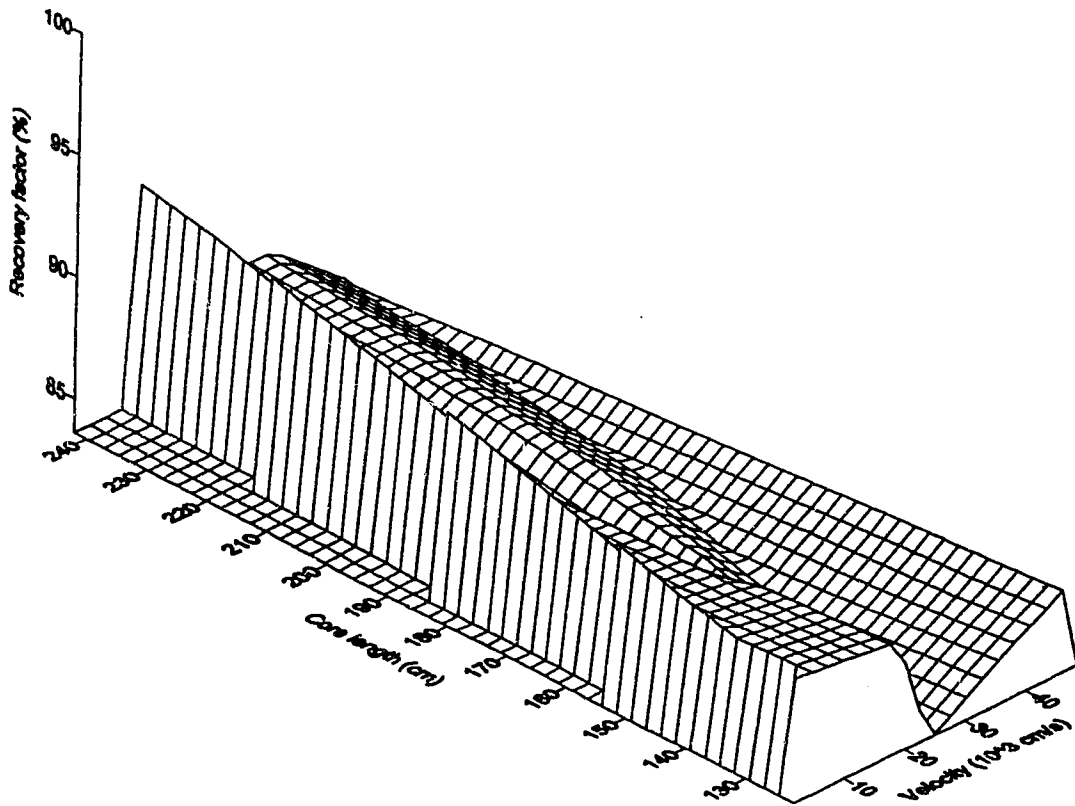


Figure 5.2.10 : The effect of core length and velocity on the recovery factor at 1 PV

increases with increasing core length for all flow rates. For short cores, the recovery factor improves at low velocities. The lowest recovery factor is observed at a velocity of 0.0025 cm/s for the short core case; this may be just another experimental error. Generally, the plot shows that the both core length and velocity affect the recovery factor.

5.3 Miscible displacement in unfavourable mobility case

Miscible displacement, where the displacing fluid has a lower viscosity than that of the displaced fluid, is unstable. In this case, the displacing fluid tends to finger through the medium and recovery becomes inefficient due to viscous fingering phenomena.

During the process of cleaning the cyclohexane-filled core which is called reflush, n-hexane was injected into the core continuously until the effluent is 100% n-hexane. The first 2 pore volumes of injection were carried out at exactly the same conditions as the previous n-hexane displacement test. This data was processed to study the effect of mobility ratio on miscible displacement.

The concentration profiles shown in Figure 5.3.1 confirm the existence of viscous fingering in the unfavourable mobility case. The concentration curve is not an "S" shaped curve as was the case for the favourable mobility case. This means that the solution to the diffusivity equation is no longer valid for miscible displacement under the effect of viscous fingering. Therefore, the method of calculating the effective dispersion coefficient from Equation (2.3.1.8) can not be used.

It is also observed that the effect of viscous fingering worsens as the flow rate increases. Figure 5.3.2 shows the concentration curves deviate from the normal "S" shape of an error function with many perturbations along the curve. This agrees

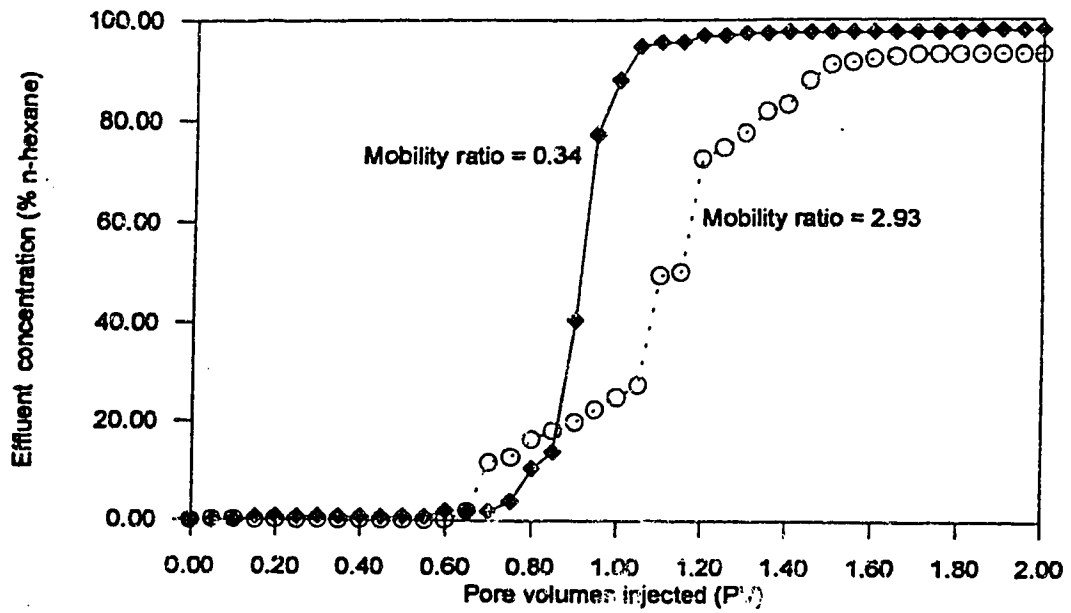


Figure 5.3.1 : The effect of mobility ratio on the concentration profile
 Core length = 122cm - Fluid velocity = 0.0118 cm/s

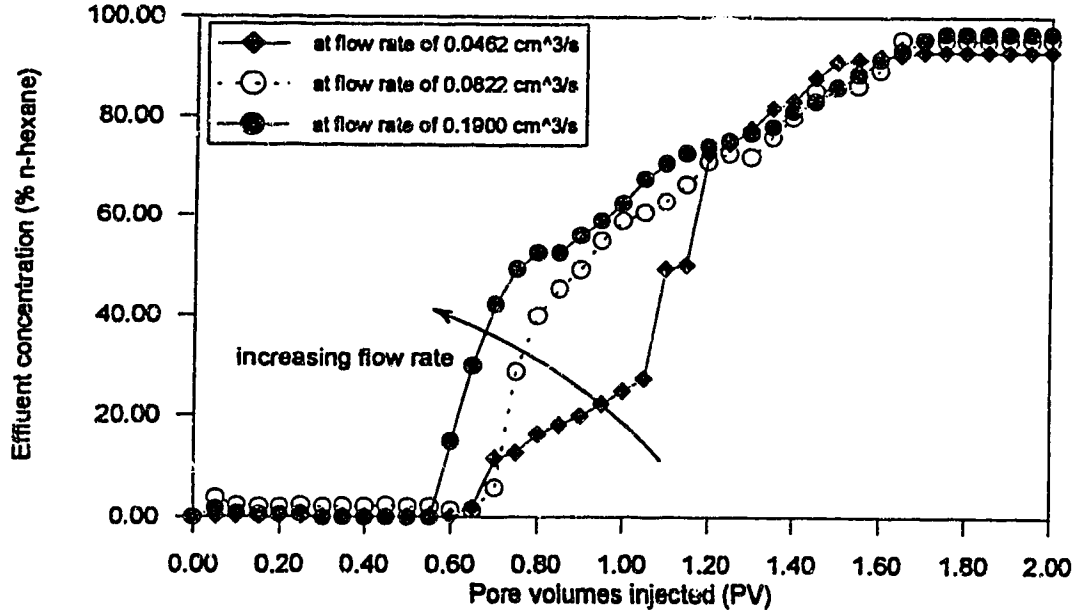


Figure 5.3.2 : The effect of flow rate on the concentration profile
 for an unfavourable mobility case.

well with what was found by Brigham³.

Since the reflush data does not follow the error-function solution, the effective dispersion coefficient is not calculated for comparison with the favourable case. If a comparison of the dispersion coefficient between the two cases, favourable and unfavourable mobility, is to be undertaken, then another model has to be tried.

The effluent concentration data for the unfavourable mobility case are reported in Appendix B.

5.4 Comparison of theoretical and experimental concentration profiles

One of the most effective methods of evaluating the efficiency of a miscible flood in the field is to conduct a similar miscible displacement test in the laboratory and use the experimental data to scale up to field conditions. However, such a scaling procedure is only possible if the laboratory experimental results match the theoretical prediction and a positive correlation between the factors studied can be established.

The laboratory experiments provide data in the form of effluent concentration versus pore volumes which can be used to construct experimental concentration profiles. The predicted concentration profiles are calculated using Brigham's model³ which is a convective dispersion model based entirely on Fickian miscible displacement theory. In the laboratory, the effluent concentration at the outlet of the core was measured and plotted as concentration versus pore volumes injected. The predicted concentration profiles, which are to be compared with the experimental concentration profiles, are calculated using Equation (2.3.1.5) as shown in Appendix C.

Before matching the laboratory displacement to Brigham's model, the effluent data were plotted as a lambda-function on probability paper to see whether a straight line

resulted because, if it does not, then the model does not apply. In addition, such a plot can be used to determine the value of the dimensionless dispersion coefficient, γ , from the slope of the line between effluent concentrations of 10% and 90%. This value γ is used to calculate the experimental dispersion coefficient as follows :

$$\gamma = \frac{vL}{K_e} \quad (5.4.1)$$

where

v = pore velocity (cm/s)

L = the length of the porous medium (cm)

and

K_e = the effective longitudinal dispersion coefficient (cm^2/s)

For each core length, the experimental dispersion coefficients were plotted as a function of solvent velocity. Curve fitting was done at each core length to yield the average dispersion coefficient for every combination of core length and velocity. The value of γ was then calculated from Equation 5.4.1 and the predicted concentration profile was calculated using Brigham's model³ as follows :

$$C' = \frac{1}{2} \operatorname{erfc} \left(\frac{1-I}{2\sqrt{I/\gamma}} \right) + \frac{1}{2\sqrt{\pi\gamma I}} e^{-\left(\frac{1-I}{2\sqrt{I/\gamma}}\right)^2} \quad (2.3.1.5)$$

where

C' = the effluent concentration

and

I = injected pore volumes (V_i/V_p)

Figure 5.4.1 is the concentration profile for the 122 cm core at a fluid velocity of 0.0118 cm/s. It is expected that the predicted concentration profile will match the experimental one. However, in this case, the predicted curve is displaced to the right of the experimental curve. In order to verify this lack of agreement, the experimental and the predicted lambda-functions were plotted in Figure 5.4.2 to determine the experimental and the predicted γ values, respectively. It is observed that both sets of data yield straight lines between effluent concentrations of 10% and 90% and that they are parallel to each other thus giving the same slope; hence, the experimental and the predicted values of γ are the same. This suggests that the method of calculating the predicted concentration profile is correct but that the model itself does not apply very well in the case of a consolidated core. It is thought that the poor match in this case, where Berea sandstone core was used, is caused by the effect of heterogeneity on the miscible displacement process.

Figures 5.4.3 and 5.4.4 display the experimental and predicted concentration profiles obtained at a low flow rate for core lengths of 183 cm and 242 cm, respectively. It is observed that the best match between the experimental curve and the predicted curve is obtained for the longest (242 cm) core. However, the match between the the experimental and the predicted curve is poorer for the intermediate length core (183 cm) than that obtained for either the shortest core (122 cm) or the longest core (242 cm).

Figures 5.4.5, 5.4.6 and 5.4.7 depict the experimental and predicted concentration profiles obtained at a high flow rate for three core lengths, 122 cm, 183 cm and

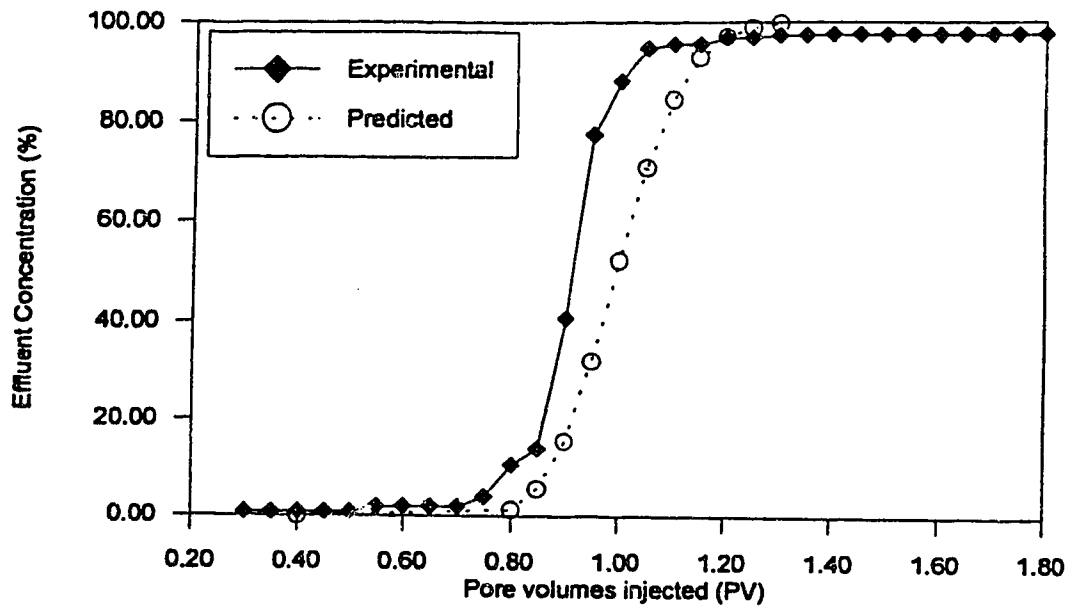


Figure 5.4.1 : Concentration profile - experimental versus predicted
Core length = 122cm - fluid velocity = 0.0118 cm/s

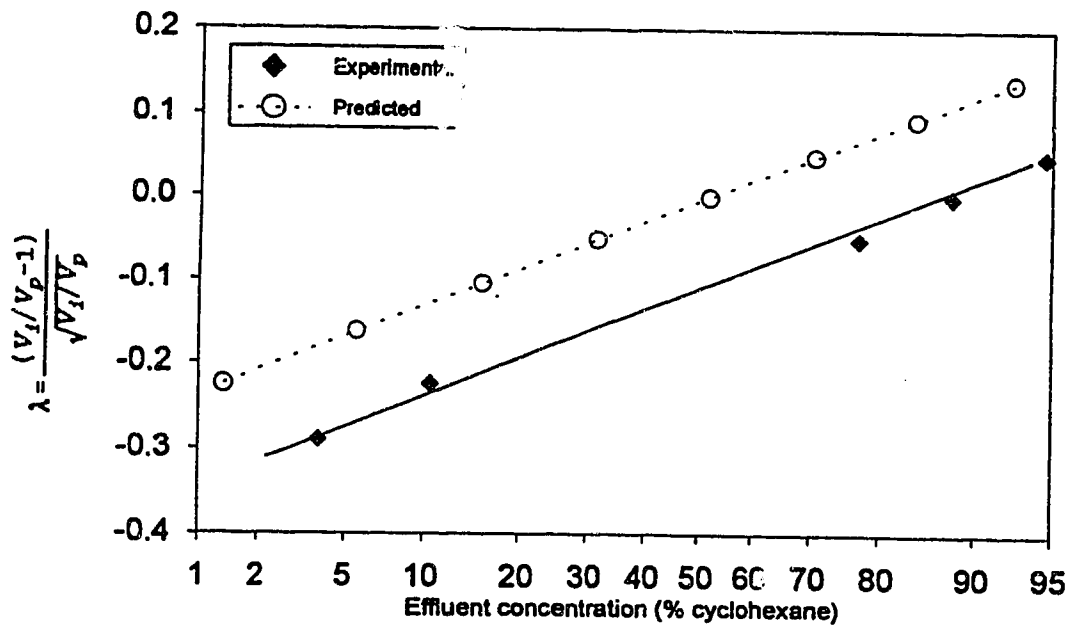


Figure 5.4.2 : Concentration plotted on arithmetic probability paper
Core length = 122 cm - fluid velocity = 0.0118 cm/s

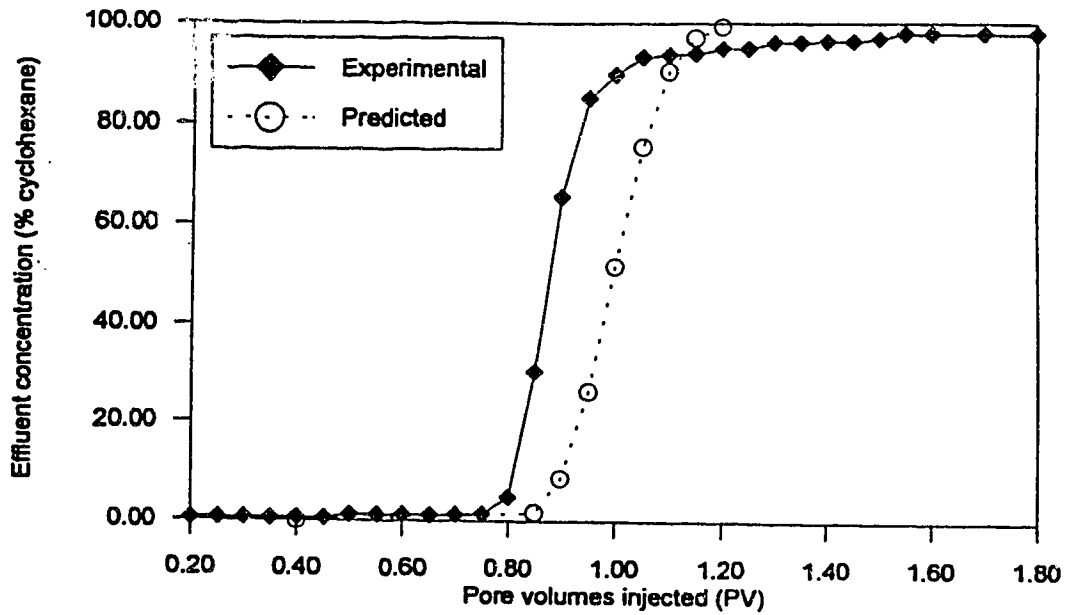


Figure 5.4.3 : Concentration profile - experimental versus predicted
Core length = 183 cm - fluid velocity = 0.0146 cm/s

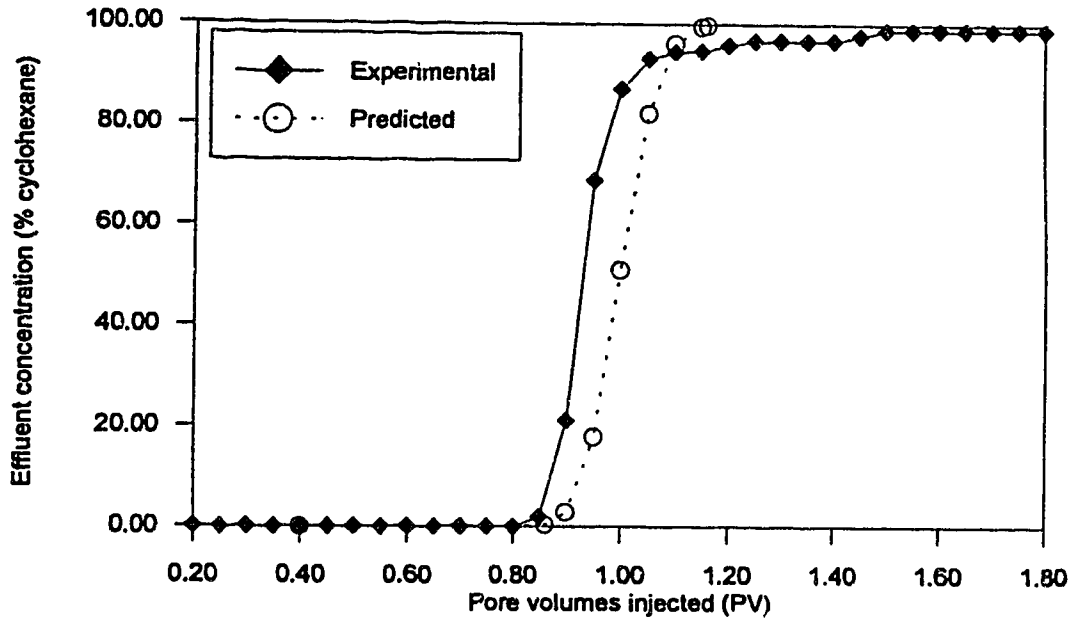


Figure 5.4.4 : Concentration profile - experimental versus predicted
Core length = 242 cm - fluid velocity = 0.0115 cm/s

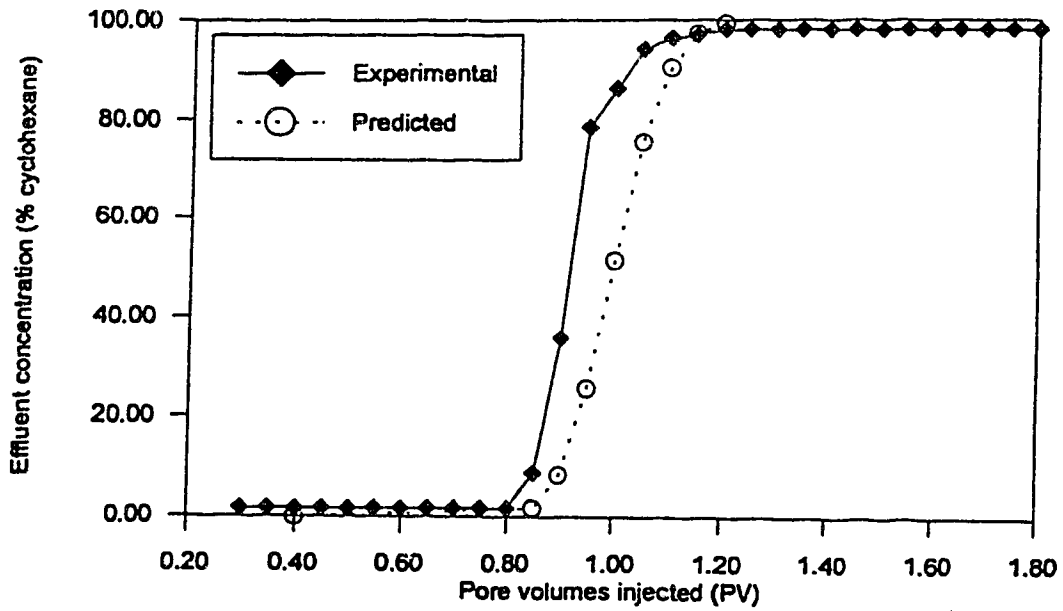


Figure 5.4.5 : Concentration profile - experimental versus predicted
Core length = 122cm - fluid velocity = 0.0483cm/s

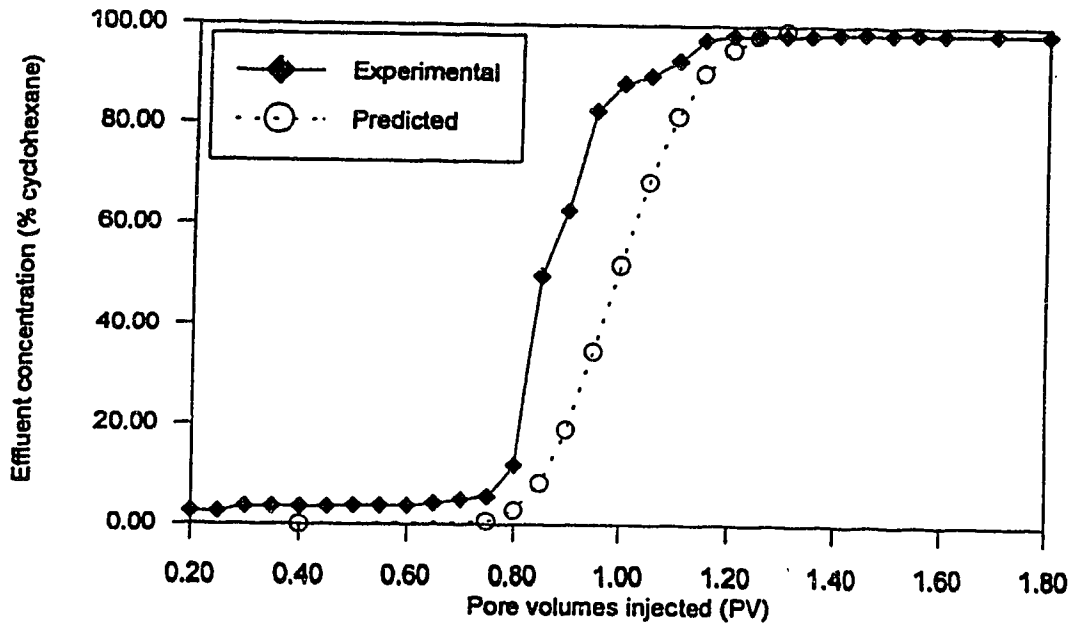


Figure 5.4.6 : Concentration profile - experimental versus predicted
Core length = 183 cm - fluid velocity = 0.0391 cm/s

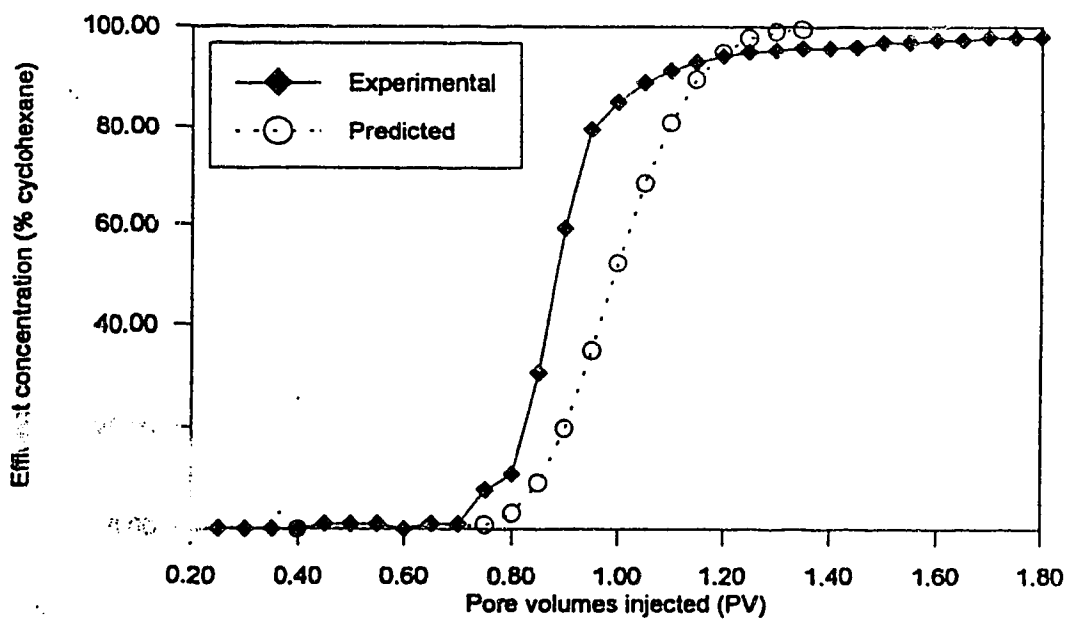


Figure 5.4.7 : Concentration profile - experimental versus predicted
 Core length = 242 cm - fluid velocity = 0.0461 cm/s

242 cm, respectively. It is observed that again the agreement between the experimental curves and the predicted curves is poor. Moreover, the poorest agreement between the experimental and the predicted curves was again obtained for the 183 cm core. This may be due to the way the 183 cm core was made. The 183 cm core was made by putting a 122 cm core and a 61 cm core together and an imperfect connection may have interrupted the continuity of the fluid flow. Hence, the experimental concentration profile for the 183 cm core may be anomalous.

The reason for the deviation of the predicted concentration profiles from the experimental ones is the inability of Brigham's model to predict miscible displacement in heterogeneous media.

In the laboratory experiments, there were errors in collecting the raw data such as core porosity, permeability and the measurements of the effluent concentration by refractive index. Since Berea sandstone cores were used for all the tests, the errors caused by errors in porosity and permeability were minimal if not negligible. The error caused by the reading of the refractive index has been minimized by careful calibration of the reading prior to each test and by creating a standard curve which was used for all tests.

It is suggested that the observed deviations between the experimental and the predicted profiles are likely due to the estimation of the dispersion coefficient using Brigham's model. While the shape of the experimental and the predicted concentration profiles match relatively well, it is observed that the mixing growth zone does not match as well. This is because the predicted data were generated using Fickian dispersion theory which can not take proper account of the effect of core heterogeneity on the dispersion process. Walsh and Withjack¹⁷ found that the mixing zone grows proportional to time, and not to square root of time, as dictated by Fickian theory.

They proposed a new model, which is based on the combined effects of spatially varying permeability and Fickian dispersion, which works much better in predicting the mixing zone growth as well as the elution history performance in Berea sandstone.

There is no doubt from this work, as well as other work ^{17,18}, that both core length and velocity affect the dispersion coefficient. As a consequence, it appears that analysis based on pure Fickian theory is incapable of adequately predicting the miscible displacement process in Berea sandstone cores.

CONCLUSIONS AND RECOMMENDATIONS

Experiments have been conducted with Berea sandstone cores to determine the effect of flow rate and core length on the dispersion coefficient. There were three core lengths under investigation : 122 cm, 183 cm and 242 cm . At each core length, the miscible displacement test was performed at six different flow rates with hexane as the displaced fluid and cyclohexane as the displacing fluid. The purpose of the study was to search for a relationship between the dispersion coefficient and core length and flow rate. The interpretation of the experimental results was based on displacement by dispersion which was based mainly on the Brigham model.

The result of this study leads to the following conclusions :

1. The dispersion coefficient depends on both core length and fluid velocity.
2. The dispersion coefficient increases with increasing velocity. The effect is minor in the short core, but becomes more significant in the longer cores.
3. The dispersion coefficient increases with increasing core length. As the velocity increases, the dispersion coefficient appears to become independent of length.
4. The parameter m (from Equation 5.1.4) increases with increasing core length.
5. The recovery factor passes through a minimum at the intermediate core length of 183 cm.

6. It was not possible, using the Brigham model, to generate concentration profiles for favourable mobility displacements which matched those obtained experimentally. While both measured and predicted profiles had essentially similar shapes, the predicted profiles were displaced to the right of the measured profiles, and the length of the transition region for the predicted profiles was longer than that of the measured profiles.
7. In the case of an unfavorable mobility ratio, the Brigham model did not work at all. This is consistent with what has been reported in the literature.

Recommendations

1. An attempt should be made to interpret the data using the non-Fickian dispersion theory suggested by Walsh and ~~W~~.
2. Repeated miscible displacement tests should be conducted with more heterogeneous cores to investigate the effect of heterogeneity on the dispersion coefficient.

REFERENCES

1. Blackwell, R.J. : " Laboratory Studies of Microscopic Dispersion Phenomena "; SPE Journal, Mar. 1962 (69).
2. Blackwell, R.J., Rayne, J.R. and Terry, W.M. : " Factors Influencing the Efficiency of Miscible Displacement "; Trans. AIME, Vol.217, 1959 (1).
3. Brigham, W.E. : " Mixing Equation in Short Laboratory Cores "; SPE Journal, Feb. 1974 (91).
4. Brigham, W.E., Reed, P.W. and Dew, J.N. : " Experiments on Mixing During Miscible Displacement in Porous Media "; SPE Journal, Mar . 1961 (1).
5. Carman, P.C. : " Permeability of Saturated Sands, Soils and Clays "; Jour. Agri. Sci. (1939), Vol.29 (262).
6. Coats, K.H. and Smith, B.D. : " Dead-End Pore Volume and Dispersion in Porous Media "; SPE Journal, Mar. 1964 (73).
7. Coskuner, G. and Bentsen, R.G. : " Effect of Length on Unstable Miscible Displacement "; JCPT, July-August 1989, Vol. 28, No. 4 (34).
8. Crane, F.E. and Gardner, G.H.F. : " Measurements of Transverse Dispersion in Granular Media "; Journal of Chemical Engineering Data (1961), Vol.6 (283).

9. Giesbrecht, D. : " An Analysis of Heterogeneity "; MSc Dissertation, University of Alberta, June 1990.
10. Farouq Ali, S. M. and Thomas, S. : " Development of chemical flooding process for light oil reservoirs in Alberta " ; Hydrocarbon Research Centre Contract 59-65002, April 1, 1982 - March 31, 1983.
11. Houseworth, J.E. : " Characterizing Permeability Heterogeneity in Core Samples From Standard Miscible Displacement Experiments "; SPE Formation Evaluation, June 1993 (112).
12. Jasti, J.K., Vaidya, R.N. and Fogler, U. : " Capacitance Effects in Porous Media ", SPE #16707, 62nd Annual Technical Conference and Exhibition of the Society of Petroleum Engineers, Dallas, Sept.27-30, 1987.
13. Perkins, T.K. and Johnston, O.C. : " A Review of Diffusion and Dispersion in Porous Media "; SPE Journal, Mar. 1963 (70).
14. Pozzi, A.L. and Blackwell, R.J. : " Design of Laboratory Models for Study of Miscible Displacement "; SPE Journal, Mar. 1963 (28).
15. Stalkup, F.I., Jr. : " Miscible Displacement "; Henry L Doherty Series, SPE, Monograph Vol. 8.
16. Van der Poel, C. : " Effect of Lateral Diffusivity on Miscible Displacement in Horizontal Reservoirs "; SPE Journal, Dec. 1963 (317).

17. Walsh, M.P. and Withjack, E.M.: " On Some Remarkable Observations Of Laboratory Dispersion Based On Computed Tomography (CT) "; Petroleum Society of CIM, CIM # 93-22, Annual Technical Conference, Calgary, May 9-12, 1993.

18. Zhang, X. : " The Effect of Core Length on the Instability of Miscible Displacement " ; MSc. Dissertation, University of Alberta, May 1993.

APPENDIX A

```

*****
*      PROGRAM EFFPLOT      *
*
* THIS PROGRAM APPLIES THE EXPERIMENTAL *
* CALIBRATION CURVE TO THE RAW EFFLUENT *
* CONCENTRATION DATA IN ORDER TO OBTAIN *
* A PROFILE OF CYCLOHEXANE CONCENTRATION *
* VS PORE VOLUMES OF CYCLOHEXANE INJECTED *
* THIS PROFILE IS THEN USED TO          *
* CALCULATE VALUES FOR HEXANE RECOVERY *
* AFTER INJECTION OF 1.0, 1.5 AND 2.0 PV *
* OF CYCLOHEXANE.              *
*****
C
  REAL A(41),B(11),C(41),D(41),PV(41),U(41),NUMB
  REAL AAREA1,AAREA2,AAREA3
  INTEGER I,J,K
C
  READ(5,*) (B(J),J=1,11)
  READ(5,*) (PV(I),I=1,41)
  READ(5,*) (A(I),I=1,41)
C
  DO 10 I=1,41
    IF (PV(I).GT.0.0) THEN
      U(I)=(PV(I)-1.0)/SQRT(PV(I))
    ENDIF
    DO 20 J=1,10
      IF (A(I).LE.B(J)) THEN
        C(I)=0.0
        D(I)=C(I)/100.0
        GO TO 10
      ELSEIF (A(I).GT.B(J).AND.A(I).LE.B(J+1)) THEN
        NUMB=A(I)-B(J)
        RATIO=NUMB/(B(J+1)-B(J))
        C(I)=RATIO*10.0+(10.0*(J-1))
        D(I)=C(I)/100.0
        GO TO 10
      ELSEIF (A(I).GT.B(11)) THEN
        C(I)=100.0
        D(I)=C(I)/100.0
        GO TO 10
      ELSE
        GO TO 20
      ENDIF
    20 CONTINUE
  10 CONTINUE

```

```

C
  WRITE(6,4)
  4 FORMAT('1','EFFLUENT CONCENTRATION PROFILE')
  WRITE(6,5)
  5 FORMAT('CORE 4ft - RATE=.....CM3/S (RUN #..)/')
  WRITE(6,6)
  6 FORMAT('PV',8X,'PERCENT C6H12',8X,'LAMBDA'/)
C
  DO 30 K=1,41
    PRINT 25, PV(K),C(K),U(K)
  30 CONTINUE
  25 FORMAT(' ',F6.3,6X,F8.3,7X,F6.3)
C
C*****
C* CALCULATE AREAS UNDER      *
C* EFFLUENT CONCENTRATION     *
C* PROFILES USING SIMPSON'S   *
C* 1/3 RULE                    *
C*****
C
C*****
C* AREA TO 1.0 PV *
C*****
C
  AAREA1=C(1)+4.0*C(2)+2.0*C(3)+4.0*C(4)+2.0*C(5)+4.0*C(6)
  +
  +2.0*C(7)+4.0*C(8)+2.0*C(9)+4.0*C(10)+2.0*C(11)+4.0*C(12)
  +   +2.0*C(13)+4.0*C(14)+2.0*C(15)+4.0*C(16)+2.0*C(17)
  +   +4.0*C(18)+2.0*C(19)+4.0*C(20)
C
  AFREA1=AAREA1+C(21)
C
C*****
C* AREA TO 1.5 PV *
C*****
C
  AAREA2=AAREA1+2.0*C(21)+4.0*C(22)+2.0*C(23)+4.0*C(24)
  +   +2.0*C(25)+4.0*C(26)+2.0*C(27)+4.0*C(28)
  +   +2.0*C(29)+4.0*C(30)
C
  AFREA2=AAREA2+C(31)
C
C*****
C* AREA TO 2.0 PV *
C*****
C

```

```

      AAREA3=AAREA2+2.0*C(31)+4.0*C(32)+2.0*C(33)+4.0*C(34)
      +   +2.0*C(35)+4.0*C(36)+2.0*C(37)+4.0*C(38)
      +   +2.0*C(39)+4.0*C(40)
C
      AFREA3=AAREA3+C(41)
C
C*****
C* CALCULATE % HEXANE RECOVERY *
C*****
C
      HEX1=100.0-(0.05/3.0*AFREA1)
      HEX2=150.0-(0.05/3.0*AFREA2)
      HEX3=200.0-(0.05/3.0*AFREA3)
C
      IF (HEX2 .GT. 100.000) HEX2=100.00
      IF (HEX3 .GT. 100.000) HEX3=100.00
C
      WRITE(6,7) HEX1
      7 FORMAT('HEXANE RECOVERY @ 1.0 PV = ',F8.3,'%')
      WRITE(6,8) HEX2
      8 FORMAT('HEXANE RECOVERY @ 1.5 PV = ',F8.3,'%')
      WRITE(6,9) HEX3
      9 FORMAT('HEXANE RECOVERY @ 2.0 PV = ',F8.3,'%')
      STOP
      END

```

APPENDIX B

1. Standard concentration curve

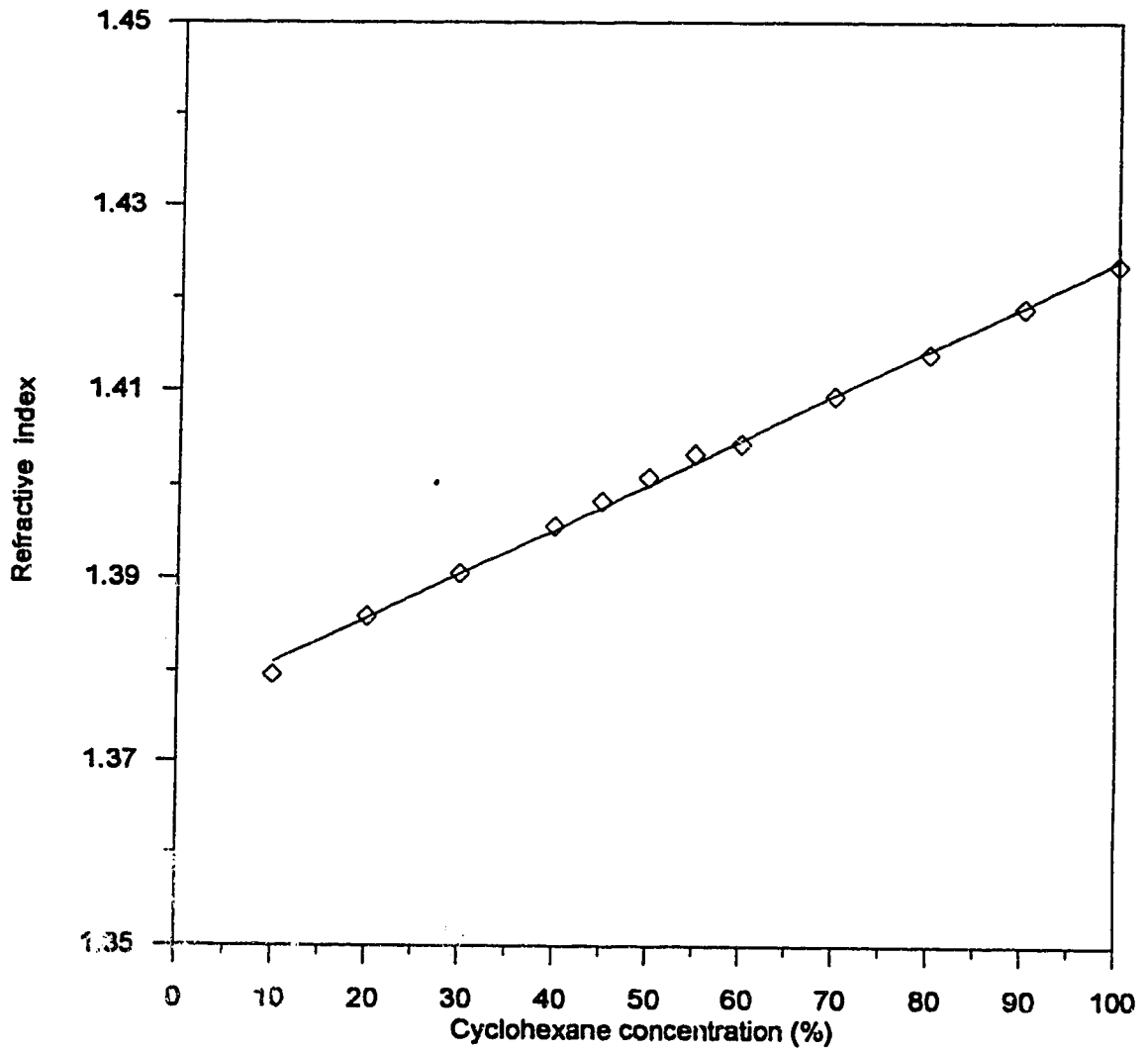


Figure B1 : Standard concentration curve
Refractive index versus % cyclohexane

2. Experimental effluent concentration for the favourable mobility cases

Table B1. 122 cm core length

PV	Lambda	Cyclohexane concentration (%) at velocity					
		0.0118 (cm/s)	0.0187 (cm/s)	0.0211 (cm/s)	0.0241 (cm/s)	0.0368 (cm/s)	0.0483 (cm/s)
0.00	*****	0.000	0.000	0.000	0.000	0.000	0.000
0.05	-4.249	0.000	0.000	0.417	1.022	1.458	1.667
0.10	-2.846	0.000	0.000	0.417	1.022	1.458	1.667
0.15	-2.195	0.770	1.922	0.417	1.022	1.458	1.667
0.20	-1.789	0.770	1.922	0.417	1.922	1.458	1.667
0.25	-1.500	0.770	1.922	1.917	1.922	1.458	1.667
0.30	-1.278	0.770	1.922	1.917	1.922	5.418	1.667
0.35	-1.099	0.770	1.922	1.917	1.922	5.418	1.667
0.40	-0.949	0.770	1.922	1.917	1.922	5.418	1.667
0.45	-0.820	0.770	1.922	1.917	1.922	5.418	1.667
0.50	-0.707	0.770	1.922	1.917	1.922	5.418	1.667
0.55	-0.607	1.922	1.922	1.917	1.922	5.418	1.667
0.60	-0.516	1.922	1.922	1.917	1.922	5.418	1.667
0.65	-0.434	1.922	1.922	1.917	1.922	5.418	5.625
0.70	-0.359	1.922	1.922	1.917	3.848	5.418	5.625
0.75	-0.289	3.848	5.770	1.917	5.770	5.418	7.709
0.80	-0.224	10.626	5.770	1.917	18.282	5.418	7.918
0.85	-0.163	13.907	5.770	1.917	51.289	5.418	8.750
0.90	-0.105	40.578	17.345	1.917	78.537	5.625	35.871
0.95	-0.051	77.316	73.901	4.584	87.858	6.459	78.537
1.00	0.000	88.035	82.679	4.792	92.857	38.696	86.250
1.05	0.049	94.694	85.179	43.799	93.468	74.145	94.081
1.10	0.095	95.510	90.815	73.901	93.877	88.750	96.325
1.15	0.140	95.510	93.468	87.142	95.101	93.061	96.938
1.20	0.183	96.938	96.530	91.837	96.123	94.897	98.163
1.25	0.224	96.938	96.938	94.081	96.938	95.919	98.163
1.30	0.263	97.347	96.938	94.897	97.958	96.123	98.163
1.35	0.301	97.347	96.938	96.123	98.367	96.325	98.163
1.40	0.338	97.552	96.938	96.938	97.958	96.938	98.163
1.45	0.374	97.552	97.347	97.347	98.980	97.958	98.163
1.50	0.408	97.552	97.347	97.347	98.980	97.958	98.776
1.55	0.442	97.552	97.347	96.938	98.980	97.347	97.347
1.60	0.474	97.552	97.958	96.938	98.980	97.958	98.163
1.65	0.506	97.552	98.163	97.756	98.980	97.958	98.163
1.70	0.537	97.552	98.571	97.756	98.980	97.958	98.163
1.75	0.567	97.552	98.571	97.756	99.184	97.958	98.163
1.80	0.596	97.552	98.980	97.756	99.184	97.958	98.163
1.85	0.625	97.958	98.980	97.756	99.184	97.958	98.163
1.90	0.653	97.958	99.184	97.756	99.184	97.958	98.776
1.95	0.680	97.958	99.387	97.756	99.184	97.958	97.347
2.00	0.707	97.958	99.387	97.756	99.184	97.958	98.163

Table B2. 183 cm core length

PV	Lambda	Cyclohexane concentration (%) at velocity				
		0.0146 (cm/s)	0.0166 (cm/s)	0.0195 (cm/s)	0.0293 (cm/s)	0.0391 (cm/s)
0.00	*****	0.000	0.000	0.000	1.293	0.000
0.05	-4.249	0.209	0.209	0.209	1.293	0.000
0.10	-2.846	0.417	0.209	0.417	1.293	0.000
0.15	-2.195	0.417	0.417	0.417	2.375	2.501
0.20	-1.789	0.417	0.417	1.458	2.375	2.501
0.25	-1.500	0.626	1.043	1.458	2.375	2.501
0.30	-1.278	0.626	1.458	3.543	5.625	3.543
0.35	-1.099	0.626	1.458	3.543	5.625	3.543
0.40	-0.949	0.626	1.458	3.543	6.459	3.543
0.45	-0.820	1.250	1.667	3.543	6.459	3.543
0.50	-0.707	1.458	1.876	3.543	6.459	3.751
0.55	-0.607	1.458	2.708	3.751	6.459	3.751
0.60	-0.516	1.458	2.708	4.584	6.668	3.543
0.65	-0.434	1.250	2.917	4.584	6.668	4.167
0.70	-0.359	1.250	2.917	4.584	6.668	5.001
0.75	-0.289	1.458	2.917	4.584	7.709	5.625
0.80	-0.224	4.792	7.292	11.800	18.800	12.001
0.85	-0.163	30.218	39.131	44.999	49.399	50.000
0.90	-0.105	65.416	73.171	79.023	77.074	62.917
0.95	-0.051	85.000	88.035	89.108	88.035	82.679
1.00	0.000	89.642	92.448	94.081	90.000	85.214
1.05	0.049	93.266	92.653	94.081	92.040	89.821
1.10	0.095	93.673	94.490	94.081	92.448	92.857
1.15	0.140	93.877	94.490	95.919	93.266	97.143
1.20	0.183	94.897	94.897	96.938	94.897	98.163
1.25	0.224	94.897	96.123	96.938	96.123	98.163
1.30	0.263	96.123	96.123	96.938	96.123	98.163
1.35	0.301	96.123	96.123	97.756	96.123	98.571
1.40	0.338	96.325	96.734	97.756	96.123	98.571
1.45	0.374	96.325	98.163	97.756	97.143	98.571
1.50	0.408	96.938	96.938	97.958	97.143	98.571
1.55	0.442	97.958	97.756	98.163	96.530	98.571
1.60	0.474	97.958	97.756	98.163	96.530	98.571
1.65	0.506	97.958	97.756	98.367	96.938	98.571
1.70	0.537	97.958	97.756	98.980	96.938	98.571
1.75	0.567	97.958	97.756	98.980	96.938	98.571
1.80	0.596	97.958	97.756	98.980	96.938	98.571
1.85	0.625	97.958	97.756	99.796	96.938	98.571
1.90	0.653	97.958	97.756	99.796	96.938	98.571
1.95	0.680	97.958	97.756	99.796	96.938	98.571
2.00	0.707	97.958	97.756	99.796	96.938	98.571

Table B3. 242 cm core length

PV	Lambda	Cyclohexane concentration (%) @ velocity					
		0.0115 (cm/s)	0.0178 (cm/s)	0.0192 (cm/s)	0.0221 (cm/s)	0.0338 (cm/s)	0.0461 (cm/s)
0.00	*****	0.000	0.000	0.000	0.000	0.000	0.000
0.05	-4.249	0.000	1.458	1.922	2.708	2.501	2.501
0.10	-2.846	0.000	1.458	1.922	2.501	2.501	3.751
0.15	-2.195	0.000	1.458	1.922	2.501	2.501	3.751
0.20	-1.789	0.000	1.250	1.922	2.501	2.501	4.167
0.25	-1.500	1.922	1.458	1.922	3.543	4.167	4.584
0.30	-1.270	0.000	1.250	1.922	3.543	4.167	5.833
0.35	-1.099	0.000	1.458	1.922	4.584	4.167	5.833
0.40	-0.949	0.000	1.458	1.922	4.584	4.584	6.251
0.45	-0.820	0.000	1.458	1.922	4.584	4.584	6.251
0.50	-0.707	0.000	1.458	1.922	4.584	4.584	6.668
0.55	-0.607	0.000	1.458	1.922	4.584	4.584	7.709
0.60	-0.516	0.000	1.458	1.922	4.584	4.584	7.709
0.65	-0.434	0.000	1.667	1.922	4.584	5.625	7.709
0.70	-0.359	0.000	2.084	1.922	4.584	5.625	7.709
0.75	-0.289	0.000	2.501	0.385	4.584	5.625	7.709
0.80	-0.224	0.000	2.501	7.693	5.625	5.625	10.801
0.85	-0.163	1.922	28.335	32.693	12.800	15.800	30.871
0.90	-0.105	21.088	50.980	77.804	53.921	55.686	58.411
0.95	-0.051	68.862	77.316	90.000	83.571	78.781	79.512
1.00	0.000	87.119	84.642	93.673	91.837	86.608	85.000
1.05	0.049	93.261		94.081	92.857	88.750	88.929
1.10	0.095	94.565		94.081	92.857	91.020	91.224
1.15	0.140	94.782		95.101	93.877	91.837	92.857
1.20	0.183	95.871		95.101	93.877	91.837	94.081
1.25	0.224	96.7		95.306	94.694	91.837	94.697
1.30	0.263			94.897	94.897	92.244	95.306
1.35	0.301			95.306	94.897	92.244	95.714
1.40	0.338			94.897	95.101	92.244	95.714
1.45	0.374			94.897	94.897	93.877	95.919
1.50	0.408			95.306	95.101	93.877	96.938
1.55	0.442			95.306	95.101	93.877	96.938
1.60	0.474			94.897	95.101	96.530	97.347
1.65	0.506			95.306	94.897	96.530	97.347
1.70	0.537			94.897	95.101	96.530	97.958
1.75	0.567		96.938	94.897	95.101	96.530	97.958
1.80	0.596	98.914	96.938	94.897	94.897	96.530	97.958
1.85	0.625	98.914	96.938	94.897	95.101	96.530	97.958
1.90	0.653	98.914	96.938	94.897	95.101	96.530	98.571
1.95	0.680	98.914	96.938	95.306	95.101	96.530	98.571
2.00	0.707	98.914	96.938	95.306	95.101	96.530	98.571

3. Experimental effluent concentration for the unfavourable mobility cases

Table B4. 122 cm core length

PV	Lambda	N-hexane concentration (%) at flow rate of				
		0.0462 (cm ³ /s)	0.0822 (cm ³ /s)	0.0944 (cm ³ /s)	0.1484 (cm ³ /s)	0.1900 (cm ³ /s)
0.00	*****	0.000	0.000	0.000	0.000	0.000
0.05	-4.249	1.020	3.877	0.000	3.062	1.633
0.10	-2.846	1.020	2.448	0.000	2.042	0.816
0.15	-2.195	1.020	2.042	0.000	1.633	0.622
0.20	-1.789	1.020	2.042	0.000	1.224	0.622
0.25	-1.500	1.020	2.042	0.000	1.020	0.622
0.30	-1.278	0.204	2.072	0.000	1.020	0.000
0.35	-1.099	0.204	2.042	0.000	1.020	0.000
0.40	-0.949	0.204	2.042	0.000	1.020	0.000
0.45	-0.820	0.204	2.042	0.000	1.020	0.000
0.50	-0.707	0.204	2.042	0.000	1.020	0.000
0.55	-0.607	0.204	2.042	0.000	1.020	0.000
0.60	-0.516	0.204	1.429	0.000	1.020	15.000
0.65	-0.434	1.837	1.429	0.000	1.020	29.756
0.70	-0.359	11.786	5.919	13.392	5.306	42.158
0.75	-0.289	12.858	28.537	15.358	19.286	49.020
0.80	-0.224	16.429	40.000	28.537	30.000	52.399
0.85	-0.163	18.215	45.295	38.126	38.542	52.399
0.90	-0.105	2.000	49.015	41.569	47.648	56.000
0.95	-0.051	22.440	55.001	50.801	56.000	59.001
1.00	0.000	24.878	59.001	54.000	60.435	62.608
1.05	0.049	27.318	60.869	59.201	63.261	67.608
1.10	0.095	49.217	63.043	64.347	65.433	70.833
1.15	0.140	50.000	66.522	68.694	68.694	72.917
1.20	0.183	72.708	71.250	71.041	70.833	74.167
1.25	0.224	74.790	72.917	79.166	74.999	75.208
1.30	0.263	77.083	72.082	88.400	79.374	76.875
1.35	0.301	81.200	76.249	89.199	83.000	78.124
1.40	0.338	83.199	80.200	91.041	84.000	81.200
1.45	0.374	87.999	85.199	91.458	85.199	83.199
1.50	0.408	91.041	86.199	92.291	85.199	85.998
1.55	0.442	91.458	86.399	92.291	87.200	88.600
1.60	0.474	92.082	89.599	92.291	89.399	91.458
1.65	0.506	92.500	95.416	92.291	94.375	93.332
1.70	0.537	93.123	95.416	93.332	95.625	95.416
1.75	0.567	93.123	95.416	96.457	95.625	96.666
1.80	0.596	93.123	95.416	96.457	95.625	96.666
1.85	0.625	93.123	95.416	92.291	95.625	96.666
1.90	0.653	93.123	95.416	96.457	95.625	96.666
1.95	0.680	93.123	95.416	96.457	95.625	96.666
2.00	0.707	93.123	95.416	96.457	95.625	96.666
3.00	1.155	100.000	100.000	100.000	100.000	100.000
4.00	1.500	100.000	100.000	100.000	100.000	100.000

Table B5. 183 cm core length

PV	Lambda	N-hexane concentration (%) at flow rate of			
		0.0785 (cm ³ /s)	0.0919 (cm ³ /s)	0.1374 (cm ³ /s)	0.1852 (cm ³ /s)
0.00	*****	0.000	0.000	0.000	0.000
0.05	-4.249	2.244	1.020	4.899	4.899
0.10	-2.846	2.244	0.816	3.877	3.266
0.15	-2.195	2.244	0.816	3.062	2.857
0.20	-1.789	1.837	0.816	3.062	1.837
0.25	-1.500	1.429	0.816	3.062	1.837
0.30	-1.279	1.429	0.816	3.062	1.837
0.35	-1.020	1.429	0.816	3.062	2.653
0.40	-0.949	4.286	3.062	2.857	2.653
0.45	-0.820	4.286	4.081	2.857	4.081
0.50	-0.707	3.877	3.062	2.244	3.877
0.55	-0.607	3.877	2.653	2.244	2.857
0.60	-0.516	3.062	12.858	2.244	1.837
0.65	-0.434	15.536	32.708	2.244	16.429
0.70	-0.359	34.792	44.903	28.293	33.543
0.75	-0.289	45.099	52.001	43.138	37.292
0.80	-0.224	50.999	55.001	48.040	38.216
0.85	-0.163	54.000	58.800	50.000	55.800
0.90	-0.105	50.999	66.086	48.824	63.043
0.95	-0.051	57.999	67.608	52.800	70.000
1.00	0.000	70.624	70.415	66.086	71.874
1.05	0.049	78.124	75.834	72.917	69.782
1.10	0.095	83.799	75.834	77.916	72.917
1.15	0.140	85.998	77.707	81.200	82.199
1.20	0.183	93.332	82.399	87.000	90.833
1.25	0.224	96.666	86.199	93.332	93.332
1.30	0.263	96.666	93.332	95.208	94.582
1.35	0.301	97.499	95.625	95.416	94.582
1.40	0.338	97.499	96.457	95.416	94.375
1.45	0.374	97.499	96.457	95.416	94.375
1.50	0.408	97.499	96.457	95.416	95.416
1.55	0.442	97.499	96.457	95.416	95.416
1.60	0.474	97.499	96.457	95.416	95.416
1.65	0.506	97.499	96.457	95.416	95.416
1.70	0.537	97.499	97.499	95.416	95.416
1.75	0.567	97.499	97.499	95.416	95.416
1.80	0.596	97.499	97.499	95.416	95.416
1.85	0.625	97.499	97.499	95.416	95.416
1.90	0.653	97.499	97.499	95.416	95.416
1.95	0.680	97.499	97.499	95.416	95.416
2.00	0.707	97.499	97.499	95.416	95.416
3.00	1.155	100.000	100.000	100.000	100.000
4.00	1.500	100.000	100.000	100.000	100.000

Table B6. 242 cm core length

PV	Lambda	N-hexane concentration (%) at flow rate of					
		0.0694 (cm ³ /s)	0.0455 (cm ³ /s)	0.0930 (cm ³ /s)	0.0789 (cm ³ /s)	0.1255 (cm ³ /s)	0.1391 (cm ³ /s)
0.00	*****	0.000	0.000	0.000	0.000	0.000	0.000
0.05	-4.249	11.808	1.020	4.899	3.062	8.776	2.042
0.10	-2.848	4.081	1.020	4.081	3.062	2.042	2.042
0.15	-2.195	4.081	1.020	4.081	3.470	1.020	3.062
0.20	-1.789	4.081	1.020	4.081	3.470	1.224	2.042
0.25	-1.500	3.877	1.020	3.675	3.470	1.224	1.837
0.30	-1.278	3.877	2.244	3.675	3.470	1.224	1.020
0.35	-1.099	3.877	2.244	3.675	3.470	1.224	1.837
0.40	-0.949	3.877	2.244	3.675	2.857	1.224	1.837
0.45	-0.820	3.062	2.244	3.675	3.062	1.224	1.837
0.50	-0.707	2.042	2.042	3.675	2.042	3.877	1.837
0.55	-0.607	2.042	2.244	2.857	2.042	1.877	1.020
0.60	-0.516	3.062	16.608	2.448	2.042	23.415	0.613
0.65	-0.434	14.286	29.514	6.123	11.965	36.459	0.613
0.70	-0.359	15.538	33.860	16.608	23.415	47.059	0.613
0.75	-0.289	23.415	43.334	22.926	28.293	56.800	4.081
0.80	-0.224	33.960	47.648	25.855	40.196	65.651	22.440
0.85	-0.163	50.200	52.001	35.834	40.196	78.750	28.537
0.90	-0.105	58.800	55.001	45.490	43.727	87.200	33.960
0.95	-0.051	70.000	69.782	57.999	52.001	89.199	40.785
1.00	0.000	81.200	83.199	72.708	63.478	90.624	50.801
1.05	0.049	88.999	92.500	77.916	73.123	91.250	63.261
1.10	0.095	91.458	94.375	85.400	81.600	92.291	77.499
1.15	0.140	92.291	94.375	90.415	89.599	92.291	84.200
1.20	0.183	92.500	94.375	91.458	93.332	92.500	88.999
1.25	0.224	92.500	94.375	92.291	93.332	92.291	90.000
1.30	0.263	94.167	94.582	93.332	94.375	92.291	91.250
1.35	0.301	94.375	94.582	93.332	94.375	92.291	93.123
1.40	0.338	94.375	94.375	94.375	94.375	93.123	94.375
1.45	0.374	94.375	94.375	94.375	94.375	93.123	93.332
1.50	0.408	95.416	95.416	95.416	95.416	93.123	93.320
1.55	0.442	95.416	95.416	95.416	95.416	93.123	94.375
1.60	0.474	95.416	95.416	95.416	95.416	93.123	95.208
1.65	0.506	95.416	95.416	95.416	95.416	93.123	94.375
1.70	0.537	95.416	95.416	95.416	95.416	93.123	94.375
1.75	0.567	95.416	95.416	95.416	95.416	93.123	93.123
1.80	0.596	95.416	95.416	95.416	95.416	93.123	94.375
1.85	0.625	95.416	95.416	95.416	95.416	93.123	94.375
1.90	0.653	95.416	95.416	95.416	95.416	93.123	94.375
1.95	0.680	95.416	95.416	95.416	95.416	93.123	94.375
2.00	0.707	95.416	95.416	95.416	95.416	93.123	94.375
3.00	1.155	100.000	100.000	100.000	100.000	100.000	100.000
4.00	1.500	100.000	100.000	100.000	100.000	100.000	100.000

APPENDIX C

CALCULATION OF THE PREDICTED CONCENTRATION PROFILES

The predicted concentration profiles were calculated using the following formula :

$$C' = \frac{1}{2} \operatorname{erfc} \frac{1-I}{2\sqrt{I/\gamma}} + \frac{1}{2\sqrt{\pi\gamma I}} e^{-\left(\frac{1-I}{2\sqrt{I/\gamma}}\right)^2} \quad (1)$$

where

C' = effluent concentration (% cyclohexane)

I = pore volumes injected, (PV)

and

γ = dimensionless dispersion

The dispersion coefficients obtained from miscible displacement experiments were plotted as a function of fluid velocity and curve fitting the data was performed for each core length. The resulting dispersion coefficient was used to determine the dimensionless dispersion as follows :

$$\gamma = \frac{vL}{K_e} \quad (2)$$

where

v = the pore velocity (cm/s)

L = the core length (cm)

and

K_e = the dispersion coefficient (cm^2/s)

Spread sheets were created to calculate the effluent concentration using the dimensionless dispersion, γ , from Equation (2) and substitute it into Equation (1).

The terms used in the spread sheets are :

$$A = \left(\frac{1-I}{2\sqrt{I/\gamma}} \right)$$

$$B = \frac{1}{2\sqrt{\pi\gamma I}}$$

and

$$2^{nd} term = \frac{1}{2\sqrt{\pi\gamma I}} e^{-\left(\frac{1-I}{2\sqrt{I/\gamma}}\right)^2}$$

CORE LENGTH = 122cm

Curve fit K_e versus Velocity excluding 2 error points yields:

$$K_e = 0.1002 v^{0.5982}$$

● Fluid velocity = 0.0118cm/s

$K_e = 0.0070383 \text{ (cm}^2\text{/s)}$
 and
 $\gamma = 204.538139$

PV	A	B	A*A	erf(A)	erfc(A)	e ^{-(A*A)}	2ndterm	Eff.Conc.
0.80	1.60	0.0221	2.5567	0.97634	0.02366	0.07754	0.0017	0.0135
0.85	1.16	0.0214	1.3536	0.89909	0.10091	0.25821	0.0055	0.0560
0.90	0.75	0.0208	0.5682	0.71115	0.28885	0.56666	0.0118	0.1562
0.95	0.37	0.0202	0.1346	0.39920	0.60080	0.87372	0.0177	0.3181
1.00	0.00	0.0197	0.0000	0.00000	1.00000	1.00000	0.0197	0.5197
1.05	-0.35	0.0192	0.1217		1.37938	0.88515	0.0170	0.7067
1.10	-0.68	0.0188	0.4649		1.66378	0.62814	0.0118	0.8437
1.15	-1.00	0.0184	1.0005		1.84270	0.36788	0.0068	0.9281
1.20	-1.31	0.0180	1.7045		1.93606	0.18195	0.0033	0.9713
1.25	-1.60	0.0176	2.5567		1.97634	0.07754	0.0014	0.9895
1.30	-1.88	0.0173	3.5401		1.99215	0.02901	0.0005	0.9966

● Fluid velocity = 0.0187cm/s

$K_e = 0.00927008 \text{ (cm}^2\text{/s)}$
 and
 $\gamma = 246.103657$

PV	A	B	A*A	erf(A)	erfc(A)	e ^{-(A*A)}	2ndterm	Eff.Conc.
0.80	1.75	0.0201	3.0763	0.98667	0.01333	0.04610	0.0009	0.0076
0.85	1.28	0.0195	1.6286	0.92973	0.07027	0.19620	0.0038	0.0390
0.90	0.83	0.0190	0.6836	0.75952	0.24048	0.50480	0.0096	0.1298
0.95	0.40	0.0184	0.1619	0.42839	0.57161	0.85050	0.0157	0.3015
1.00	0.00	0.0180	0.0000	0.00000	1.00000	1.00000	0.0180	0.5180
1.05	-0.38	0.0175	0.1465		1.40900	0.86370	0.0152	0.7197
1.10	-0.75	0.0171	0.5593		1.71115	0.57160	0.0098	0.8654
1.15	-1.10	0.0168	1.2038		1.88020	0.30010	0.0050	0.9451
1.20	-1.43	0.0164	2.0509		1.95685	0.12860	0.0021	0.9805
1.25	-1.75	0.0161	3.0763		1.98667	0.04610	0.0007	0.9941
1.30	-2.06	0.0158	4.2595					

② Fluid velocity = 0.0241cm/s

Ke = 0.01078923 (cm²/s)
and
gamma = 272.512581

PV	A	B	A*A	erf(A)	erfc(A)	e ^{-(A*A)}	2ndterm	Eff.Conc.
0.80	1.85	0.0191	3.4064	0.99111	0.00889	0.03320	0.0006	0.0051
0.85	1.34	0.0185	1.8034	0.94191	0.05809	0.16470	0.0031	0.0321
0.90	0.87	0.0180	0.7570	0.78143	0.21857	0.46910	0.0084	0.1177
0.95	0.42	0.0175	0.1793	0.44746	0.55254	0.83590	0.0147	0.2909
1.00	0.00	0.0171	0.0000	0	1.00000	1.00000	0.0171	0.5171
1.05	-0.40	0.0167	0.1622		1.42839	0.85030	0.3142	0.7284
1.10	-0.79	0.0163	0.6193		1.73610	0.53830	0.0088	0.8768
1.15	-1.15	0.0159	1.3329		1.89612	0.26370	0.0042	0.9523
1.20	-1.51	0.0156	2.2709		1.96727	0.10320	0.0016	0.9852
1.25	-1.85	0.0153	3.4064		1.99111	0.03320	0.0005	0.9961

③ Fluid velocity = 0.0483cm/s

Ke = 0.01635328 (cm²/s)
and
gamma = 360.331365

PV	A	B	A*A	erf(A)	erfc(A)	e ^{-(A*A)}	2ndterm	Eff.Conc.
0.80	2.12	0.0166	4.5041					
0.85	1.54	0.0161	2.3845	0.97058	0.02942	0.09210	0.0015	0.0162
0.90	1.00	0.0157	1.0009	0.84270	0.15730	0.36460	0.0057	0.0844
0.95	0.49	0.0152	0.2371	0.51166	0.48834	0.78890	0.0120	0.2562
1.00	0.00	0.0149	0.0000	0	1.00000	1.00000	0.0149	0.5149
1.05	-0.46	0.0145	0.2145		1.48465	0.80690	0.0117	0.7540
1.10	-0.90	0.0142	0.8189		1.79690	0.44090	0.0062	0.9047
1.15	-1.33	0.0139	1.7625		1.94001	0.17160	0.0024	0.9724
1.20	-1.73	0.0136	3.0028		1.98557	0.04960	0.0007	0.9935
1.25	-2.12	0.0133	4.5041					

CORE LENGTH = 183cm

Curve fit K_e versus velocity yields :

$$K_e = 16.672 v^{1.8218}$$

Ⓒ Fluid velocity = 0.0146cm/s

$K_e = 0.00754755 \text{ (cm}^2\text{/s)}$
and
 $\gamma = 353.995883$

PV	A	B	A*A	erf(A)	erfc(A)	e ^{-(A*A)}	2ndterm	Eff.Conc.
0.80	2.10	0.0168						
0.85	1.53	0.0163	2.3426	0.96951	0.03049	0.09610	0.0016	0.0168
0.90	0.99	0.0158	0.9833	0.83850	0.16150	0.37410	0.0059	0.0867
0.95	0.48	0.0154	0.2329	0.50274	0.49726	0.79220	0.0122	0.2608
1.00	0.00	0.0150	0.0000	0.00000	1.00000	1.00000	0.0150	0.5150
1.05	-0.46	0.0146	0.2107		1.48465	0.81000	0.0119	0.7542
1.10	-0.90	0.0143	0.8045		1.79690	0.44730	0.0064	0.9048
1.15	-1.32	0.0140	1.7315		1.93806	0.17700	0.0025	0.9715
1.20	-1.72	0.0137	2.9500		1.98500	0.05230	0.0007	0.9932
1.25	-2.10	0.0134						

Ⓒ Fluid velocity = 0.0166cm/s

$K_e = 0.00953632 \text{ (cm}^2\text{/s)}$
and
 $\gamma = 318.550698$

PV	A	B	A*A	erf(A)	erfc(A)	e ^{-(A*A)}	2ndterm	Eff.Conc.
0.80	2.00	0.0177	3.9819	0.99532	0.00468	0.01870	0.0003	0.0027
0.85	1.45	0.0171	2.1081	0.95969	0.04031	0.13290	0.0023	0.0224
0.90	0.94	0.0167	0.8849	0.81227	0.18373	0.41280	0.0069	0.0987
0.95	0.46	0.0162	0.2096	0.48465	0.51535	0.81090	0.0131	0.2708
1.00	0.00	0.0158	0.0000	0.00000	1.00000	1.00000	0.0158	0.5158
1.05	-0.44	0.0154	0.1896		1.46622	0.82730	0.0128	0.7459
1.10	-0.85	0.0151	0.7240		1.77766	0.48480	0.0073	0.8926
1.15	-1.25	0.0147	1.5581		1.92290	0.21050	0.0031	0.9646
1.20	-1.63	0.0144	2.6546		1.97884	0.07030	0.0010	0.9904
1.25	-2.00	0.0141	3.9819		1.99532	0.01870	0.0003	0.9979

Ⓒ Fluid velocity = 0.0195cm/s

$K_e = 0.01278712 \text{ (cm}^2\text{/s)}$
and
 $\gamma = 279.069866$

PV	A	B	A*A	erf(A)	erfc(A)	e ^{-(A*A)}	2ndterm	Eff.Conc.
0.80	1.87	0.0189	3.4884	0.99182	0.00818	0.03050	0.0006	0.0047
0.85	1.36	0.0183	1.8468	0.94556	0.05444	0.15770	0.0029	0.0301
0.90	0.88	0.0178	0.7752	0.78668	0.21332	0.46060	0.0082	0.1149
0.95	0.43	0.0173	0.1836	0.45688	0.54312	0.83230	0.0144	0.2860
1.00	0.00	0.0169	0.0000	0.00000	1.00000	1.00000	0.0169	0.5169
1.05	-0.41	0.0165	0.1661		1.43796	0.24700	0.0140	0.7329
1.10	-0.80	0.0161	0.6342		1.74210	0.53040	0.0085	0.8786
1.15	-1.17	0.0157	1.3650		1.90200	0.25540	0.0040	0.9350
1.20	-1.52	0.0154	2.3256		1.96841	0.09770	0.0015	0.9857
1.25	-1.87	0.0151	3.4884		1.99182	0.03050	0.0005	0.9964

⊙ Fluid velocity = 0.0293cm/s

Ke = 0.02684894 (cm²/s)
and
gamma = 199.706214

PV	A	B	A*A	erf(A)	erfc(A)	e ^{-(A*A)}	2ndterm	Eff.Conc.
0.80	1.58	0.0223	2.4963	0.97454	0.02546	0.08240	0.0018	0.0146
0.85	1.15	0.0217	1.3216	0.89612	0.10388	0.26670	0.0058	0.0577
0.90	0.74	0.0210	0.5547	0.70467	0.29533	0.57420	0.0121	0.1597
0.95	0.36	0.0205	0.1314	0.38932	0.61068	0.87690	0.0180	0.3233
1.00	0.00	0.0200	0.0000	0.00000	1.00000	1.00000	0.0200	0.5200
1.05	-0.34	0.0195	0.1189		1.36936	0.88790	0.0173	0.7020
1.10	-0.67	0.0190	0.4539		1.65662	0.63510	0.0121	0.8404
1.15	-0.99	0.0186	0.9768		1.8385	0.37650	0.0070	0.9263
1.20	-1.29	0.0182	1.6642		1.93189	0.18930	0.0034	0.9694
1.25	-1.58	0.0179	2.4963		1.97454	0.08240	0.0015	0.9887

⊙ Fluid velocity = 0.0391cm/s

Ke = 0.04541667 (cm²/s)
and
gamma = 157.547867

PV	A	B	A*A	erf(A)	erfc(A)	e ^{-(A*A)}	2ndterm	Eff.Conc.
0.75	1.81	0.0260	3.2822	0.98952	0.01048	0.03750	0.0010	0.0082
0.80	1.40	0.0251	1.9693	0.95228	0.04772	0.13960	0.0035	0.0274
0.85	1.02	0.0244	1.0426	0.85083	0.14917	0.35250	0.0086	0.0832
0.90	0.66	0.0237	0.4376	0.64937	0.35063	0.64560	0.0153	0.1906
0.95	0.32	0.0231	0.1036	0.34912	0.65088	0.90160	0.0208	0.3462
1.00	0.00	0.0225	0.0000	0.00000	1.00000	1.00000	0.0225	0.5225
1.05	-0.31	0.0219	0.0938		1.3389	0.91050	0.0200	0.6894
1.10	-0.60	0.0214	0.3581		1.60385	0.69900	0.0150	0.8169
1.15	-0.88	0.0210	0.7706		1.78688	0.46270	0.0097	0.9030
1.20	-1.15	0.0205	1.3129		1.89612	0.26900	0.0055	0.9538
1.25	-1.40	0.0201	1.9693		1.95228	0.13960	0.0028	0.9789
1.3	-1.65	0.0197	2.7268		1.98037	0.06540	0.0013	0.9915

CORE LENGTH = 242 cm

Curve fit K_e versus velocity yields:

$$K_e = 45.8861 v^{2.0865}$$

• Fluid velocity = 0.0115 cm/s

$$K_e = 0.00412408 \text{ (cm}^2\text{/s)}$$

and

$$\gamma = 674.817001$$

PV	A	B	A*A	erf(A)	erfc(A)	e ^{-(A*A)}	2ndterm...	Eff.Conc.
0.86	1.96	0.0117	3.8449	0.99442	0.00558	0.02140	0.0003	0.0030
0.90	1.37	0.0114	1.8745	0.84731	0.05269	0.15340	0.0018	0.0281
0.95	0.67	0.0111	0.4440	0.65662	0.34338	0.64150	0.0071	0.1788
1.00	0.00	0.0109	0.0000	0.00000	1.00000	1.00000	0.0109	0.5109
1.05	-0.63	0.0106	0.4017		1.62704	0.66920	0.0071	0.8206
1.10	-1.24	0.0104	1.5337		1.92050	0.21570	0.0022	0.9625
1.15	-1.82	0.0101	3.3007		1.98994	0.03690	0.0004	0.9953
1.16	-1.93	0.0101	3.7231		1.99365	0.02420	0.0002	0.9971

• Fluid velocity = 0.0178 cm/s

$$K_e = 0.01026083 \text{ (cm}^2\text{/s)}$$

and

$$\gamma = 419.810103$$

PV	A	B	A*A	erf(A)	erfc(A)	e ^{-(A*A)}	2ndterm	Eff.Conc.
0.85	1.67	0.0149	2.7782	0.98181	0.01819	0.06290	0.0009	0.0100
0.9	1.08	0.0145	1.1661	0.87332	0.12668	0.31130	0.0045	0.0679
0.95	0.53	0.0141	0.2762	0.54646	0.45354	0.75570	0.0107	0.2375
1.00	0.00	0.0138	0.0000	0.00000	1.00000	1.00000	0.0138	0.5138
1.05	-0.50	0.0134	0.2499		1.52049	0.77890	0.0105	0.7707
1.10	-0.98	0.0131	0.9541		1.83423	0.38520	0.0051	0.9222
1.15	-1.43	0.0128	2.0534		1.95685	0.12830	0.0016	0.9801
1.2	-1.87	0.0126	3.4984		1.99182	0.03020	0.0004	0.9963

• Fluid velocity = 0.0192 cm/s

$$K_e = 0.01201681 \text{ (cm}^2\text{/s)}$$

and

$$\gamma = 386.658386$$

PV	A	B	A*A	erf(A)	erfc(A)	e ^{-(A*A)}	2ndterm	Eff.Conc.
0.85	1.60	0.0156	2.5588	0.97634	0.02366	0.07740	0.0012	0.0130
0.90	1.04	0.0151	1.0741	0.85864	0.14136	0.34100	0.0052	0.0758
0.95	0.50	0.0147	0.2544	0.52049	0.47951	0.77530	0.0114	0.2512
1.00	0.00	0.0143	0.0000	0.00000	1.00000	1.00000	0.0143	0.5143
1.05	-0.48	0.0140	0.2302		1.50274	0.79440	0.0111	0.7625
1.10	-0.94	0.0137	0.8788		1.81627	0.41530	0.0057	0.9138
1.15	-1.38	0.0134	1.8913		1.94901	0.15090	0.0020	0.9765
1.20	-1.80	0.0131	3.2222		1.98909	0.03990	0.0005	0.9951

Ⓔ Flow rate = 0.0221cm/s

Ke = 0.01611594 (cm²/s)
and
gamma = 331.857787

PV	A	B	A*A	erf(A)	erfc(A)	e ^{-(A*A)}	2ndterm	Eff.Conc.
0.81	1.92	0.0172	3.6976	0.99337	0.00663	0.02480	0.0004	0.0037
0.85	1.48	0.0168	2.1961	0.96365	0.03635	0.11120	0.0019	0.0200
0.90	0.96	0.0163	0.9218	0.82542	0.17458	0.39780	0.0065	0.0938
0.95	0.47	0.0159	0.2183	0.49374	0.50626	0.80390	0.0128	0.2659
1.00	0.00	0.0155	0.0000	0.00000	1.00000	1.00000	0.0155	0.5155
1.05	-0.44	0.0151	0.1975		1.46622	0.82080	0.0124	0.7455
1.10	-0.87	0.0148	0.7542		1.78143	0.47040	0.0069	0.8977
1.15	-1.27	0.0144	1.6232		1.92751	0.19730	0.0026	0.9666
1.20	-1.66	0.0141	2.7655		1.98110	0.06280	0.0009	0.9914

Ⓕ Fluid velocity = 0.0338cm/s

Ke = 0.03910802 (cm²/s)
and
gamma = 209.154024

PV	A	B	A*A	erf(A)	erfc(A)	e ^{-(A*A)}	2ndterm	Eff.Conc.
0.80	1.62	0.0218	2.6144	0.97803	0.02197	0.07320	0.0016	0.0126
0.85	1.18	0.0212	1.3841	0.90483	0.09517	0.25050	0.0053	0.0529
0.90	0.76	0.0206	0.5810	0.71753	0.28247	0.55930	0.0115	0.1527
0.95	0.37	0.0200	0.1376	0.39920	0.60080	0.87140	0.0174	0.3178
1.00	0.00	0.0195	0.0000	0.00000	1.00000	1.00000	0.0195	0.5195
1.05	-0.35	0.0190	0.1245		1.37938	0.88290	0.0168	0.7065
1.10	-0.69	0.0186	0.4754		1.67084	0.62160	0.0116	0.8470
1.15	-1.01	0.0182	1.0230		1.84681	0.35950	0.0065	0.9289
1.20	-1.32	0.0178	1.7429		1.93806	0.17500	0.0031	0.9721
1.25	-1.62	0.0174	2.6144		1.97803	0.07320	0.0013	0.9903
1.30	-1.90	0.0171	3.6200		1.99279	0.02680	0.0005	0.9969

② Fluid velocity = 0.0461cm/s

Ke = 0.07472968 (cm²/s)
 and
 gamma = 149.287403

PV	A	B	A*A	erf(A)	erfc(A)	e ^{-(A*A)}	2ndterm	Eff.Conc.
0.75	1.76	0.0267	3.1102	0.98719	0.01281	0.04460	0.0012	0.0076
0.80	1.37	0.0258	1.8661	0.94731	0.05269	0.15470	0.0040	0.0303
0.85	0.99	0.0250	0.9879	0.83850	0.16150	0.37240	0.0093	0.0901
0.90	0.64	0.0243	0.4147	0.63458	0.36542	0.66050	0.0161	0.1988
0.95	0.31	0.0237	0.0962	0.33890	0.66110	0.90650	0.0215	0.3520
1.00	0.00	0.0231	0.0000	0.00000	1.00000	1.00000	0.0231	0.5231
1.05	-0.30	0.0225	0.0889		1.32862	0.91490	0.0206	0.6849
1.10	-0.58	0.0220	0.3393		1.58792	0.71230	0.0157	0.8096
1.15	-0.85	0.0215	0.7302		1.77066	0.48180	0.0104	0.8957
1.20	-1.12	0.0211	1.2441		1.88678	0.28820	0.0061	0.9495
1.25	-1.37	0.0207	1.8661		1.94731	0.15470	0.0032	0.9768
1.30	-1.61	0.0202	2.5838		1.97720	0.07550	0.0015	0.9901
1.35	-1.84	0.0199	3.3866		1.99073	0.03380	0.0007	0.9960

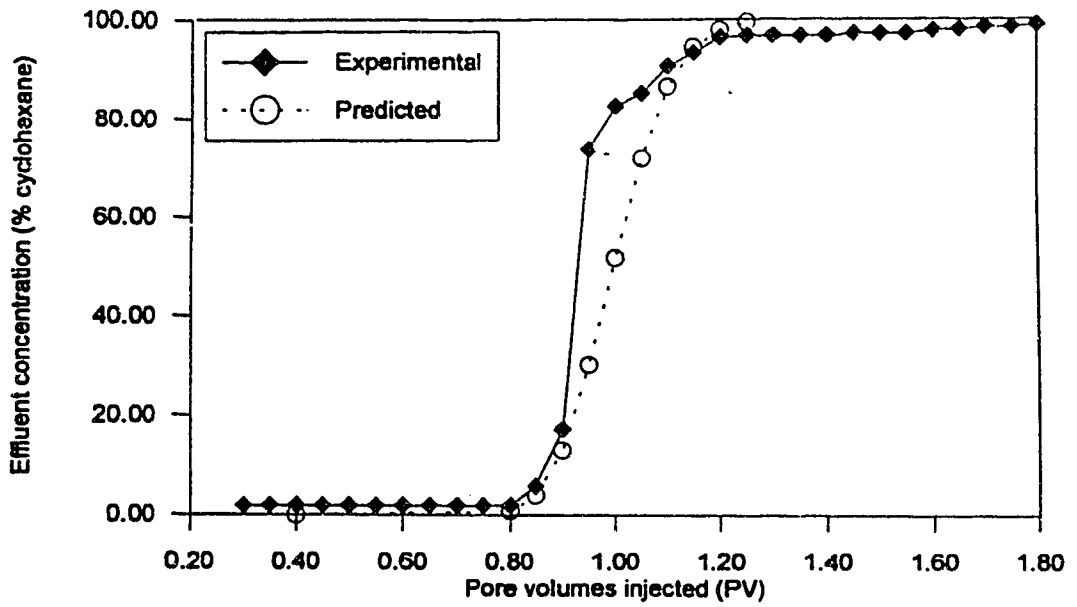


Figure C1 : Concentration profile - experimental versus predicted
Core length = 122cm - fluid velocity = 0.0187 cm/s

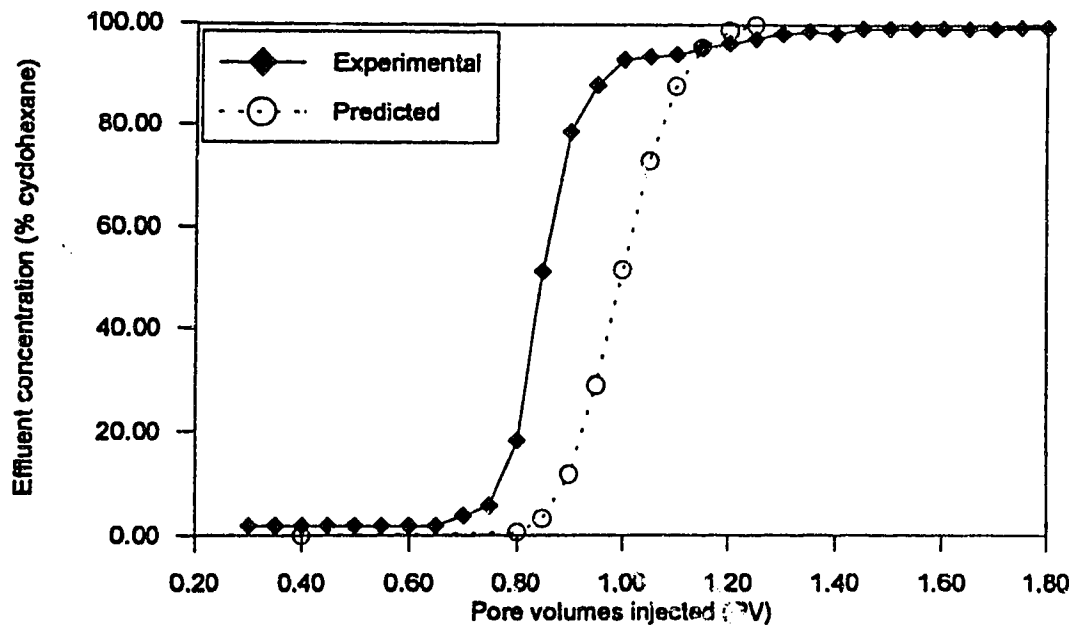


Figure C2 : Concentration profile - experimental versus predicted
Core length = 122cm - fluid velocity = 0.0241cm/s

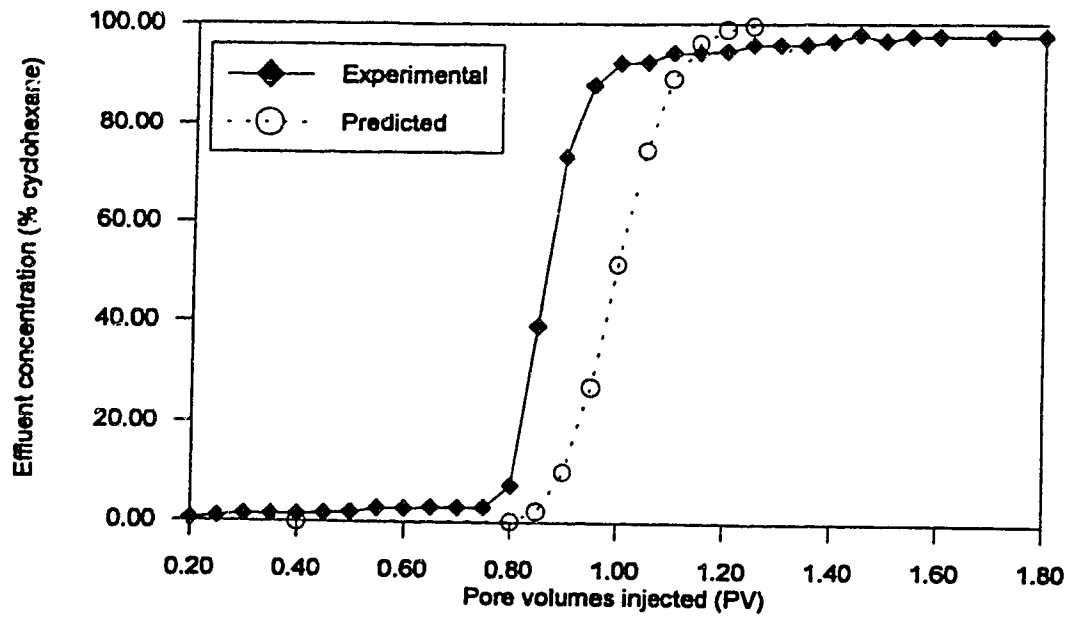


Figure C3 : Concentration profile - experimental versus predicted
Core length = 183 cm - fluid velocity = 0.0166 cm/s

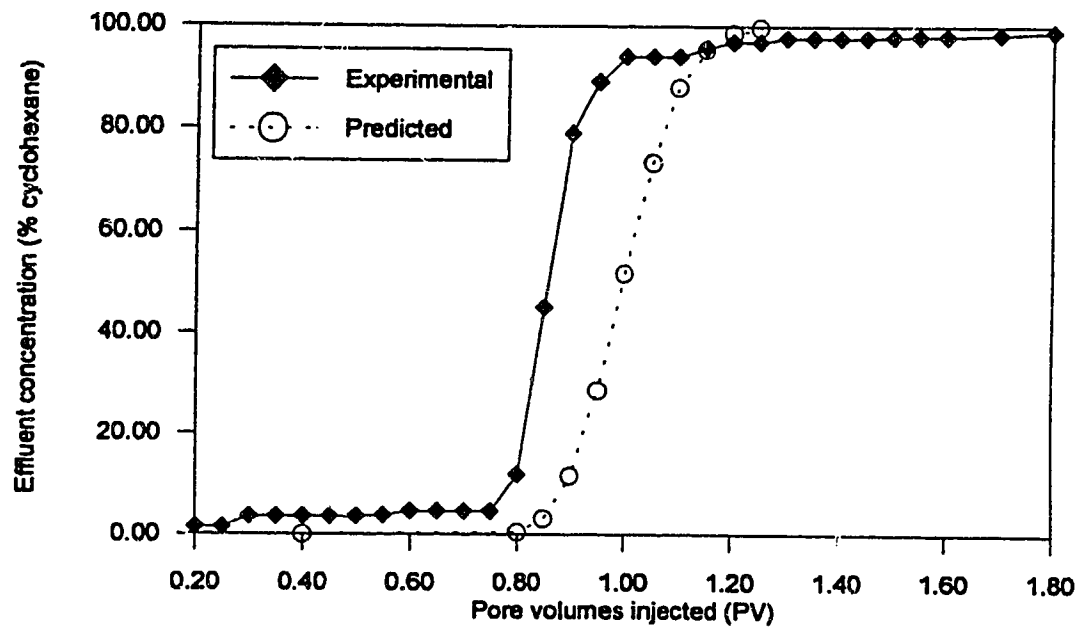


Figure C4 : Concentration profile - experimental versus predicted
Core length = 183 cm - fluid velocity = 0.0195 cm/s

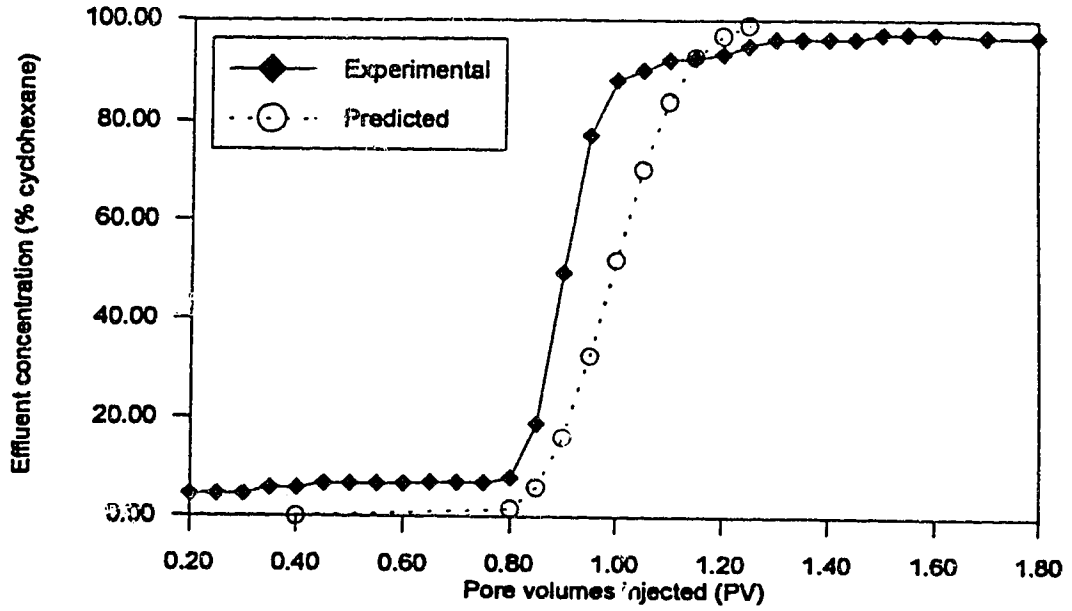


Figure C5 : Concentration profile - experimental versus predicted
 Core length = 183 cm - fluid velocity = 0.0293 cm/s

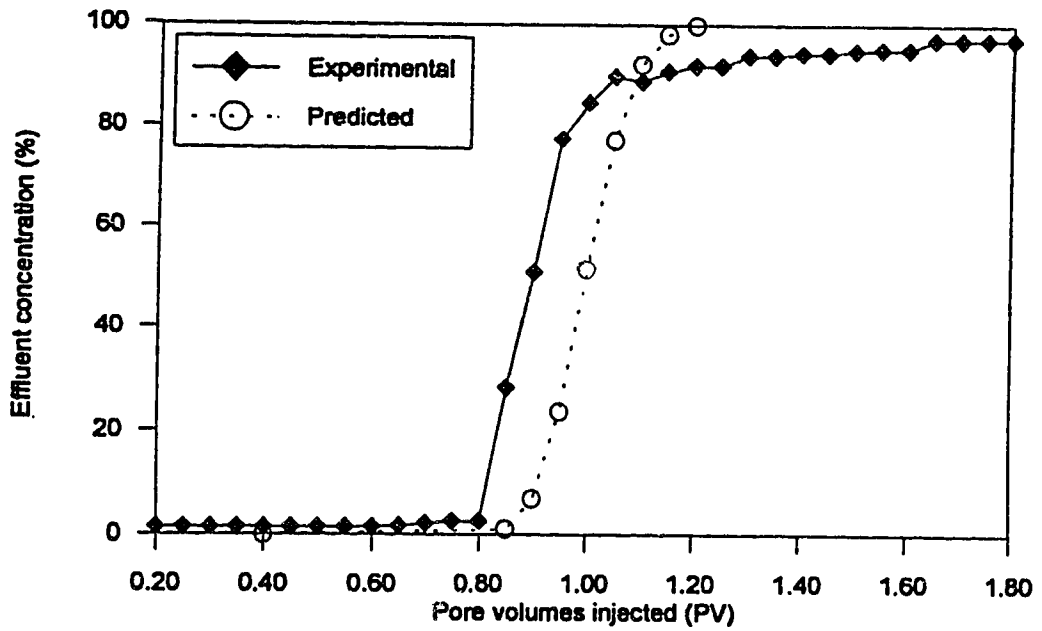


Figure C6 : Concentration profile - experimental versus predicted
 Core length = 242 cm - fluid velocity = 0.0178 cm/s

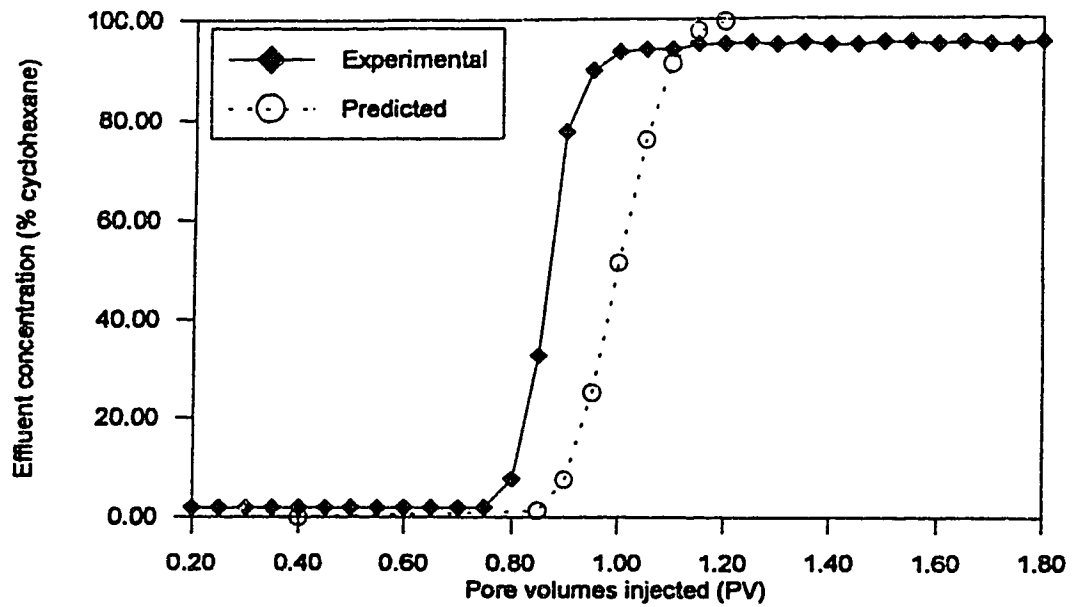


Figure C7 : Concentration profile - experimental versus predicted
Core length = 242 cm - fluid velocity = 0.0192 cm/s

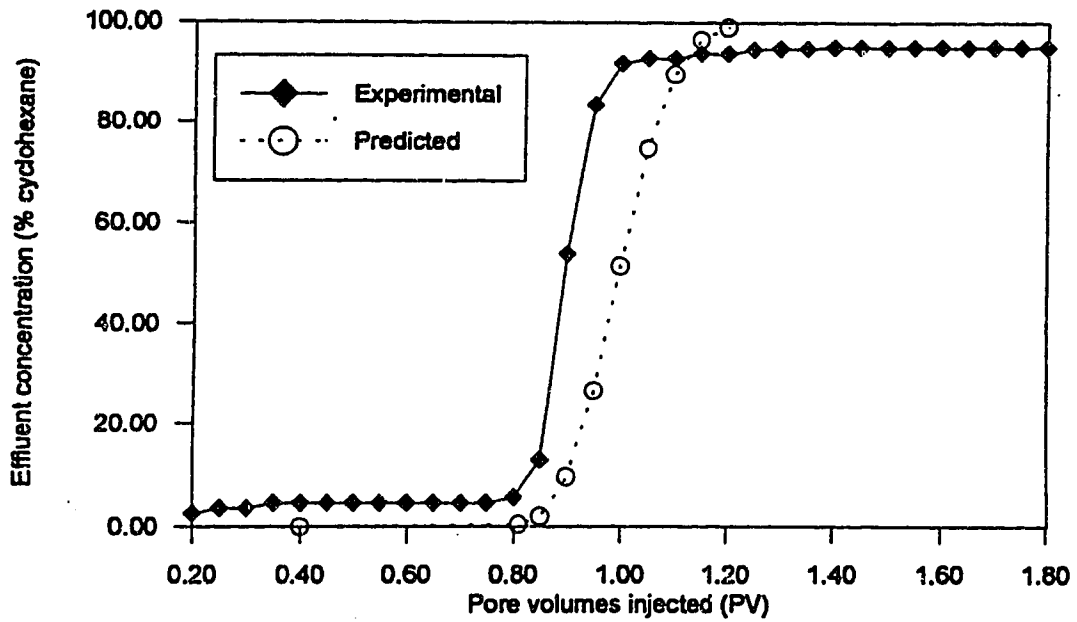


Figure C8 : Concentration profile - experimental versus predicted
Core length = 242 cm - fluid velocity = 0.0221 cm/s

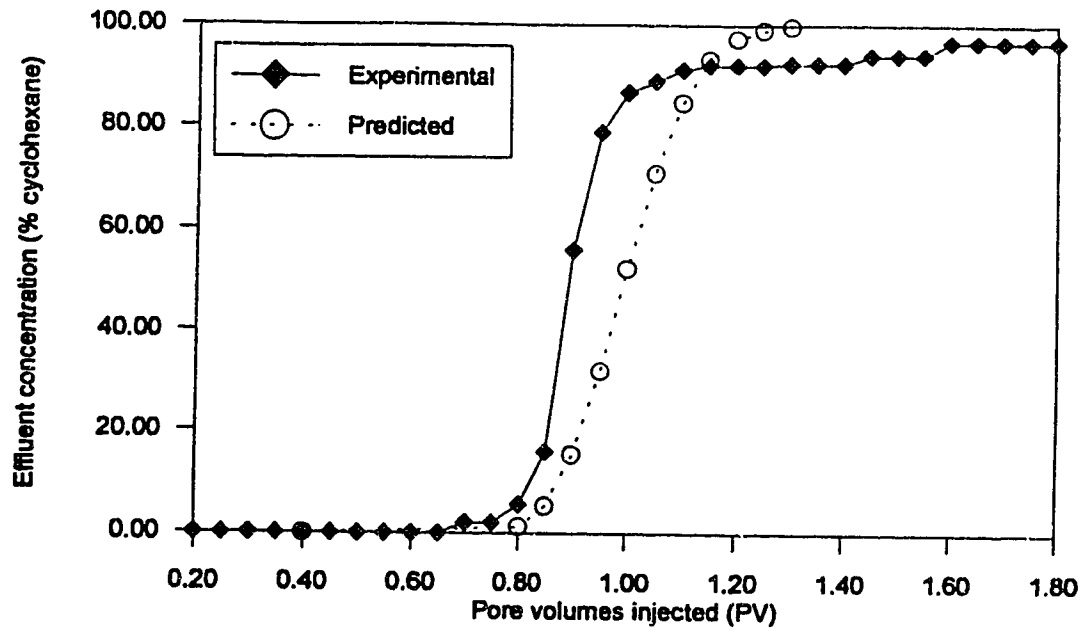


Figure C9 : Concentration profile - experimental versus predicted
Core length = 242 cm - fluid velocity = 0.0338 cm/s